THE IMPACT OF PERMITTED TREE REMOVAL ON LAND SURFACE TEMPERATURE CHANGE IN AUSTIN, TEXAS

by

Hannah Elese Buckhalter

Bachelor of Science, 2022
University of Montana
Missoula, Montana

Submitted to the Graduate Faculty of the College of Science and Engineering
Texas Christian University
in partial fulfillment of the requirements
for the degree of

Master of Science

Environmental Science

May 2025

APPROVAL PAGE

THE IMPACT OF PERMITTED TREE REMOVAL ON LAND SURFACE TEMPERATURE CHANGE IN AUSTIN, TEXAS

By

Hannah Elese Buckhalter

Thesis approved:

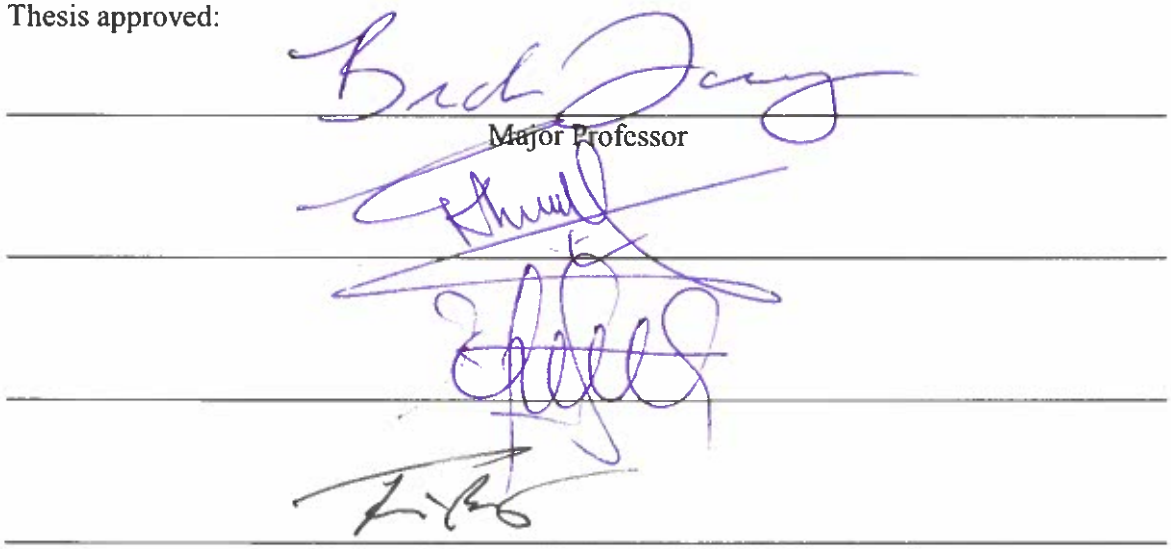

Major Professor

For the College of Science and Engineering

Acknowledgements

First and foremost, I would like to thank my family for their continued and unwavering support throughout this entire process and helping me through multiple cross-country moves that brought me to where I am today. I would like to thank my mother, Kim Buckhalter, for always picking up the phone when I was having a bad day, and my father, Brad Buckhalter, for always being available to provide guidance and support. I would also like to thank my younger brother, Owen, for making me laugh over FaceTime for hours and reminding me that I was capable of doing anything that I set my mind to.

I would also like to thank my close friends and peers, Adam Buckmeier, Abi Welch, Kate Davis, Elizabeth Hargis, Hill Nystrom, Portia Asare, Peyton Harper, Camden Butterworth and Simoon Nice for supporting me, encouraging me, and reminding me of the amazing things that we are all doing as a part of this department. To my best friends Maddie Rzucidlo and Emmersen Cook, I cannot thank you enough for providing me with endless memories and so much love during my time in Fort Worth. This would not have been possible without you two as a part of my support system. And to my closest friends out of state and across the country, Adam Hensley, Brooklynn Henderson, Brook Ploot, Kihana Turner, Skye O'Connell, Caitlyn Pregana, Cooper Heimer, Mady Rodriguez, and Thomas Ke, I thank you all for never forgetting about me and for always cheering me on, even though I am a thousand miles away.

This research would not have been possible without the support and guidance from my advisor, Dr. Brendan Lavy. Thank you for pushing me to not only be a better student, but to also be a better writer and better research. You have taught me how to look deeper, how to ask the harder questions, and how to make the world a better place. Thank you for forever changing how I understand research and science. This research could not have been done alone, and I am so grateful for your support. A special thanks to my committee members, Dr. Gehendra Kharel and Dr. Esayas Gebremichael, for lending their expertise to ensure that my research was the best that it could be.

Lastly, I would like to thank all the faculty within this department for continuously expanding my knowledge and for making me a better student.

Contents

List of Figures

List of Tables

1. Introduction

Over half of the world's population lives in cities, with urban populations increasing from 751 million in 1950 up to 4.2 billion in 2018 (United Nations 2018). In the United States, 83% of Americans live in urban areas, where urban populations grew by 6.4% between 2010 and 2020 (United States Census Bureau 2022; University of Michigan Center for Sustainable Systems 2023). Urbanization has many environmental impacts. Land use changes brought about by rapid urbanization leads to higher levels of urban and industrial runoff, creating a higher concentration of pollutants, toxins, and nutrients entering nearby water bodies (DiDonato et al. 2009; Paerl & Scott 2010). Urbanization also leads to increases in a host of air pollutants, such as carbon dioxide (CO_2), nitrogen oxides (NOx), sulfur dioxide (SO_2), particulate matter (PM), and volatile organic compounds (VOC) (Wang 2018). Urban development also contributes to habitat fragmentation (Liu et al. 2016).

Construction and development associated with urban expansion and urban redevelopment also impacts cities' urban forests (Morgenroth et al., 2017; Zhang et al., 2022). In the United States, urbanization is contributing to forest loss and increasing impervious surface cover. Between the years 2009 and 2014, urban tree canopy cover decreased from 40.4% to 39.4%, while urban impervious surface cover increased from 25.6% to 26.6%. This is equal to a loss of 138,000 acres of forests or 28.5 million trees per year (Nowak & Greenfield 2018a). These trends are likely to continue as US urban areas continue to grow. Moreover, urban tree loss is compounded by climate hazards, such as hurricanes, as well as trees becoming more vulnerable to pathogenesis due to increasing temperatures caused by climate change (Cole et al. 2021; Tubby & Webber 2010).

1.1 Urban Forest benefits

Urban forests provide important benefits to cities. Trees help to mitigate flood risks by intercepting rainfall, increasing soil infiltration, and storing water (Qin, 2020). Trees aid in the removal of harmful pollutants from the air such as PM2.5, PM10, NO_2, O_3, SO_2, cadmium, and benzopyrene (Wolf et al. 2020). Trees store and sequester CO_2 from the atmosphere, while also playing a role in oxygen production through photosynthesis. Annual carbon sequestration by urban forests in the United States is around 36.7 million tons (Nowak & Greenfield 2018b). Trees increase soil fertility by enriching soil with carbon, as well as providing the soil with additional organic material from their leaf litter (Pinho et al. 2012). Tree canopy helps reduce exposure to ultraviolet radiation, reducing chances of skin cancer caused by sun exposure (Wolf et al. 2020). Trees also provide habitat and shelter for multiple animal species. Urban forests support various species of bats, birds, winged pollinators, and invertebrates, providing habitat and contributing to biodiversity (Jiguet et al. 2012; Harvey et al. 2006; Kowarik et al. 2019).

A particularly important service provided by urban forests is their contribution to public health. Urban forests are important for people who engage in all levels of outdoor activity (Stangierska et al. 2023). Exposure to nature and spending time outdoors lowers blood pressure, increases immune function, reduces inflammation, and decreases stress hormone levels. Spending time in nature decreases symptoms of anxiety and depression and increases overall mood (Oh et al. 2017). Urban forests have also been associated with better self-reported health and social cohesion within neighborhoods (Ulmer et al. 2016). Urban forests are also essential to reducing land surface temperature (LST) in urban areas, making

spaces that are prone to experiencing higher temperatures more enjoyable for humans (Greene & Millward 2017).

1.2 Urban Heat Island Effects on Human Health

Urban areas are typically warmer than surrounding rural areas. This is referred to as the urban heat island (UHI) effect and is described as the temperature within an urban area being higher than that of rural areas due to reduced canopy cover, excessive impervious surface cover, and increased pollution (Greene & Millward 2017). Excessive exposure to heat caused by the UHI effect can have negative side effects such as dehydration, heat stress, heat stroke, organ damage, and even death (Ebi et al. 2021). Climate change has also been linked to increases in human heat stress both during the day and at night in urban areas (Oleson et al. 2015). Because of this, there has been a rise in heat mortality attributed to climate change (Vicedo-Cabrera et al. 2021). Urban forests play a role in mitigating the risks associated with the UHI effects that are compounded by climate change, as they can lower both air and land surface temperatures through their cooling effects (Upreti et al. 2017).

1.3 Urban forests and urban temperatures

In urban areas, greenspaces are correlated with lower temperatures compared to areas with less vegetation and green cover and more impervious cover (Estoque et al. 2017). Extensive greenspaces exhibit a cooling effect of approximately 0.94°C during the day (Bowler et al. 2010). Trees demonstrate better temperature-reducing abilities compared to other forms of vegetation, such as grasslands (Fan et al. 2015). The extent of temperature reduction related to increasing canopy cover or its spatial distribution varies widely based on local climate and weather patterns and the existing urban forest. For example, research done by Zhou et al. (2017) in Baltimore, Maryland, demonstrated the importance of canopy percentage in

regulating temperature. In Sacramento, California, however, the spatial arrangement of trees plays a more important role in temperature reduction.

Similar influences by urban canopy cover are seen at neighborhood scales or smaller with certain neighborhoods having lower ambient air temperatures by as much as 4°C in the presence of urban canopy cover (Wang & Akbari 2016). The strategic and well-thought-out placement of urban greenspaces is important, as prior research indicates that specifically targeting high heat risk areas for tree planting shows more significant reductions in temperature than simply expanding greenspaces (Zölch et al. 2016). Prioritizing the increase of tree canopy in these high-risk areas is likely to significantly lower temperatures. Urban forests also reduce temperatures in areas with extensive impervious surfaces, like roads, and parking lots (Vailshery et al. 2013). The diversity of urban trees also has an important role in how trees can reduce urban temperature, as an abundant and diverse array of tree species in an urban area are linked to lower daytime temperatures (Rendon et al. 2024).

The reduction of urban temperature will only become more important in future, as temperatures are predicted to rise as the result of climate change (Lindsey and Dahlman 2024). Yet, despite extensive research into the cooling benefits of urban trees and greenspaces, less is known about the effects of urban tree removal on LST. This area of inquiry is an important dimension of urban climate dynamics that warrants further investigation to assess the implications of urban tree management strategies more comprehensively. Addressing this knowledge gap will help urban planners, foresters, developers, and municipalities implement sustainable urban forest programs to safeguard human health.

1.4 Purpose Statement and Research Questions

The purpose of this research is to examine the influence of tree removal on LST. By exploring the relationship between urban deforestation and heat, this research contributes to the growing body of literature on urban forests and microclimates and provides information to support the conservation of urban trees.

1.5 Research Questions

To examine the relationship between forest loss and urban temperature, this research asks the following questions:

Q1: Does tree removal impact LST in the city, and if so, at what scales?

Q2: To what degree does tree removals influence urban temperatures compared to other variables associated with greater LST in the city?

2. Literature Review

As of the year 2022, over half of the world's population lives in cities. This mass urban migration comes with an increase in demolition, construction, and inevitable change to a city's urban forest (Zhang 2022; Morgenroth et al. 2017). An urban forest, in short, is a collection of trees that grow within a city. Across the nation, cities are facing the tandem challenges of an influx of people moving into the city and the effects on the city's urban forest. The increase in construction and demolitions constitute the need for tree removal, whether for development and aesthetic reasons or for safety reasons (Morgenroth et al. 2017). Trees have a vital role in urban living. They provide shade in sunny areas, retain water during storm events, remove pollution from the atmosphere, provide aesthetic value, and provide homes for native animal species (Dai et al. 2023; Wu et al. 2019; Conway 2016). This literature review will cover the multifaceted relationship between urbanization and urban forests around the world. By exploring the social, economic, and ecological factors at play, the challenges that urban forests face will be presented alongside their benefits.

2.1 Urban Development's Effect on Canopy Cover

The primary research theme within the literature explores the influence of urban and suburban development on urban forest tree removal and canopy cover. Much of the world's population has made the migration to urban living, and with this migration comes urban development to adapt to this increase in population (Morgenroth et al., 2017). Croeser et al. (2020) discovered that 19,739 trees were removed in the city of Melbourne between the years 2008-2017. Most canopy decreases resulted in removals from parks and private property, but a slight increase was shown in canopy cover from street trees. The slight increase in tree

canopy cover for trees could not counteract the overall canopy loss of 53 hectares (Croeser et al., 2020).

Lee et al. (2017) investigated the effects of home size increases in Los Angeles County on green cover in single-family home neighborhoods. It was found that home redevelopment decreased the amount of green cover and increased the amount of building structures and hardscapes in neighborhoods. Over a span of 10 years, green cover decreased in a range of 14-55% in these single-family lots. Through extrapolation, it was determined that redevelopment at this rate for single family home neighborhoods would lead to a 1.2% annual decrease in green cover (Lee et al., 2017).

Guo et al. (2018) investigated tree removal due to redevelopment on private property in Christchurch, New Zealand, monitoring 450 properties between the years of 2011 to 2015 and part of 2016. 321 of the monitored properties underwent development and 129 did not. 44% of trees were removed on developed properties, while 13% of trees were removed on non-redeveloped properties (Guo et al., 2018). Morgenroth et al. (2017) also had similar findings in residential communities in Christchurch, New Zealand. 123 properties that were adjacent to construction projects were monitored for trees before and after demolition. They found that 21.6% of the trees on these properties were removed, leading to a 19% canopy cover reduction in these residential communities (Morgenroth et al., 2017).

In Philadelphia, Pennsylvania, a study was done to investigate the loss of trees on a highly urbanized college campus. The mortality rate of the trees was 4.3% higher than that of similar studies done in other cities. This high mortality rate was associated with proactive management of trees for safety reasons and other construction projects on campus. Approximately 48.5% of the removals on campus were a result of a construction project

(Roman et al., 2022). However, with these high removal levels, there were also new tree plantings equivalent to the number of trees removed. The tree diversity on campus was also notable, showing the attention to tree planting and removal by the campus landscape architects and other officials (Roman et al., 2022).

The impact of urban and suburban development on tree removal and canopy cover underscores a significant concern as global populations gravitate towards urban living. These findings emphasize the urgency for appropriate strategies to mitigate urban development's adverse impact on tree cover and prioritize the need for a balanced approach to urban growth and environmental preservation.

2.2 Urban Forest Benefits and Ecosystem Services

The second theme within the literature explored the contribution of trees through their ecosystem services. In the face of extensive tree removal because of development and boundary expansion, urban and suburban systems are facing a loss of ecosystem services that are provided by trees and other greenery. Major ecosystem services include the removal or sequestration of air pollution, runoff reduction, and the reduction of air temperature by canopy cover (Qin, 2020; Wu et al., 2019; Ziter et al., 2019). Trees also provide valuable social services, ranging from elevating mood to increasing levels of physical activity (Wolf et al., 2020).

A study done by Ziter et al. (2019) in Madison, Wisconsin used bicycle-based sensors to determine air temperature over multiple transects. Air temperature sampling was done over multiple days, three times a day during the hottest portions of the day, and the air temperatures recorded were compared to urban forest canopy cover. They found that found that canopy cover decreased air temperature at an average 0.7 °C at a 10m radius from either

one of the three urban lake locations that were considered in the study. Temperatures continued to decrease the larger the radius from the lake became, with an average 1.3 degrees °C decrease at a 30m radius, and >1.5 °C decrease between a 60m radius and a 90m radius. The decreasing temperatures leading away from the lake were attributed to an increase in canopy cover (Ziter et al., 2019). When considering both canopy cover and impervious surfaces at the same time, canopy cover reduced daytime air temperature at all levels impervious surface cover. Even at the 10m radius from the nearest water body, an area with >50% impervious surface cover experiences a reduction in air temperature 1-1.3 °C with >75% canopy cover (Ziter et al., 2019).

Urban forests also play a crucial role in removing or sequestering pollutants from the atmosphere. A common way to quantify pollution removal or other ecosystem services is to employ the program iTree Eco, which is used in tandem with data pulled from pollution monitoring stations and meteorological stations, which was the method used in a study done by Wu et al. in 2019. This study determined that the trees in Shenzen City, China, removed a total of 1000.1 tons of PM2.5, a harmful particulate pollutant, from the atmosphere. Evergreen shrubs, evergreen needle-leaf forests, and evergreen broad-leaf forests showed the highest pollutant removal efficiency (Wu et al., 2019).

Similar to the Wu et al. study done in a 2019, a study done by Bottalico et al. (2016) found that both O3 (ozone particles formed in the lower atmosphere due to pollution) and PM10, another harmful particle pollutant, were removed from the atmosphere in large quantities in Florence, Italy through sequestration by urban vegetation. Different species of trees removed different amounts of O3 and PM10, with evergreen broadleaf forests removing the most O3 and mixed species forests removing the most PM10. There seemed to be a

slightly higher performance for O3 removal than PM10 removal, but that does not diminish the importance of urban forests in removing particulate matter from the air (Bottalico et al. 2016).

Greene and Millward (2017) performed a study to investigate the effects of canopy cover on LST in Toronto, Canada. Through spatial regression and satellite images, they discovered a significant relationship between tree canopy cover and LST, with observed LST decreasing in spaces with closed tree canopy or high canopy density. Even in areas with low density canopy cover, tree canopies can still play a role in reducing surface temperature when accompanied by other forms of vegetation (Greene and Millward, 2017). Dai et al. (2023) made strikingly similar discoveries through their study in Luoping County, China. Through ArcGIS software and an LST inversion, they quantified the distribution of LST in relation to various land cover types, with LST being the lowest under tree canopy cover and on water. The average LST with tree canopy cover was 29.98 °C, and the average LST on impervious surfaces was 31.44 °C (Dai et al., 2023). The results from these studies emphasize the significant impact that tree canopy cover has on the reduction of LST.

Trees also play an important role in flood mitigation through intercepting rainfall increasing water infiltration (Qin, 2020). Approximately 10-50% of annual rainfall is intercepted by trees, with interception rates varying by tree species. Trees increase soil infiltration because their root systems create conduits in the soil, allowing water to infiltrate faster and reduce stormwater runoff. These paths created in the soil have been found to increase soil infiltration by 150%. Trees then return water to the atmosphere through photosynthesis, maintaining the healthy balance of water in the soil, on the surface, and in the air (Qin, 2020).

Trees and urban forests are also associated with a general increase in overall health and mood (Wolf et al., 2020). Higher levels of urban forests increase outdoor activity levels of all kinds such as walking, cycling, and playing amongst children. Physical activity in nature enhances cognitive function and performance and increases mood, bringing feelings of happiness and vitality. Those with exposure to urban forests self-report lower levels of hostility and anger (Wolf et al., 2020).

This research underscores urban forests' important role in moderating temperatures, mitigating environmental stressors in densely populated areas, removing harmful air pollutants, mitigating flood risks, and even increasing the health and well-being of people in urban communities. These findings stress the urgency of preserving and nurturing urban forests for their contributions to environmental quality and public health and well-being.

2.3 Public Consensus on Urban Forests

The third theme within the literature explored the weight of public opinions and feelings about trees and their influence on tree retention. When studying urban forest management, it is critical to consider the role that public perception and opinions play in tree removal decision making or tree protections. Many trees in urban, western cities are located on private property and are managed by homeowners or property owners, which often serves as a drawback in the context of urban forest management, as individual attitudes towards trees, socioeconomic status, and other determining factors can influence how people feel about the trees on their property (Guo et al., 2019).

Collecting public consensus data on tree removal and retention is often done as a survey. Most surveys are short and easy to understand to prevent fatigue or boredom from respondents (Koeser et al., 2023). The survey respondents are most often selected to be

individuals that live in single family homes with greenspace on the ground (Conway, 2016). These surveys will typically include sections for demographic data too, including information such as the age, gender, ethnicity, and economic status of the respondent (Conway, 2016). The survey will include information inquiring about attitudes towards trees, tree aesthetics, tree removals, and property redevelopment (Guo et al., 2019).

Results from these surveys tend to show similar findings. In a Koeser et al. study (2023), only 17% of the survey respondents supported the removal of large trees for development, and 82% said that they would highly consider planting a new tree on their property for monetary compensation. Most people find trees to be important and support federal and local funding for urban forest initiatives. Some residents in a Guo et al. (2019) study noted that they would keep their trees and consider planting more trees to help improve air quality (Guo et al., 2019). The most common reasons for keeping a tree included aesthetic value, privacy, animal habitat, and creating shade (Conway, 2016; Kirkpatrick et al., 2012). Trees were often removed or would be considered for removal if they were dead, diseased, a hazard, or were too much to maintain (Conway, 2016; Guo et al., 2019; Kirkpatrick et al., 2012).

A public consensus survey can also show the effectiveness of a tree ordinance (Koeser et al., 2023). Many local government agencies have made moves to prioritize the protection and health of trees in the urban forests through urban forest governance, the practice of making and upholding laws and regulations, and management, which stems from typical environmental and ecological management (Clark et al., 2020). Surveys regarding tree ordinances and urban forest management can be conducted by asking citizens how they feel about urban foresters and planning professionals similarly, and their answers are recorded and

transcribed using NVivo software (Clark et al., 2020; Conway 2016). A study done by Clark et al. (2020) showed that local authority tree initiatives are not always effective when protecting urban trees. A ‘significant tree’ is a tree nominated by a local government authority in the greater Melbourne, Australia vicinity. The tree is nominated for its size, age and value, and a significant tree is considered protected under most urban forest initiatives. However, many residents opted to not accept the significant tree nomination for trees on their property in fear of the nomination hindering their ability to develop their property in the future and lowering property value (Clark et al., 2020).

Surveys assessing public sentiment reveal strong support for tree preservation and habitat creation, but many residents prioritize aesthetics and privacy, showcasing a complex relationship between tree value and property concerns. Residents also tend to show hesitation in giving trees on their property a higher level of protection for fear of lowering their property value. These findings indicate the need for comprehensive urban forest governance that navigates diverse community perspectives while prioritizing environmental sustainability.

2.4 Urban Forests and Environmental Justice

The fourth theme within the literature explored the relationship between socioeconomic status, race and ethnicity, and urban forests and urban heat exposure. The community of environmental justice (EJ) scholars and professionals have long been concerned with how low income and minority communities are unevenly exposed to environmental inequity and environmental hazards (Schwarz et al., 2015). Urban tree canopy (UTC) is typically regarded as an environmental amenity or good and is associated with local water cycles and local climate. The presence of UTC has often been linked to negative and significant relationships with minority races and low-income communities (Schwarz et al.,

2015). Disproportionate access to UTC and urban forests implies disproportionate access to physical, mental and social health benefits that trees provide to individuals and to communities (Gerrish & Watkins, 2017).

There are a variety of ways to effectively study and observe the relationship between urban forests, race, and income, as well as ways to analyze how we research and describe these relationships. A common way to research the relationship between socioeconomic status or race against UTC is to input socioeconomic and UTC data into the iTree Landscape program, which can also provide an output of monetary values for trees and their ecosystem services (Riley and Gardiner, 2020). The most valuable ecosystem services include carbon sequestration, stormwater runoff reduction, and atmospheric pollution removal (Riley and Gardiner, 2020). A geographic information system is then used to divide and spatially illustrate census block groups for the desired study areas and visually display UTC and socioeconomic status (Schwarz et al., 2015).

Results from the studies on the spatial distribution of UTC against socioeconomic status and or race and ethnicity proved to be similar, albeit with slight differences. Riley and Gardiner (2020) found that areas with median income and a higher presence of undergraduate degrees showed to have either neutral or a slightly positive relationship with UTC. They also found that communities with a higher percentage of minorities, poverty, or with less of an educational background have connotations of missing out on the benefits of UTC (Riley & Gardiner, 2020). Schwarz et al. (2015) had similar results with socioeconomic status generally having a negative relationship to UTC, but with variation in areas such as areas in California that have higher Asian populations than many urban areas across the

United States. In Los Angeles, the relationship between being an Asian racial minority and UTC was positive. (Schwarz et al., 2015).

Many cities are developing Urban Forest Masters Plans (UFMPs) to combat urban forest loss and promote urban forest growth and biodiversity. These planning documents provide local planting and stewardship goals within their territory (Grant et al., 2022). The question remains as to how well or effectively these cities are pledging to commit to environmental justice in the UFMPs. A study done by Grant et al. (2022) consisted of a content analysis of 107 UFMPs in the United States to determine how environmental justice was addressed in these documents. A keyword search was performed, and the keywords were divided into one of the three environmental justice pillars, those being distributional, procedural, and recognitional justice, and then further subdivided to determine whether they were briefly mentioned or explained in detail (Grant et al., 2022).

The UFMP analysis conducted by Grant et al. (2022) revealed that, out of 107 UFMPs analyzed, these plans averaged 2.2 per 1000 words in reference to distributional, procedural, and recognitional justice all together. A UFMP from Seattle, Washington was the only plan to give an in-depth explanation and plan for recognitional justice. Overall, it was found that these documents place the heaviest emphasis on procedural justice, which is due to how the words were coded and counted, using words and phrases such as “engagement/outreach” and “public education” (Grant et al., 2022).

UTC is also essential to combating the UHI effect, as urban forests are essential to reducing or otherwise influencing LST in urban areas, making spaces that are prone to experiencing higher temperatures more enjoyable to the human experience (Greene and Millward, 2017; Ziter et al. 2019). A study done by (Hsu et al., 2021) compared urban heat

exposure against census track data to determine the inequity of heat exposure across major cities in the United States. UHI exposure across major cities in the United States is highest for Black and Hispanic residents across all climatic regions, while non-Hispanic white residents have the lowest exposure (Hsu et al., 2021). UHI is higher for people of poor or lower-class backgrounds as compared to people from wealthy, upper class backgrounds. Minority and low-income communities face the most exposure to the heat island effect (Hsu et al., 2021).

Understanding the relationship between UTC, race, and income is pivotal in addressing EJ concerns. These studies show how the disproportionate access to UTC correlates with disparities in health and well-being for minority and low-income communities, as well as show how income and education correlate with UTC presence. These complexities emphasize the complicated nature of addressing EJ in UTC distribution.

These studies have expressed the impact of urban expansion on tree removal and canopy cover, emphasizing the consequences of private property redevelopment and public property management. From Austin to Melbourne, the data shows the substantial loss in canopy cover due to development, raising concerns about sustainable urban growth. The role of urban forests in providing essential ecosystem services has been illustrated. From regulating surface temperatures to effectively sequestering pollutants, trees are essential to urban environments. The integration of public opinions into urban forest management decisions has been explored in the literature, revealing diverse attitudes toward tree preservation. Homeowners' opinions on trees are shaped by various factors from aesthetics to environmental concerns and play an important role in the management of urban trees. Furthermore, the research done on environmental equity has shown the disparities in access to urban tree canopy and shows the impact on marginalized communities. The findings have

shown the intricacies of socioeconomic status and race in relation to tree coverage, advocating for more inclusive urban forest management.

3. Materials and Methods

3.1 Site and Situation

The study area for this research is Austin, Texas (Fig. 1). Austin is in Central Texas and is the state's capital city. Austin is the 10th largest city in the United States and has become a hotspot for urban growth due to its ample recreational and economic opportunities. From 2010 to 2020, Austin's population increased by 33.0%, making it one of the fastest growing U.S. cities (Austin Chamber, 2023).

The city of Austin adopted a tree ordinance in 1984 to protect trees on both private and public property. Most urban forest regulations fall into one of four categories: 1) street tree ordinances; 2) tree protection or preservation ordinances; 3) buffer or view ordinances; and 4) landscape ordinances (Lavy & Hagelman, 2019). A tree preservation or protection ordinance (TPO) typically includes the following information: 1) the parameters of protection, 2) the extent of protection, and 3) the conditions of protection. (Lavy & Hagelman, 2019).

The ordinance for Austin has been amended and edited over the years and was eventually given a heritage tree clause, where trees with a diameter at breast height (DBH) equal to or greater than 19 inches are considered a protected tree, and those greater than or equal to 24 inches are considered a heritage tree. This heritage tree ordinance is only applicable to native Texas trees. A landowner must submit a request for a permit to remove or otherwise modify a heritage tree, which the city has the power to deny after a site inspection is done. Factors considered during the permit's pending approval or denial include tree age, species, condition, and size. The goal of Austin's tree protection ordinance is to balance re-forestation and tree preservation while always emphasizing one of the two

elements to benefit the community (Lavy & Hagelman, 2017). Even with its tree protection ordinance in place, the amount of approved tree removals increased by 30% between the years of 2002-2011 in the city of Austin, with 76% of tree loss taking place on residential properties and 54% attributed to some form of development (Lavy & Hagelman, 2017).

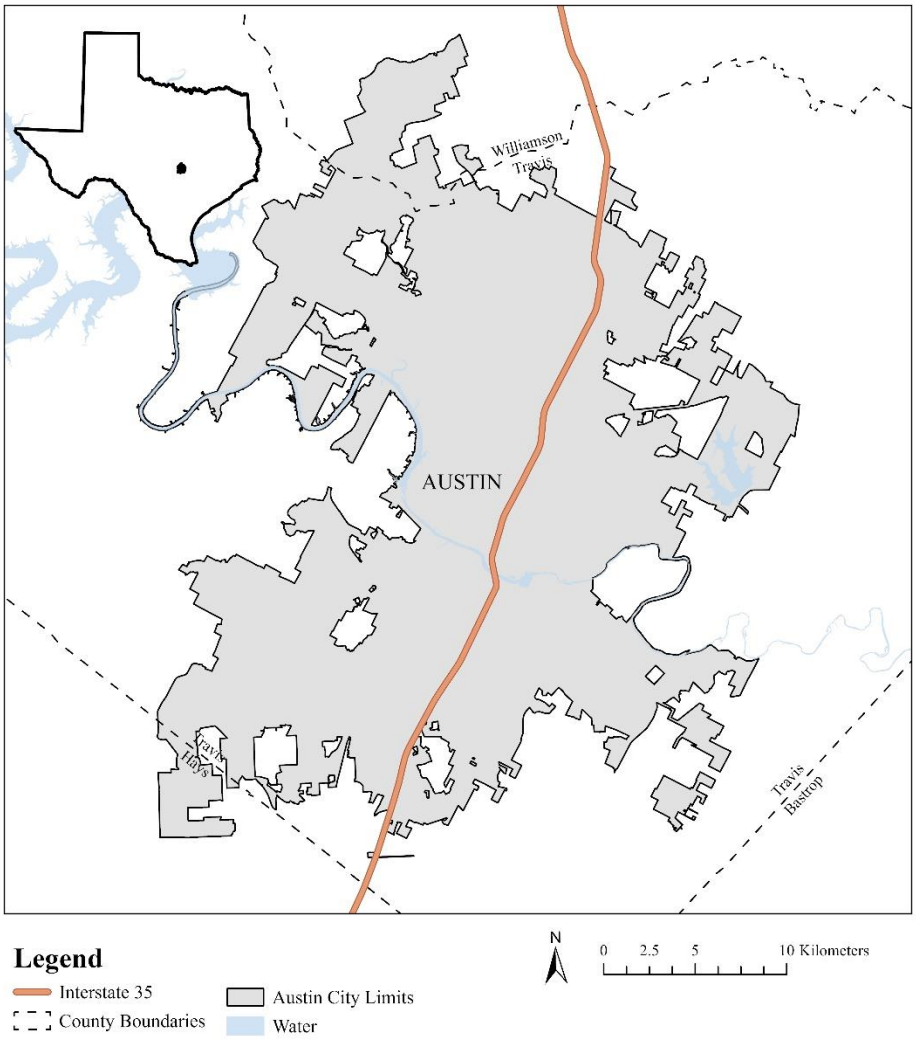

Figure 1. Austin city limits study area.

3.2 Data

Data for this research was collected from various sources (Table 1). Data included instances of tree removals, satellite imagery, developed impervious cover, and canopy cover. The following section outlines these data and their sources.

Table 1. Variables influencing LST.

Conceptual Variables	*Operational Variables*	*Metrics*	*Units*
Urban Deforestation	Tree Removal	Location	Latitude/Longitude coordinates
		Health	% healthy
		Development Related (Y/N)	% development related
Neighborhood Characteristics	Impervious Cover	0-25% 25-50% 50-75% 75-100%	% impervious cover
Urban Forest Presence	Canopy Cover		% canopy cover

The spatial analysis for this research was conducted in ESRI ArcGIS Pro. ArcGIS Pro is a geographic information system (GIS) software commonly used to explore and analyze visual and spatial data (ESRI, n.d.). Before moving forward in ArcGIS Pro, it was ensured that our map in the GIS was projected in Central Texas State Plane NAD 1983 (2011) to ensure geographic accuracy and to reduce possible geographic distortion. To begin, we uploaded the Austin City Limits boundaries to define our area of interest.

3.2.2 Tree Removals

Tree removal data for this study was obtained from the Austin City Arborist Program. The dataset contains information from every tree removal application permit, including the

address, the date of application submission, what action was requested, whether the action was requested for development reasons, and whether the permit for tree modification was granted. Modification requests fall into one of three categories: 1) total removal of the tree, 2) encroachment into the tree's critical root zone (CRZ), and 3) excessive removal of the tree's canopy (Lavy & Hagelman, 2017). It also contains data regarding tree species, DBH, and tree condition. The available data contains approximately 60,000 tree removals or major modifications and spans from 2005 to present day and is updated daily. For this study, we examined the location or address of the major modifications or removals, whether the removal was development related, and the condition of the tree. We incorporated tree removals spanning from 2013 through 2023 into our GIS to represent a decade of permitted tree removals that will be examined alongside a decade of LST variations.

We uploaded the tree removal dataset into our GIS and used the 'xy table to point' tool to plot the tree removals onto our generated map. Tree condition, a category of interest for our tree removals, was split into four separate categories: good, fair, poor, or dead. Since we were only classifying tree removals to be healthy or unhealthy for this study, we designated tree removals that were categorized as 'good' or 'fair' to be healthy trees, and then designated removals categorized as 'poor' or 'dead' as an unhealthy removal (Table 2).

Table 2. Tree Removal Condition Classification Table.

Tree Condition	***Classification***
Good/1. Good	Healthy
Fair/2. Fair	Healthy
Poor/3. Poor	Unhealthy
Dead/dying/4. Dead, dying, or imminent hazard	Unhealthy

3.2.3 LST

To obtain accurate LST readings for our study, we used Landsat 8 OLI/TIRS images courtesy of the United States Geological Survey (USGS). We used Google Earth Engine (GEE) Code Editor to extract this Landsat 8 OLI/TIRS imagery (Ermida et el. 2020). GEE is a specialized computing platform that lets users run geospatial analysis through the Google interface. The Code Editor feature within GEE is a web-based integrated development environment, accessible through log-in with a Google account (Google, n.d.). Before we moved to extract the Landsat images, we set the Austin area as the primary geometry point with a 30 km buffer. When we selected our Landsat 8 imagery through GEE, we ensured that the time span of images ranged from 2013 to 2023. Because Texas faces extreme heat during the summer months, we filtered the image selection to only select images from the summer months of June, July, or August from 2013 through 2023. We also confirmed that our images would have less than 10% cloud cover to ensure the quality of our LST readings.

After employing the prescribed code in GEE to fit our research interests, we found 25 images that matched our search criteria. While we had set our cloud cover limit to 10%, the 10% cover was applied to the entire Landsat 8 image that encompassed Austin as opposed to exclusively the city limits. This resulted in several images that displayed high cloud cover over city limits. Of the 25 images, we chose to use 8 images for our study based on relative cloud cover over Austin city limits to ensure that we get the most accurate LST readings for our research (Table 3). Our 8 selected images were exported into Google drive, we uploaded them into ESRI ArcGIS Pro for analysis.

Table 3. Landsat 8 images selected by GEE based on our search criteria.

Date	***Cloud Cover %***	***Selected***
2013-6-08	1.72	No
2013-08-31	0.33	Yes
2014-07-01	8.12	No
2015-07-20	0.44	Yes
2015-08-05	4.23	No
2016-07-06	2.71	No
2016-07-22	0.25	Yes
2016-08-07	7.26	No
2016-08-23	8.47	No
2017-06-23	6.35	No
2017-07-09	4.95	Yes
2018-07-12	2.37	No
2018-07-28	3.32	No
2018-08-29	8.29	Yes
2019-06-13	2.71	No
2019-07-31	5.92	No
2019-08-16	2.59	Yes
2020-07-17	7.46	No
2020-08-18	3.31	Yes
2022-07-07	5.22	No
2023-06-24	2.70	No
2023-07-10	0.70	No
2023-07-26	7.59	No
2023-08-11	0.00	Yes
2023-08-27	0.79	No

Since we are interested in how LST changes over time, we constructed a time series for LST from our 8 selected images in GEE. After creating the time series, we employed code to create a slope raster image based on the LST value from the selected Landsat imagery by performing a linear regression. The generated slope raster illustrates the average temperature change per pixel from the oldest LST raster in 2013 to the newest LST raster in

2023 to display average change in LST throughout that decade. When our slope raster was generated, we exported the image to Google Drive and then downloaded it to our computer to upload it into to ESRI ArcGIS Pro for further analysis.

3.2.3 Additional Landscape Characteristics

In addition to urban forest loss and LST, we quantified specific landscape features identified in the literature that may contribute to the change in LST, those being percent impervious cover and percent canopy cover. These biophysical landscape components are some of the most important parts of an urban ecosystem (Xu, 2010).

3.2.3.1 Developed Impervious Cover Percentage

Developed impervious cover data was gathered from the USGS National Land Cover Database (NLCD) 2021 Land Cover (CONUS). This product provides comprehensive and accurate information about the nation's land cover. Each 30 m × 30 m pixel is assigned a classification based on its cover type, which includes but is not limited to open water, low to high intensity development, agriculture, and wetlands (Multi-Resolution Land Characteristics Consortium n.d.). Increasing levels of impervious surfaces are associated with higher urban temperatures, as impervious surfaces have high LST, which is the basis of the UHI effect. Higher levels of impervious surface cover are also responsible for a decline in vegetation cover (Xu, 2010). Once we downloaded the land cover data from the NLCD, we uploaded it into ESRI ArcGIS Pro to move forward with our analysis.

3.2.3.2 Tree Canopy Percentage

Tree canopy cover has been shown to lessen the effects of daytime heat in urban areas (Ziter et al., 2019). Urban development and redevelopment are major factors that determine

tree canopy percentage (Morgenroth et al., 2017; Croeser et al. 2020), so it is essential to consider complete tree canopy cover as an influence for LST in this study.

4. Analysis

4.1 Scale of Analysis

This research is focused on assessing the impact of tree removals at different scales, those being city blocks and neighborhoods, which correspond to 32,400 m² and 291,600 m², respectively. We are examining changes in temperature at two different spatial scales because urban temperature dynamics and urban temperature change may vary depending on the scale of investigation. Understanding temperature dynamics at various spatial scales is imperative in understanding the key factors in urban microclimate variability alongside environmental equity issues (Karangi and Kiage 2021).

To generate these different sized grids, we used the 'Fishnet' tool. To generate our first fishnet composed of 291,600 m² grid boxes, we opened the 'Fishnet' tool and gave our output feature class a unique and easily identifiable name. To generate a fishnet, an origin coordinate is required. We ultimately selected our origin coordinate to be our NLCD land cover raster that we used in this study. The land cover raster has a 30 m × 30 m resolution. While our grid cells are be larger than 30 m × 30 m, each of our grid cells for scale needed to be both divisible by 30 m for our analysis. The fishnet grid cells needed to be lined up with a raster image to ensure that the 30 m × 30 m image pixels fit neatly within each grid cell for consistent and accurate analysis.

After setting the origin coordinate, the template extent and the Y-axis coordinate updated update automatically, so we did not change the input for those two fields. For our

cell size width and height, we set the measurements to 540 m (540 m × 540 m) to create our 291,600 m² grid cell. The opposite corner of the fishnet was automatically generated when we set our origin coordinate as the land cover raster, so we did not change this input. We unchecked the create label points box, as these are not necessary for our analysis. For the geometry type, we were given the option of choosing either polyline or polygon. We needed polygons for our analysis, so we set the geometry type to polygon. We then ran the tool. Once complete, this tool generated a grid divided into 291,600 m² cells

We repeated this process once more for our 32,400 m² fishnet. We assigned our output feature class a unique name and set our origin coordinate to the NLCD land cover raster. The only steps that changed for this process were the cell width and cell height. For the 32,400 m², we set the cell width and height to 180 m (180 m × 180 m). Identical to the first grid we generated, the template extent, Y-axis coordinate, and opposite corner of fishnet are generated automatically when we set the origin coordinate, so they do not need to be manipulated further. After all the fields for the tool were completed, we ran the tool again. At the end of this process, we had generated a grid divided into the 32,400 m² cells, and in turn two grids of different sizes to represent our scales for analysis.

Next, we had to ensure that our study area of Austin City Limits only contained whole grid cells from our generated fishnet with no partial grid cells. We achieved this by using the 'Select by Location' tool. For our input features, we first selected our 291,600 m² fishnet. We set Austin City Limits as the selecting feature and set the relationship to 'crossed by the outline of'. The selection type was set to 'new selection', we kept the search distance at '0', and then we ran the tool. This highlighted and selected all the cells from our tessellation that crossed the boundary of Austin City Limits. We chose to select these cells

because, even if they are not fully contained by the city of Austin, they are necessary to keep for accurate analysis. We returned to the ‘select by location’ tool to select the blocks from the rest of the fishnet. We kept the input features and selecting feature the same, but we changed the selection type to ‘add to the current selection’. We adjusted the relationship to ‘within’, kept the search distance at ‘0’, and then ran the tool again. This selected all the whole cells that are contained by Austin City Limits. Our result showed every cells that is within or crossed by Austin City Limits as highlighted and selected. We did not want any partial cells from either one of the grids, even if they are cut off by the city limits boundary. This tool allowed us to select these cells crossed by the boundary as whole squares, not partial. This is essential for accurate calculations of minimum, mean, and maximum LST, impervious cover, tree canopy cover, and our tree removals at each scale. Once all the cells were selected, we navigated to the 291,600 m^2 layer in the Contents pane, opened the pop-up menu for the layer, navigated to selection, and chose ‘Make layer from current selection’. This created a new layer for our analysis, a layer comprised of Austin city limits and our newly selected grid cells from our tessellation (Fig. 2).

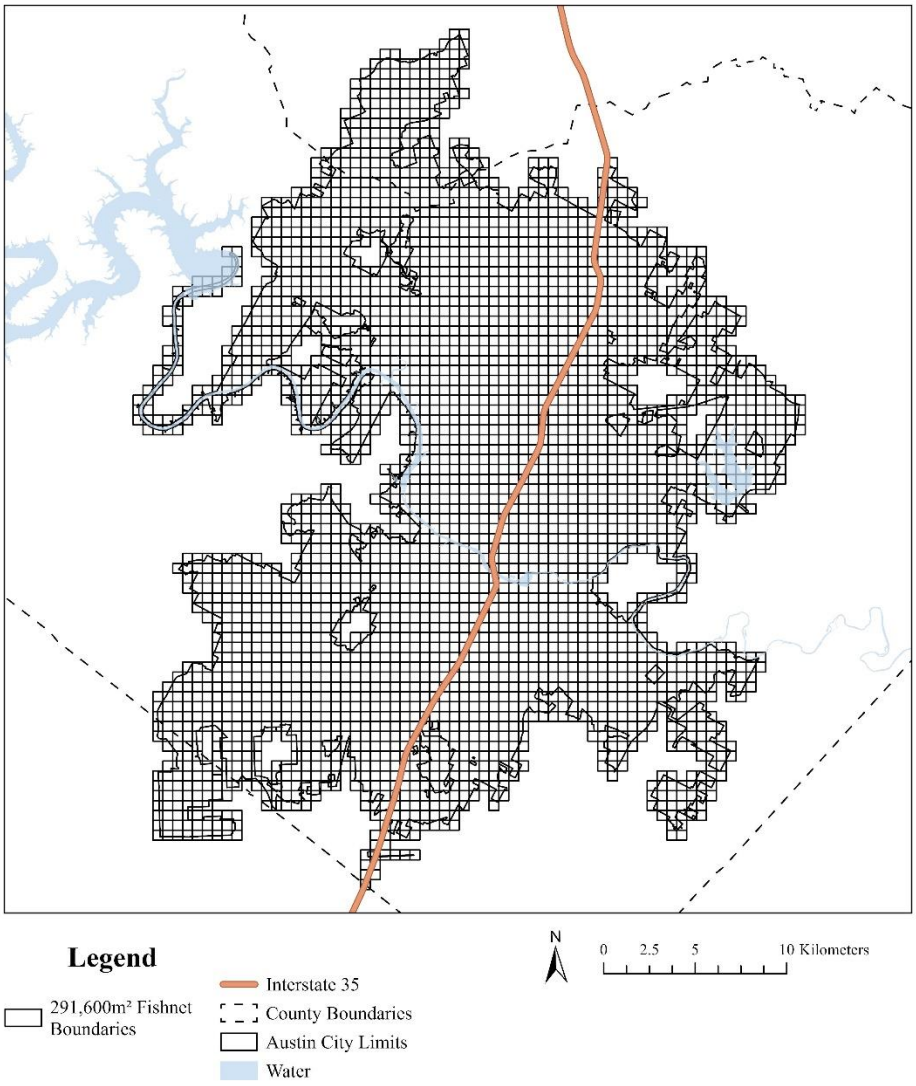

Figure 2. 291,600 m² fishnet over Austin city limits.

To ensure that both fishnets were uniform in their boundaries, we reduced the size of our 32,400 m² fishnet in a similar way. To do this, we used the 'select by location' tool again. Moving to our 32,400 m² fishnet, we set this fishnet to the input feature and we set our newly generated 291,600 m² selection layer as the selecting feature and set the relationship to 'within'. We ran the tool and were given all the selected grid cells from our 32,400 m² fishnet

that rested within the newly generated 291,600 m² selection layer. Using the ‘Select by Location’ tool in this way ensures that, even though our grid cells are different sizes to represent scale, the total area being incorporated into our analysis is still the same regardless of scale. We then navigated to our 32,400 m² fishnet in the contents pane, selected the layer, and created a new layer from the current selection (Fig. 3). We had two new layers for our fishnets that would be used for the remainder our study.

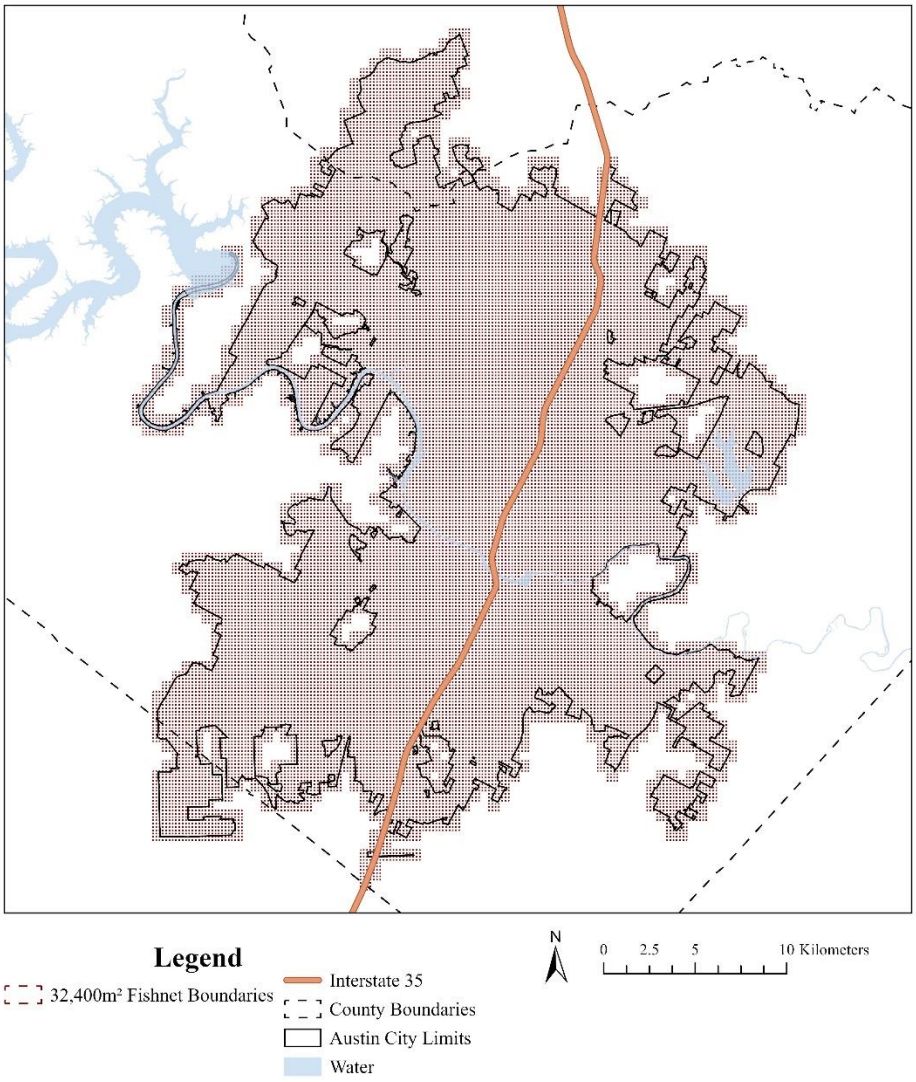

Figure 3. 32,400 m² fishnet over Austin city limits.

4.1.1 Quantifying Tree Removals

To obtain totals for all tree removals, healthy removals, and development related removals at both scales, we used the 'summarize within' tool in ESRI ArcGIS pro. When using this tool, we set the input polygon to our desired grid, starting with our 291,600 m² fishnet. For our input summary features, we chose our tree removal layer, as these are the

features that we want to summarize. We assigned the output class a unique name, as using this tool creates a new layer. We left the summary fields blank to simply generate a count of points. We ran the tool, which generated for us a new layer comprised of both the 291,600 m² fishnet and summarized information about the tree removals that includes a count of points. When we open the attribute table, we can look at individual 291,600 m² grid cell and see how many total tree removals occurred in each.

Next, we wanted to see how many healthy removals tree removals and how many development related removals occurred in each grid cell. To do this, we used the 'summarize within' tool again. This time, for our input polygon features, we selected our newly generated summarized layer that we created in the previous step. Our input summary features were our tree removals, and we gave our new output layer an identifiable name. For the summary fields, we selected development related removals and healthy removals. We ran the tool, which generated for us a new layer that, when investigated, displays a total count of removals, a total count of development removals, and a total count of healthy removals for each grid cell.

We repeated these steps for our 32,400 m² fishnet to generate a similar new layer. The only difference in this process was selecting the 32,400 m² fishnet as the input polygon when first using the 'summarize within' tool. At the end of this process, we had two new layers comprised of the total number of tree removals, the number of healthy removals, and the number of development related removals, one for each of our fishnets.

4.1.2 Calculating LST

Before we could begin extracting values from our LST slope image, we needed to do cell dimension resizing and georeferencing. By default, the Landsat images exported from

GEE have a 30 m × 30 m resolution, but the exporting and importing of data can sometimes lead to unintentional resolution changes or manipulations (Google Earth Engine, n.d.). We noticed that our slope raster pixels were not neatly aligned in either of our fishnet grids, when ideally, the y should be a perfect fit. Upon further investigation, we found that the cell resolution for the raster was 28.4 m × 28.4 m. To adjust the slope raster image to fit our grids appropriately, we used the 'resample' tool in ESRI ArcGIS Pro. For the input raster, we selected our slope raster. We gave our output raster a new name, as this would generate a new raster layer to use for analysis. For the output cell size, we set the cell size to match that of our NLCD impervious cover raster (the image used for reference when generating our fishnet grids) which has a 30 m × 30 m resolution. We elected for nearest neighbor resampling and ran the tool. This tool gave us a new layer that now had a resolution of 30 m × 30 m.

However, even with the new resampled cells sizes, the raster was still not correctly lined up with the fishnet grids. As was previously stated, the importing and exporting of images in bulk may result in unintended compression and discrepancies. To ensure that our slope image aligns with and fits appropriately within our fishnets, we used the 'georeference' tool to move our raster layer in line with our fishnets. First, we ensured that we had 'snapping' turned on. The 'snapping' feature is a drawing aid that increases accuracy when aligning a geometric element (ESRI, n.d.). Next, we selected the 'georeference' tool from the Imagery pane. We selected the 'move' function, as we wanted to move and adjust our raster layers within the map view. We then selected the 'add control points' tool, which would allow us to move a desired point on the raster layer to a corresponding point on the fishnet grid. With everything selected, we began moving the slope raster. We zoomed into the map a

considerable amount to ensure that we could easily see and identify lines and boundaries. Next, we set one control point to a vertex of a 30 m × 30 m raster pixel that was intended to be aligned within the fishnet grid. Then, we set another control point to the corresponding vertex of the fishnet, and with snapping on, our control point snapped to the fishnet grid. Our raster was then shifted, and all pixels fit accordingly into the fishnet.

For our analysis, we needed minimum, maximum, and mean values for each fishnet grid cell for the slope raster. This was done using the 'zonal statistics as table' spatial analyst tool. For our feature zone data, we started with our new 291,600 m² fishnet layer we created that encompasses all grid squares within Austin city limits and that are crossed by the city limits. Our zone field automatically sets to GRID_ID, and we left it as such. For our input value raster, we selected our slope raster, and then gave our output table a unique and easily identifiable name. For the statistics types, we selected the 'minimum, maximum, and mean' option from the drop-down menu, and then we ran the tool. The product of this tool provided us with a table containing 3,175 rows of information. Each row represents an individual grid cell from the 291,600 m² fishnet. Every row contained values for the minimum, maximum, and mean slope, or LST change over time. We repeated this process for our slope raster with the same parameters for the 32,400 m² fishnet by changing the input raster or feature zone data within the tool. We ran the tool once more, and we were given another table with 28,575 rows of information. After this process was complete, we had two tables, one for each fishnet, all containing the minimum, maximum, and mean slope values for each grid cell.

After these zonal statistics tables were generated, we needed to join each table to their designated fishnets. We first joined the 291,600 m² slope zonal statistics table to the accompanying fishnet layer. We navigated to the 291,600 m² fishnet layer in the contents

pane, clicked on the layer, selected ‘Joins’ and then ‘Add join’. When the tool opened, our input table was automatically set to the 291,600 m² fishnet. We set the input join field to the OID (ObjectID) for the fishnet. For our join table, we selected our slope table for the 291,600 m² fishnet, and set the join table field as the OID (ObjectID) for the slope table. We validated the join and then selected ‘ok’. The slope table that we generated for our 291,600 m² fishnet was then joined to that fishnet layer, allowing us to open the attribute table for that fishnet layer and view the statistics that we had calculated for it. To join the slope zonal statistic table that we created for our 32,400 m² fishnet to the fishnet layer itself, we repeated this entire process once more, which then allowed us to open the attribute table for that fishnet layer and view the statistics for the slope raster image.

4.1.3 Calculating Impervious Cover Percentage

Our next step was to calculate the percentage of impervious cover for each unit of analysis. Developed spaces from the NLCD were organized into four distinct categories of measurement: Developed, Open Space; Developed, Low Intensity; Developed, Medium Intensity; Developed, High Intensity. First, we tabulated each of our fishnets using the ‘Tabulate Area’ tool to assign zones for our NLCD land cover raster pixels according to the size of the fishnet grid cells. We opened the tool and started with our largest grid. For our input raster or feature zone data, we selected our 291,600 m² fishnet. For zone field we selected OID. Our input raster or feature class was set to the NLCD land cover raster. We set the class field to value and gave our output table a unique name. The processing cell size automatically set to the land cover raster after selecting it as our input, so we did not change the processing cell size. We then ran the tool. This tool gave us a standalone table, containing each land cover classification value in square meters per grid cell for our 291,600 m² fishnet.

Again, our land cover classifications of interest were: Developed, Open Space; Developed, Low Intensity; Developed, Medium Intensity; Developed, High Intensity. We repeated this process once more for our remaining 32,400 m² fishnet size. The only thing that changed when we repeated this process was our feature zone data, which was changed to the 32,400 m² fishnet. When we ran the tool again, we were given a new unique table containing each land cover classification value in square meters per grid cell for our 32,400 m² fishnet.

The next step in our process was to join our fishnet grids to their tabulation table, starting with our 291,600 m² fishnet. We selected our fishnet layer in the contents pane and navigated to the 'Add Join' tool. For our input table, we selected our 291,600 m² tabulation table. We set the input join field to OID and ensured that we kept all target features. We validated the join and then ran the tool. Now our 291,600 m² fishnet and tabulation are neatly placed into one table. We repeated this process for our 32,400 m² fishnet, joining each fishnet to their appropriate tabulation table.

Our final step for our land cover classification data was determining the percentage of developed impervious cover per fishnet grid cell for both grids. To do this, we needed to understand which numerical values for each pixel in our NLCD raster legend were indicative of developed imperviousness. According to the NLCD, Developed, Open Space was assigned a value of 21, Developed, Low Intensity was assigned a value of 22, Developed, Medium Intensity was assigned a value of 23, and Developed, High Intensity was assigned a value of 24 (Table 4) (Multi-Resolution Land Characteristics Consortium, n.d.).

Table 4. NLCD Land Cover Classification Numbers

Development Intensity	***NLCD Classification Number***
Developed, Open Space	21
Developed, Low Intensity	22
Developed. Medium Intensity	23
Developed, High Intensity	24

Once our tables were joined together, we were easily able to assess this relationship. Starting with our 291,600 m² fishnet, we opened the attribute table and added fields to our table by selecting the 'add fields' button within the attribute table. We added four new fields into the table, one for each level of developed imperviousness, and saved our changes to ensure these fields were added to the table. The first field that we assessed was the Developed, Open Space field. To calculate how much Developed, Open Space made up each 291,600 m² block, we needed to use the 'calculate field' function within the attribute table, which is accessed by right clicking on the desired field and selecting the 'calculate field' option. Using this tool, we calculated the percentage of Developed, Open Space by dividing the designated value 21 by the total area of the fishnet grid cell. This gave us the total percentage of the Developed, Open space. We did this for each impervious cover classification, ending with 4 different percentages, one for each impervious cover type for our 291,600 m² fishnet. We repeated this entire process for our 32,400 m² fishnet grids, also ending with 4 different impervious cover classification percentages for each fishnet grid cell. Once this process was completed for both fishnet grids, our attribute tables now displayed all our desired impervious cover percentages per fishnet block.

4.1.4 Calculating Tree Canopy Percentage

To estimate tree canopy cover across the city at two scales, the first thing that was done was estimate the total area of land per grid cell at both scales. This was done using a

land cover polygon shapefile that accounts for Travis County, as well as parts of Williamson County and Hays County. This shapefile includes land only, excluding water. We utilized this shapefile because, to calculate tree canopy cover for each grid, we must look only at pixels within each grid cell that are only made of land, as water cover is not capable of growing tree canopy, so we did not want water area measurements to skew or impact our calculations.

We then needed to calculate total land for each unit of analysis. To do this, we used the summarize within tool. We opened the tool and started with our largest grid. For our input polygons, we selected our 291,600 m^2 fishnet. For the input summary features, we selected the land shapefile. We opted to keep all input polygons. We set the shape unit to square meters, gave the output class a unique name, and then ran the tool. This tool generated a new layer that looked almost identical to the working fishnet layer. However, upon opening the table, one could see that this new layer contained total land in square meters per grid cell for our 291,600 m^2 fishnet. We repeated this process once more for our remaining 32,400 m^2 fishnet. The only thing that was changed when we repeated this process was the input polygons, which was changed to the 32,400 m^2 fishnet. When we ran the tool again, we were given another unique layer, of which the attribute table contained total land in square meters per grid cell for our 32,400 m^2 fishnet.

The next step was to calculate total canopy cover for each fishnet grid. We proceeded to add in our tree canopy cover data for the city of Austin, which was obtained from the City of Austin Open Data Portal. This polygon shapefile maps canopy cover across the city of Austin for the year 2022. This tree canopy layer was obtained using NAIP and Maxar aerial imagery, and had an accuracy assessment performed on it by the City of Austin and the

Texas A&M Forest Service to assure the quality of the data (City of Austin Development Services Department 2022). This process was very similar to determining total land cover for each fishnet grid cell. Starting with the 291,600 m², we once again opened the 'summarize within' tool. For the input polygons, we selected the newly generated 291,600 m² summarized layer for land. The input summary features were set to the canopy cover shapefile. All input polygons were kept, and we set the shape unit to square meters. We set a unique name for the output feature class and then ran the tool. Once again, a new layer was constructed. This time, upon investigation, the attribute table contained total canopy cover based on the land cover, as well as total land cover. We repeated this process once more for the 32,400 m², with the only change being the input polygon features, which were set to the newly generated 32,400 m² grid containing land cover for each grid cell. A new 32,400 m² layer was made, this time containing both total land and canopy cover.

The final step was to determine the percent canopy cover for each grid cell by manual calculation. We started with the 291,600 m² fishnet with both the land cover and tree canopy cover. We opened the attribute table, and added a new field into the table, which was named 'canopy cover'. We clicked the calculate field button, divided total tree canopy over total land, and then multiplied by 100. We verified the expression and then clicked 'ok'. When we calculated our new field, it filled with percent canopy cover for each fishnet grid block, all based on total land cover. We repeated this same process for the 32,400 m² fishnet with land cover and tree canopy cover, adding in a new field and calculating the field to illustrate percent canopy cover for each grid cell.

The last step for this process was to join these two new and updated fishnet layers. To do this, we used the Spatial Join tool. We navigated to the spatial join tool in the

geoprocessing pane and opened the tool. Starting with our 32,400 m² fishnet, we set the target feature class to the 32,400 m² fishnet. For the join feature class, we selected the newly generated layer containing both land cover and canopy cover. We set the spatial relationship to 'intersects' and gave the output feature class a unique name and then ran the tool. This tool joined our newly generated canopy cover layer to the 32,400 m² fishnet layer. Upon further investigation of the 32,400 m² layer's attribute table, it is shown that the canopy cover data is now joined to the layer based on geographic location, so we could now see the canopy cover percentage for each grid cell. We repeated this process once more for the 291,600 m², joining the new canopy cover to the fishnet layer. The only step in this process that changed was the target feature class setting, which was changed to the 291,600 m² fishnet. When the tool was ran once more, the canopy cover layer was now joined to the 291,600 m², allowing us to see the canopy cover percentage for each grid cell in that fishnet.

4.2 Multinomial Logistic Regression

To examine the relationship between tree removals, changes in LST, and various urban environmental characteristics, we employed a multinomial logistic regression model. The purpose of this model is to assess the significance of independent variables—tree removals, canopy cover, and impervious cover—in predicting the dependent variable, which, in this case, is the mean change in LST (Meyers et al. 2017). Before moving forward with our multinomial logistic regression, we explored the idea of an ordinal logistic regression. Although LST slope regimes are ordered categorical outcomes, modeling using ordinal logistic regression revealed inconsistencies that suggested a violation of the proportional odds assumption. More specifically, the ordinal model assumes that the effect of each predictor is constant across the cumulative thresholds of the dependent variable (e.g., from

Low to Moderate, Moderate to High, and so on). In practice, however, we observed that the effects of tree removals and their interaction with canopy cover varied by slope regime. In some cases, predictors showed no significant relationship or even an inverse relationship depending on the regime, suggesting that a single pooled estimate was not appropriate to capture these dynamics. As a result, we selected multinomial logistic regression as our primary model. This approach allows for category-specific estimates and does not impose an ordering constraint, making it better suited to exploring the nuanced and potentially nonlinear relationships between the urban forest and LST change. While ordinal regression was tested, its results were not consistent with the complexity of the data and are therefore not reported here. We ran our multinomial logistic regression using the Statsmodels python program (Seabold & Perktold 2010). The assumptions of a logistic regression are as follows: there must be an absence of perfect multicollinearity, there must be no specification errors, each independent variable is at ratio or interval level, there must be independence of errors, the independent variables must be linearly related to the log odds, and the dependent variable must be binary.

4.2.1 Heat Regimes

To continue designing our multinomial logistic regression model, we needed to change our independent or output variable (LST slope) into multiple categorical outputs. In the multinomial logistic regression, the outcome variable must have three or more categories (Meyers et al. 2017). Following this requirement, we categorized our mean LST slope values into heat regimes to represent difference levels of temperature change throughout the city of Austin (Table 5). These categories – Low, Moderate, High, and Very High – are based on the mean LST change natural break thresholds. The Low heat regime category is the reference

category for the analysis, which is a requirement for designing multinomial logistic regression (Meyers et al. 2017). These heat regime classifications are appropriate for the nature of our research, as temperature changes across the city are not equal and may be influenced by various factors (Unger, 2004). Allocating our LST change values into distinct categories allows us to better assess the degree of change in LST and its relationship with tree removals and canopy cover.

Table 5. Heat Regime Natural Breaks Thresholds

Heat Regime Designation	***Temperature break thresholds (C)***
Low (reference)	-0.3060 to 0.3384
Moderate	0.3384 to 0.4494
High	0.4494 to 0.5750
Very High	0.5750 to 1.6885

4.4 Addressing Multicollinearity

Before proceeding with the regression analysis, we needed to address the assumption of the absence of multicollinearity (Meyers et al. 2017). To do this, we needed to determine whether our data was normally distributed. The normality assumption is met when each variable's frequency creates an approximate bell-shaped curve. The most effective graphical approach to assessing data for normality is to use a normal probability plot, or a Normal Q-Q plot, where the values of a variable are plotted against the expected normal distribution (Meyers et al. 2017). We created a Q-Q plot for each variable we intended in incorporating into our analysis; mean LST slope (Fig. 4), minimum LST slope (Fig. 5), maximum LST slope (Fig. 6), canopy cover percentage (Fig. 7), open developed imperviousness (Fig. 8), low developed imperviousness (Fig. 9), medium developed imperviousness (Fig. 10), high developed imperviousness (Fig. 11), total removals (Fig. 12), development related removals (Fig. 13), non-development related removals (Fig. 14), healthy removals (Fig. 15), and unhealthy removals (Fig. 16).

Based on the Q-Q plots that were generated, the data appears to be not normal (Appendix H). Nevertheless, we ran an additional statistical normality test to verify that our data is not normally distributed. We ran a Kolmogorov-Smirnov normality test for our variables, an effective test to assess the normality of large data set (Table 6).

Table 6. Table depicting Kolmogorov-Smirnov normality test results for each variable. Asterisk indicates significance.

Variable	***Test statistic***	***P-value***	***Accept or Reject the Null Hypothesis***
Mean LST Slope	0.076	<0.001*	Reject; the data is not normally distributed
Minimum LST Slope	0.054	<0.001*	Reject; the data is not normally distributed
Maximum LST Slope	0.106	<0.001*	Reject; the data is not normally distributed
Canopy Cover	0.386	0.0*	Reject; the data is not normally distributed
Developed, open space	0.227	0.0*	Reject; the data is not normally distributed
Developed, low intensity	0.183	0.0*	Reject; the data is not normally distributed
Developed, medium intensity	0.159	0.0*	Reject; the data is not normally distributed
Developed, high intensity	0.291	0.0*	Reject; the data is not normally distributed
Total tree removals	0.405	0.0*	Reject; the data is not normally distributed
Development related removals	0.417	0.0*	Reject; the data is not normally distributed
Non-development related removals	0.392	0.0*	Reject; the data is not normally distributed
Healthy removals	0.416	0.0*	Reject; the data is not normally distributed
Unhealthy removals	0.396	0.0*	Reject; the data is not normally distributed

Once we had confidently determined that all of our variables were not normally distributed, we proceeded with a variance inflation factor (VIF). A VIF measures how much a predictor variable in a regression is inflated due to multicollinearity with other variables. In other words, a VIF tells one whether a variable a too related to other variables, which can influence regression results.

Table 7. Table depicting VIF for each variable of interest for the multinomial logistic regression.

	Feature	*VIF*
0	constant	13.85
1	imperv_open	1.160044
2	imperv_low	1.376454
3	imperv_med	1.241838
4	imperv_high	1.189591
5	canopy_cover	1.021585
6	removals_healthy	∞
7	removals_unhealthy	∞
8	removals_dev	∞
9	removals_nondev	∞
10	lst_slope_min	7.770123
11	lst_slope_max	8.854657
12	lst_slope_mean	22.480799

According to the VIF test (Table 7), developed open space (1.160044), developed low intensity (1.376454), developed medium intensity (1.241838), developed high intensity (1.189591) and canopy cover (1.021585) demonstrate low VIF values, indicating low multicollnearity between these predictors. Healthy removals, unhealthy removal, development removals and non-development removals show an infinite VIF, suggesting almost perfect collinearity. However, this was expected, as all of these tree removals are from the same dataset and would likely be highly correlated to one another. To address this, we decided to not analyze these different categories of tree removals in the same regression, but rather create separate regression models for each of the tree removal categories of interest. Minimum LST slope (7.770123), maximum LST slope (8.854657) and mean LST slope mean (22.480799) all show high VIF values, indicating high levels of multicollinearity. Once again, this is expected, as these measurements contain much of the same information. To create our regression, we will focus solely on mean LST slope values for analysis.

Next, for visual representation, we moved forward with generating a Spearman's rho correlation matrix for the variables of interest for our research (Figure 4). This correlation matrix is appropriate to use for our data because it does not assume normal distribution, as it is a non-parametric test (Meyers et al. 2017). Our correlation matrix revealed that several variables were highly correlated with one another, potentially affecting regression results. Specifically, each impervious cover category showed significant correlations with each of our tree removal variables, and as expected, all the tree removal categories are highly correlated with one another, and all the LST categories are highly correlated with one another as well. Since the impervious cover categories were so highly correlated with our tree removal categories, we decided to exclude impervious cover values from our regression analysis to prevent our results from being skewed. Additionally, we opted to only include two categories of tree removals; total removals and development related removals, because we are most interested in the cumulative impact of total tree removals and the specific impact of development removals on LST.

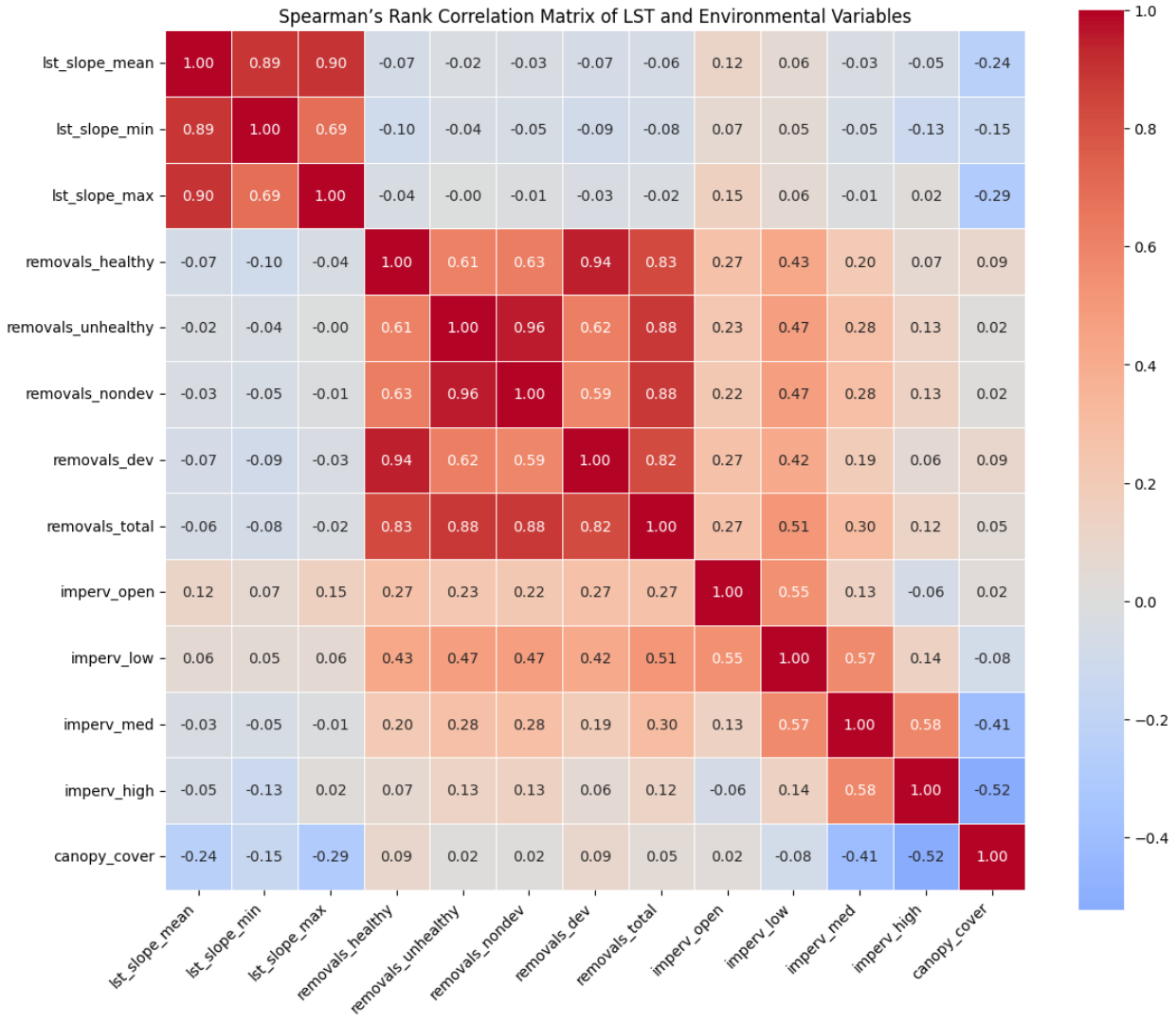

Figure 4. Spearman's rho correlation matrix for variables of interest.

4.2.2 Refining the model

To perform an accurate analysis on the effects of tree removals on LST, we only examined grids that contained permitted tree removals. There are a substantial amount of grid blocks in both the small grid and the large grid that do not have any recorded tree removals. Including these grid blocks in the analysis would likely influence our results by analyzing temperature changes with no removals. While changes in temperature variations in these grid blocks can still be assessed against other urban environment factors, such as impervious

cover or canopy cover, we excluded these grids blocks from the analysis, as we are most interested in how the removal of trees impacts LST.

Additionally, we needed to ensure that our model examined only grid blocks that contained less than 100% canopy cover. After calculating the percent canopy cover per grid block at each scale, we identified a small number of outliers for canopy cover for both grid sizes. The outliers were over 100% canopy cover, which is not a possible number. These outliers likely occurred due to small differences between the Austin City limits shape file and the canopy cover shape file in ArcGIS Pro. Removing these outliers before we proceeded with analysis ensured that our results are more representative of the true relationship between canopy cover, LST, and tree removals.

4.3 LST Slope Categories

While using the mean LST change values from each grid block is an efficient and effective way to assess the change in temperature over time, relying solely on average change in temperature does not provide the depth needed to fully understand urban forest temperature dynamics (Chang et al. 2021). Since each grid block also contains minimum and maximum LST change values, these were incorporated into part of our analysis. Examining both the minimum and the maximum temperature changes will allow us to explore relationships between canopy cover and LST in areas that are experiencing very high rates of temperature change opposed to areas that are seeing very low rates of temperature change. This approach will show whether tree removals and canopy cover have the same effect on LST in areas with vastly difference temperature changes.

To examine these two additional LST slope categories and their relationships with canopy cover and tree removals, we used simple summary statistics. First, we examined the

correlations between canopy cover, tree removals, and average LST change through a Spearman's rho correlation. Mean, minimum, and maximum LST categories were assessed against canopy cover and both total and development removals with their own mean temperature change at both the large and the small grid size. Next, we examined summary statistics at each slope regime for each LST category while considering each tree removal type at both scales. This assessment summarized the mean LST slope, mean canopy cover, and mean tree removals for each LST slope regime. For the minimum and maximum LST slope categories, the slope regimes are based on the Jenks natural breaks thresholds established for the mean LST slope category. Conducting this Spearman's rho correlation and summary statistic examinations provided further insight into the relationship dynamics between tree removals, canopy cover, and the variety of temperature changes occurring throughout the city of Austin.

5. Results

5.1 Tree Removal Comparisons

This section presents descriptive statistics through side-by-side bar charts to provide an overview of tree removals across the study area from 2013 through 2023. These visualizations compare removal counts based on key attributes such as health status, location, and removal justification, offering insight into categorical trends.

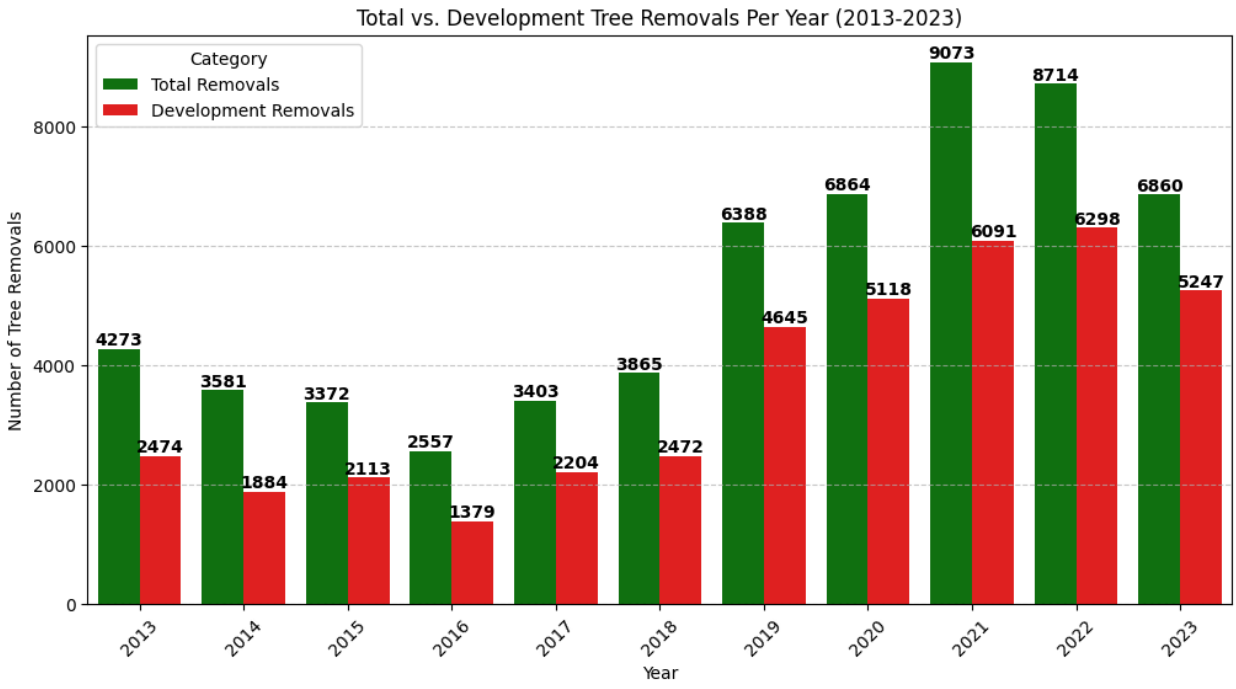

Figure 5. A side-by-side bar chart depicting total tree removals against development related tree removals from 2013 through 2023.

A large portion of total tree removals that took place from 2013 through 2023 were related to development (Figure 18). In 2021, the city permitted the highest total removals, at

9,073 removals, where 6,091 of which were related to development. In 2015, the city approve the lowest count of total removals at 2,557, of which 1,379 were development related. In 2022, the city approved the most development related tree removals, which accounted for 6,298 out of 8,714. The year 2023 had the highest percentage of development related removals, with 5,247 development removals accounting for approximately 76.5% of total removals for that year (6,860).

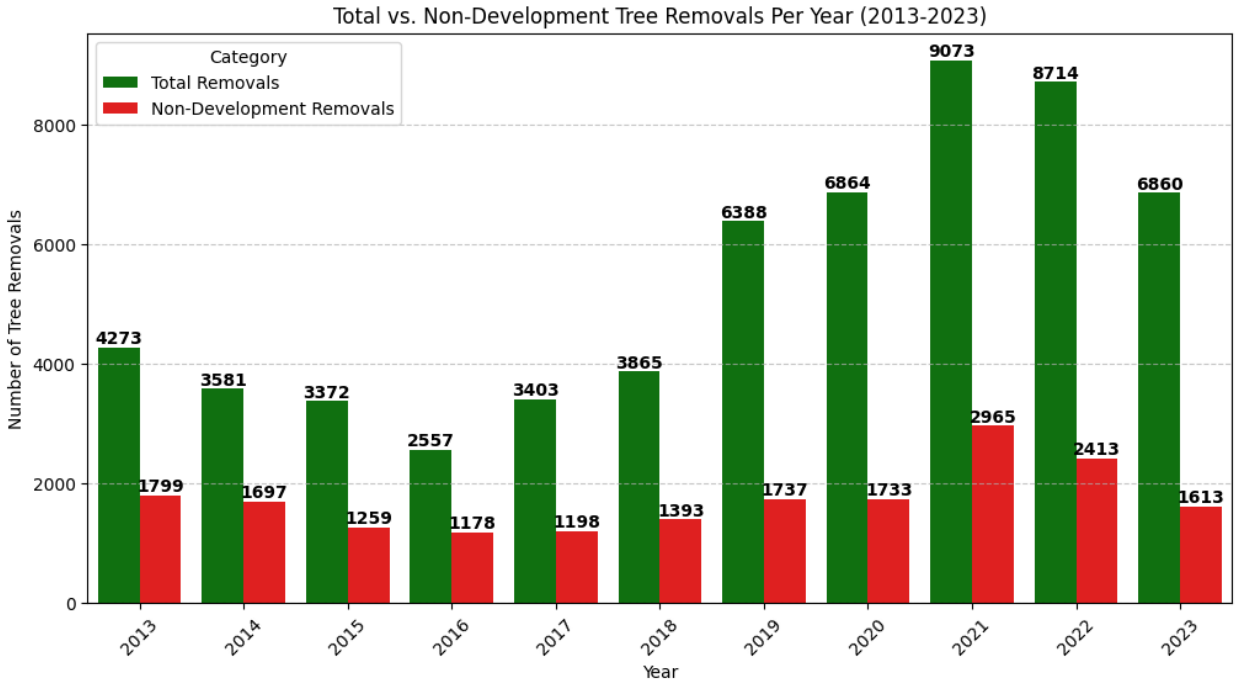

Figure 6. A side-by-side bar chart depicting total tree removals against non-development related tree removals from 2013 through 2023.

In 2021, as previously mentioned, the city approved the highest total removals, at 9,073 removals, of which 2,965 were non-development related (Figure 19). In 2015, the city permitted the lowest count of total removals at 2,557, of which 1,178 were non-development related. In 2021, the city apporved the most non-development related tree removals, which

accounted for 2,965 out of 9,073 removals. The year 2015 had the highest percentage of non-development related removals, with 1,697 non-development removals accounting for approximately 47.3% of total removals for that year (3,581).

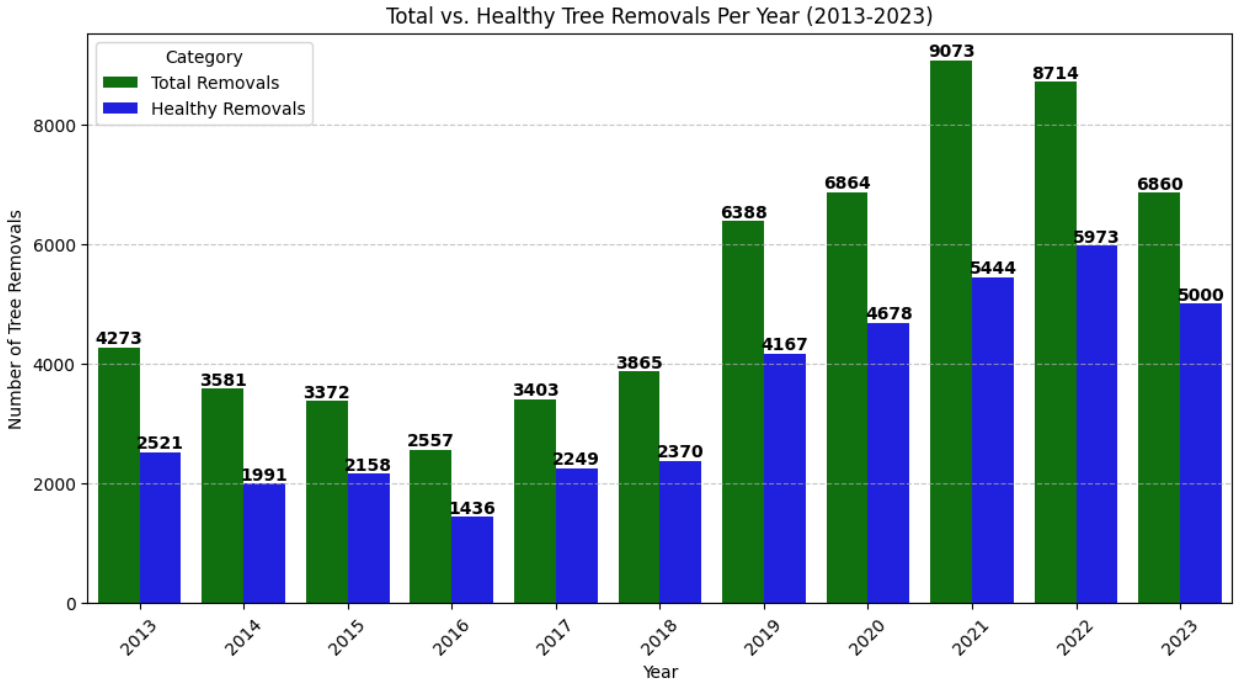

Figure 7. A side-by-side bar chart depicting total tree removals against healthy tree removals from 2013 through 2023.

In 2021, as previously mentioned, the city permitted the highest total removals, at 9,073 removals, of which 5,973 were healthy removals (Figure 20). In 2015, the city approved the lowest count of total removals at 2,557, of which 1,436 were healthy. In 2022, the city permitted the highest number of healthy tree removals, which accounted for 5,973 out of 8,714 removals. The year 2023 had the highest percentage of healthy tree removals, with 5,000 healthy removals accounting for approximately 72.9% of total removals for that year (6,860).

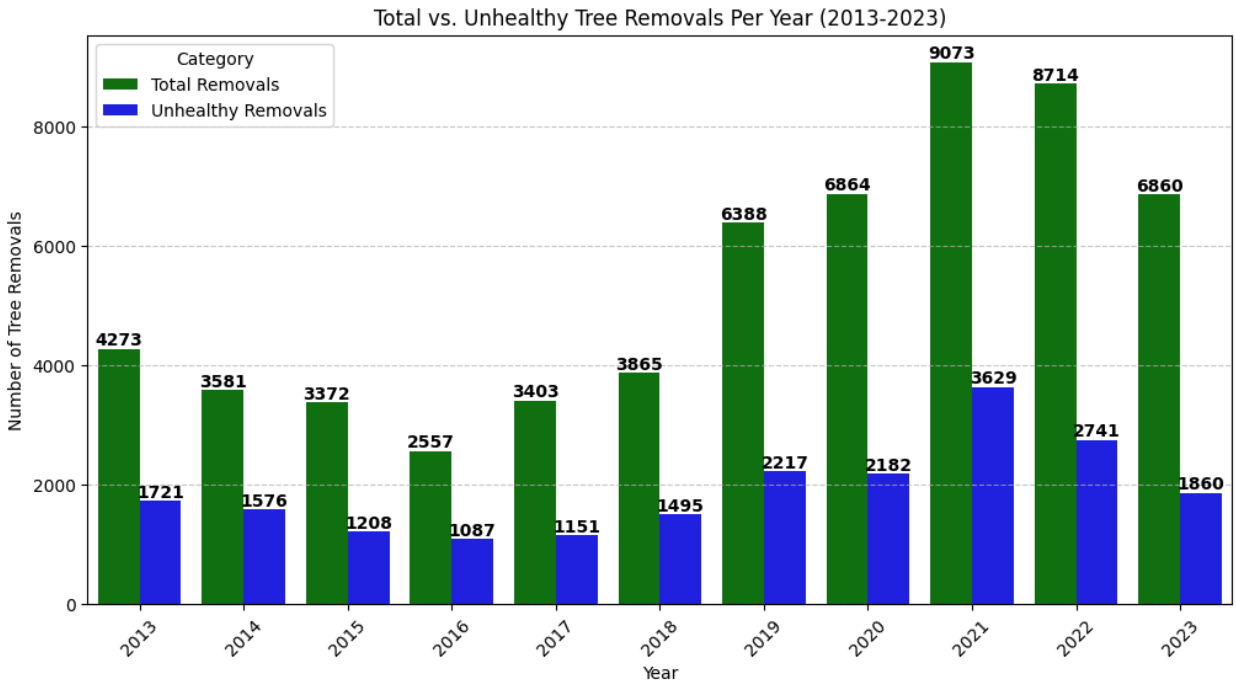

Figure 8. A side-by-side bar chart depicting total tree removals against unhealthy tree removals from 2013 through 2023.

In 2021, as previously mentioned, the city approved the highest total removals, at 9,073 removals, of which 3,629 were unhealthy removals (Figure 21). In 2015, the city permitted the lowest count of total removals at 2,557, of which 1,087 were unhealthy. In 2021, the city approved the highest number ofunhealthy tree removals, which accounted for 3,629 out of 9,073 removals. The year 2014 had the highest percentage of unhealthy tree removals, with 1,576 unhealthy removals accounting for approximately 44% of total removals for that year (3,581).

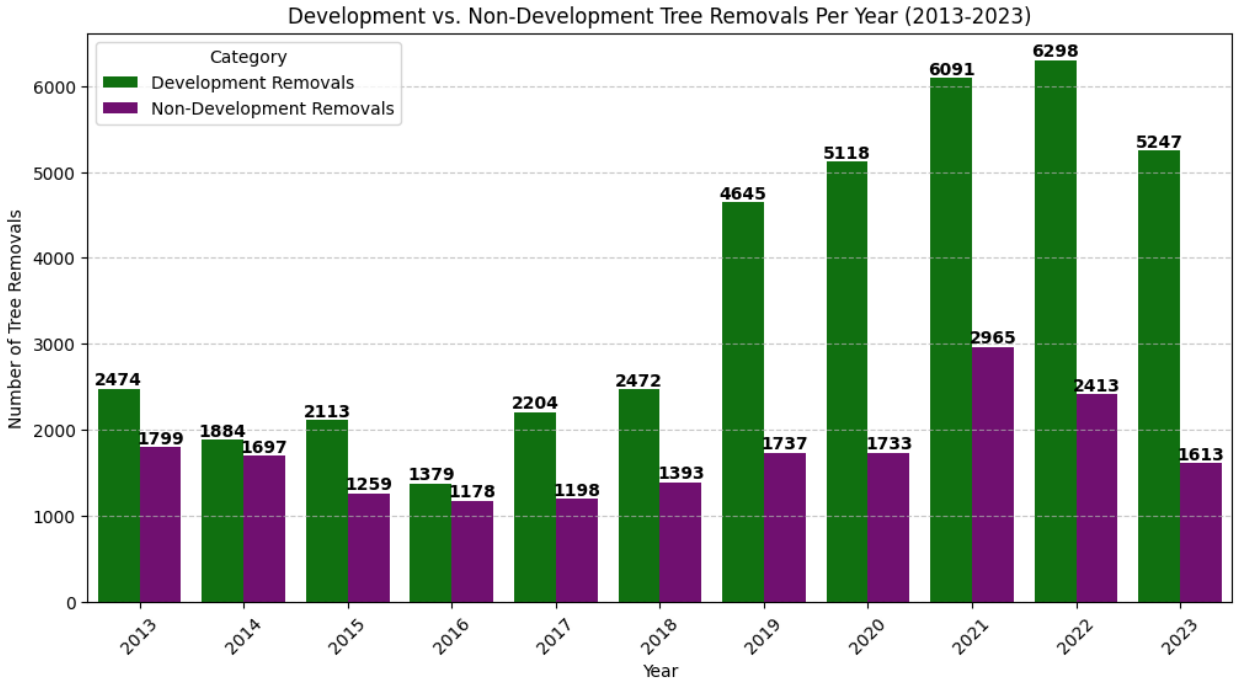

Figure 9. A side-by-side bar chart depicting development tree removals against non-development tree removals from 2013 through 2023.

In 2022, the city permitted the highest number of development removals, at 6,298 removals (Figure 22). In 2023, the city approved the highest number of non-development removals at 2,965 removals. The year 2016 had the most similar values between development and non-development removals, with 1,379 development related removals and 1,178 non development related removals.

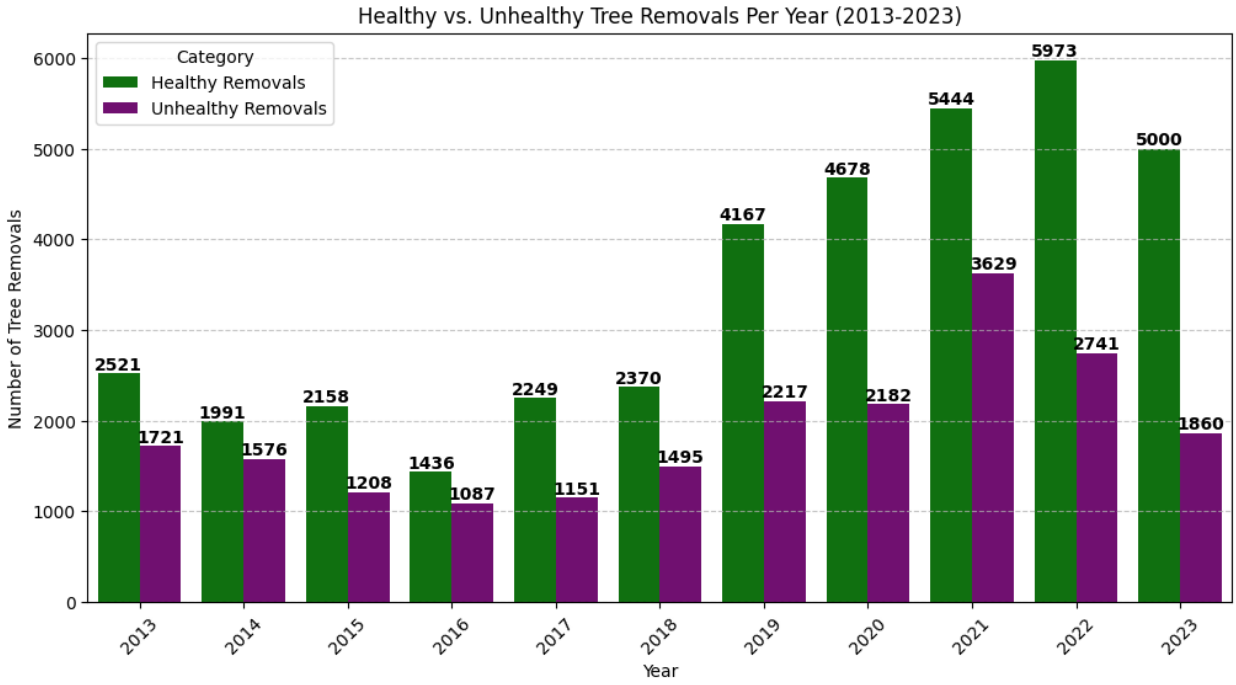

Figure 10. A side-by-side bar chart depicting healthy tree removals against unhealthy tree removals from 2013 through 2023.

In 2022, the city permitted the highest number of healthy removals, at 5,973 removals. In 2021, the city approved the highest number of unhealthy removals at 3,629 removals. The year 2016 had the most similar values between healthy and unhealthy removals, with 1,436 healthy removals and 1,087 unhealthy removals.

5.2 Heat Regime Maps

This section presents maps of heat regimes derived from the LST slope categories. These maps highlight spatial patterns of temperature change over time and identify areas experiencing different levels of LST change. The maps also provide insight into localized heat dynamics and potential environmental impacts by visualizing the heat regime distributions.

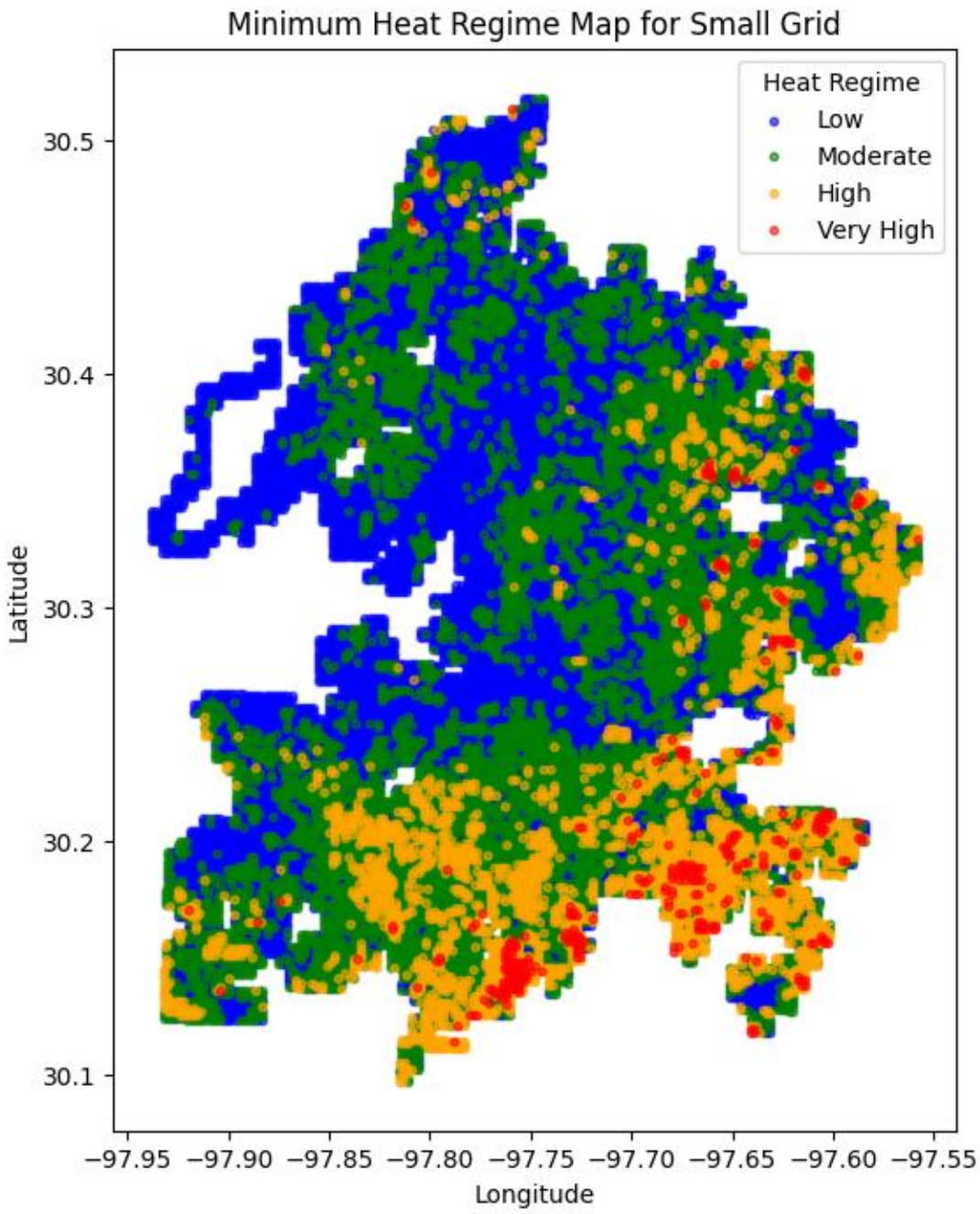

Figure 11. Heat regime distribution for the small scale throughout the city of Austin based on the minimum LST category.

The minimum LST heat regime map for the small grid shows areas in the northern and central regions primarily exhibiting low (blue) and moderate (green) heat regimes (Fig.

24). In contrast, the southern and southeastern portions of the city contain a greater concentration of high (orange) and very high (red) heat regimes, indicating high rates of LST change.

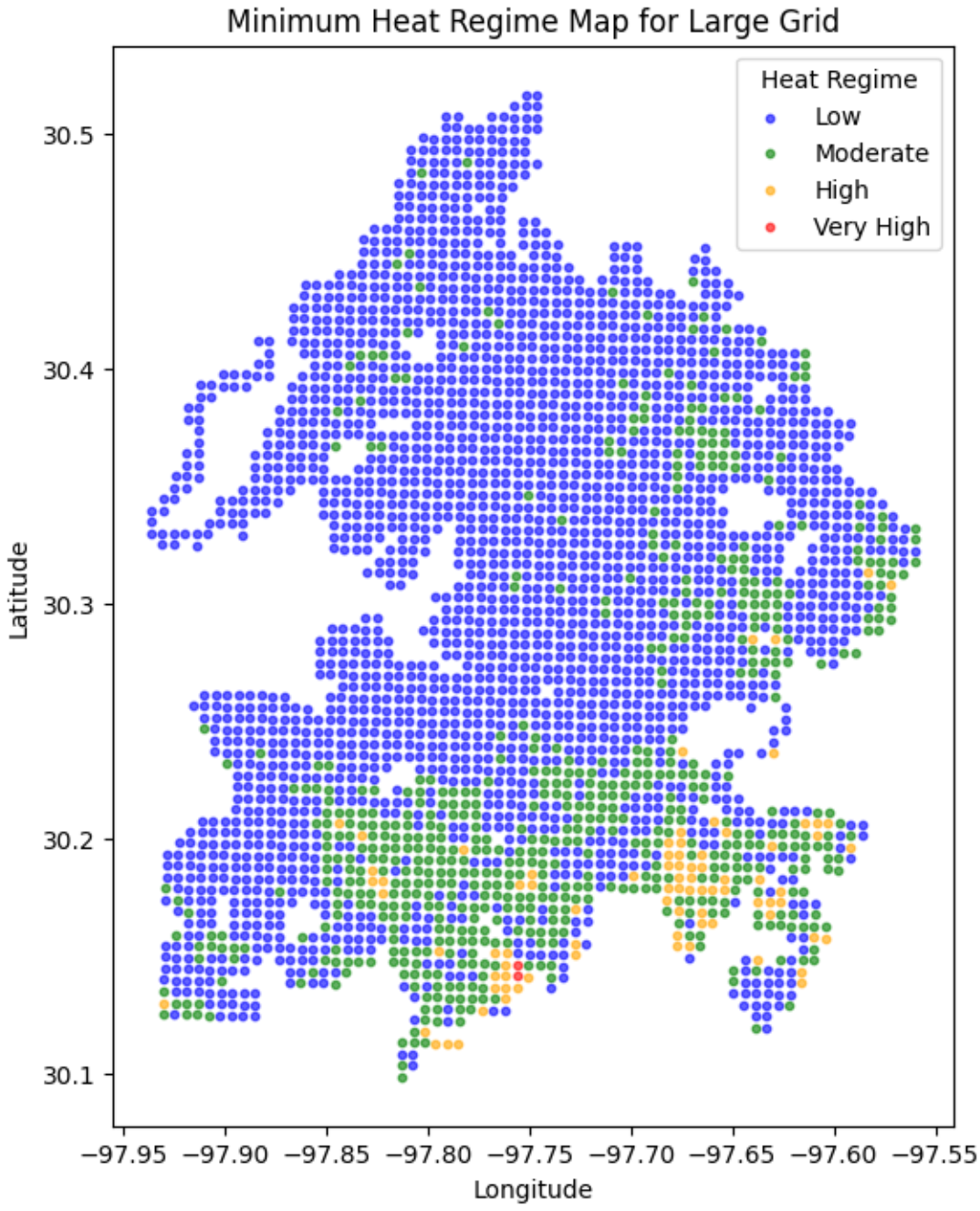

Figure 12. Heat regime distribution for the large scale throughout the city of Austin based on the minimum LST category.

Compared to the small-scale map, the larger grid for the minimum LST heat regimes aggregates temperature variations, showing a more uniform representation of low (blue) and moderate (green) heat regimes across the city (Fig. 26). However, instances of high (orange) and very high (red) heat regimes are still concentrated in the southern and southeastern regions, though their presence is less prominent.

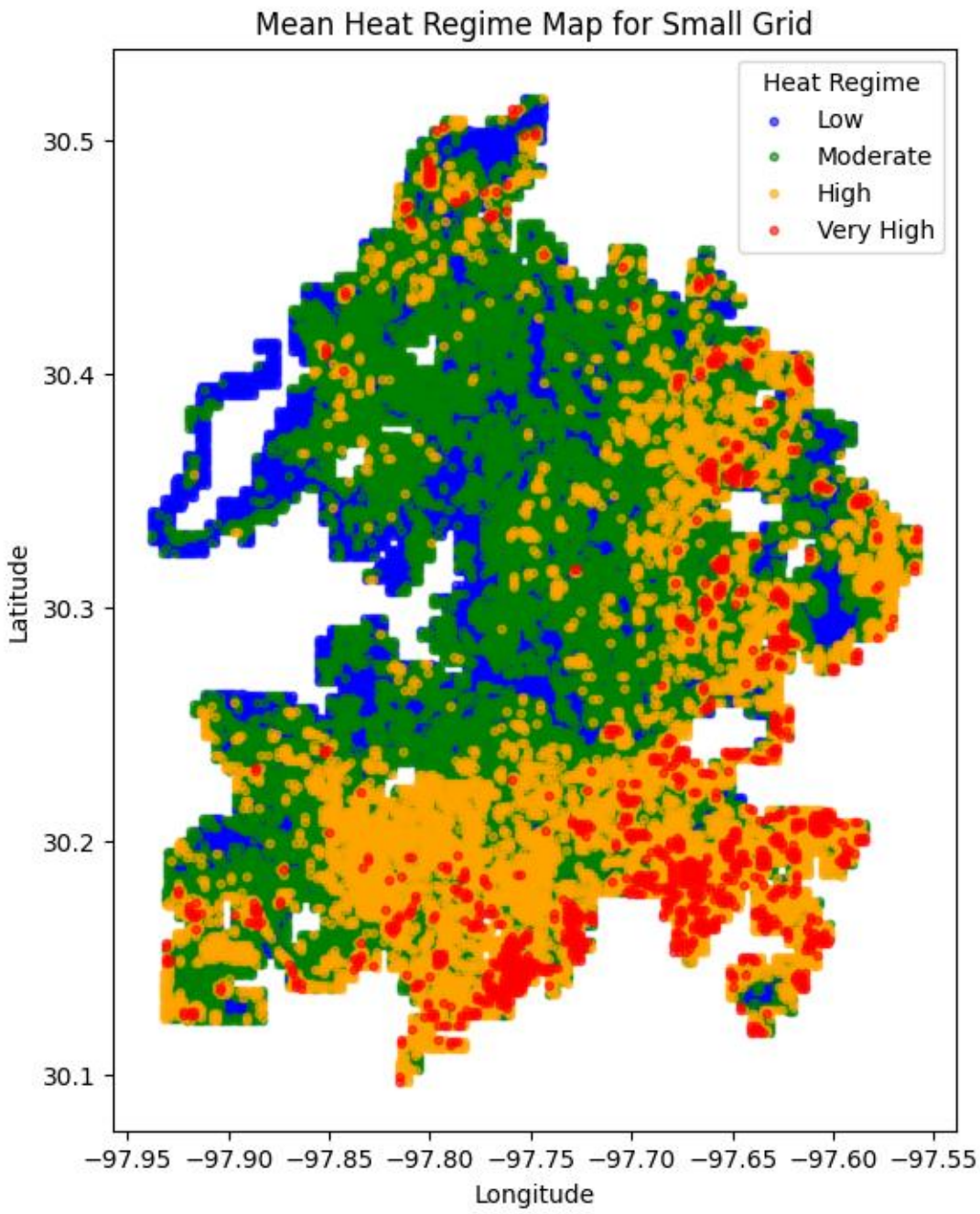

Figure 13. Heat regime distribution for the small scale throughout the city of Austin based on the mean LST category.

The mean LST heat regime map for the small grid shows areas in the northern and central regions primarily exhibiting low (blue) and moderate (green) heat regimes, but there

are several instance of high (orange) and very high (red) heat regimes in these areas as well, showing higher rates of change than at the minimum LST regimes (Fig. 27). The southern and southeastern portions of the city still show a greater concentration of high (orange) and very high (red) heat regimes, indicating high rates of LST change in these areas.

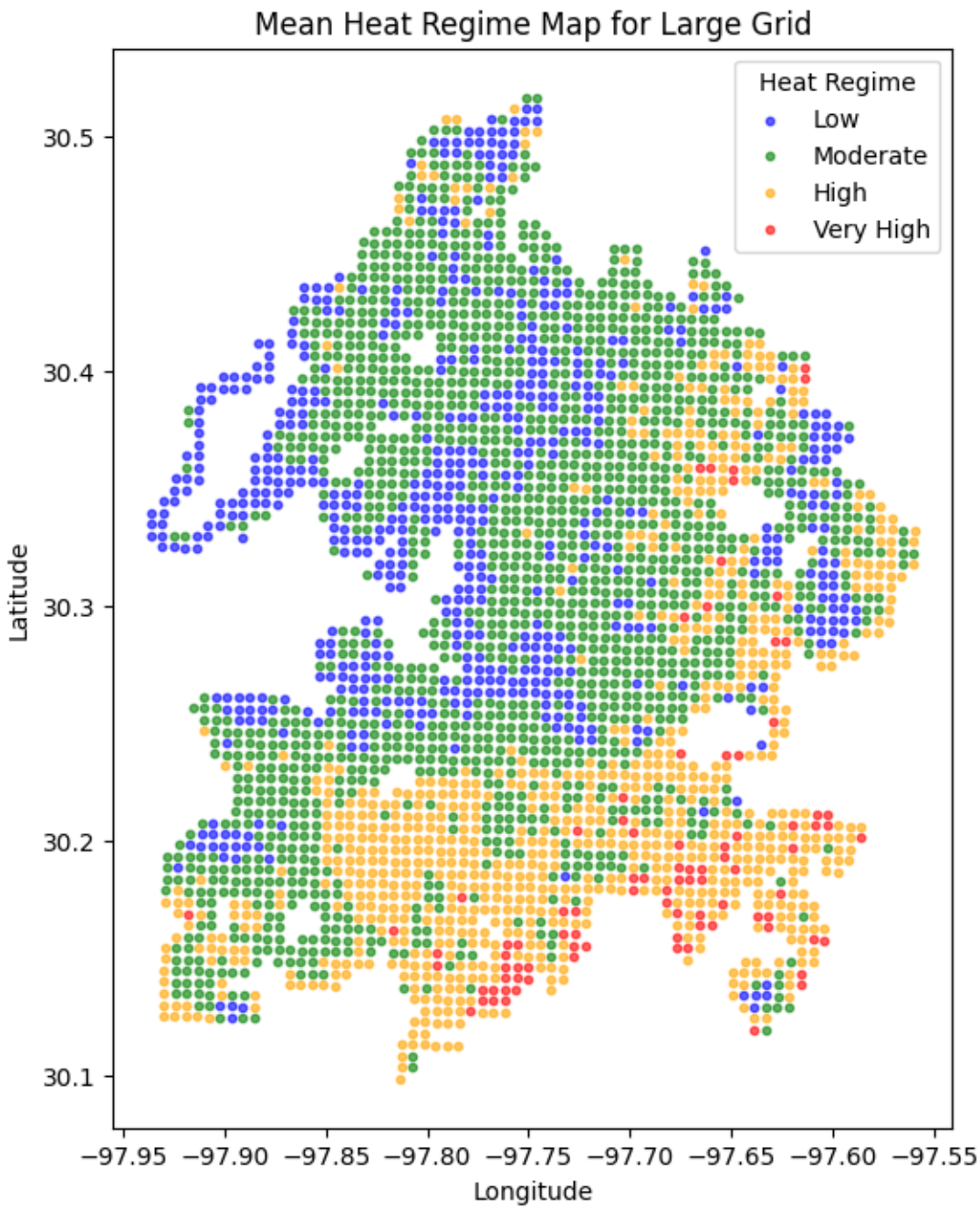

Figure 14. Heat regime distribution for the large scale throughout the city of Austin based on the mean LST category.

In comparison to the small-scale map, the larger grid for the mean LST heat regimes aggregates temperature changes, showing a more uniform representation of low

(blue) and moderate (green) heat regimes in the northwestern and west central areas of the city (Fig. 28). However, instances of high (orange) and very high (red) heat regimes are still appearing in the central and east central portion of the city, though not as concentrated as in the southern and southeastern regions.

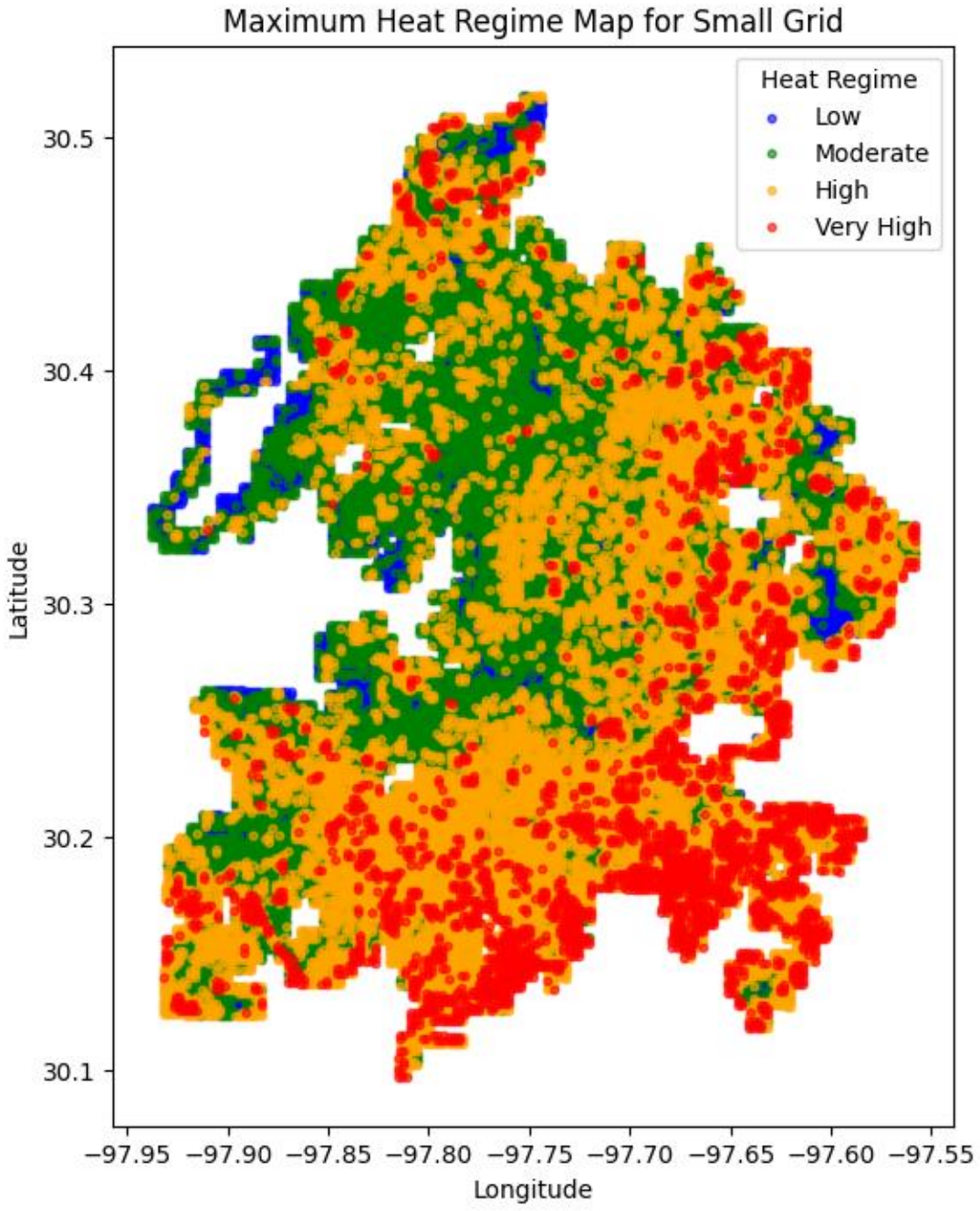

Figure 15. Heat regime distribution for the small scale throughout the city of Austin based on the maximum LST category.

The maximum LST heat regime map for the small grid shows areas in the northern and central regions exhibiting a true mixture of low (blue) moderate (green), high (orange) and very high (red) heat regimes (Fig. 29). The southern and southeastern portions of the city still exhibit a greater concentration of high (orange) and very high (red) heat regimes, indicating high rates of LST change in these areas.

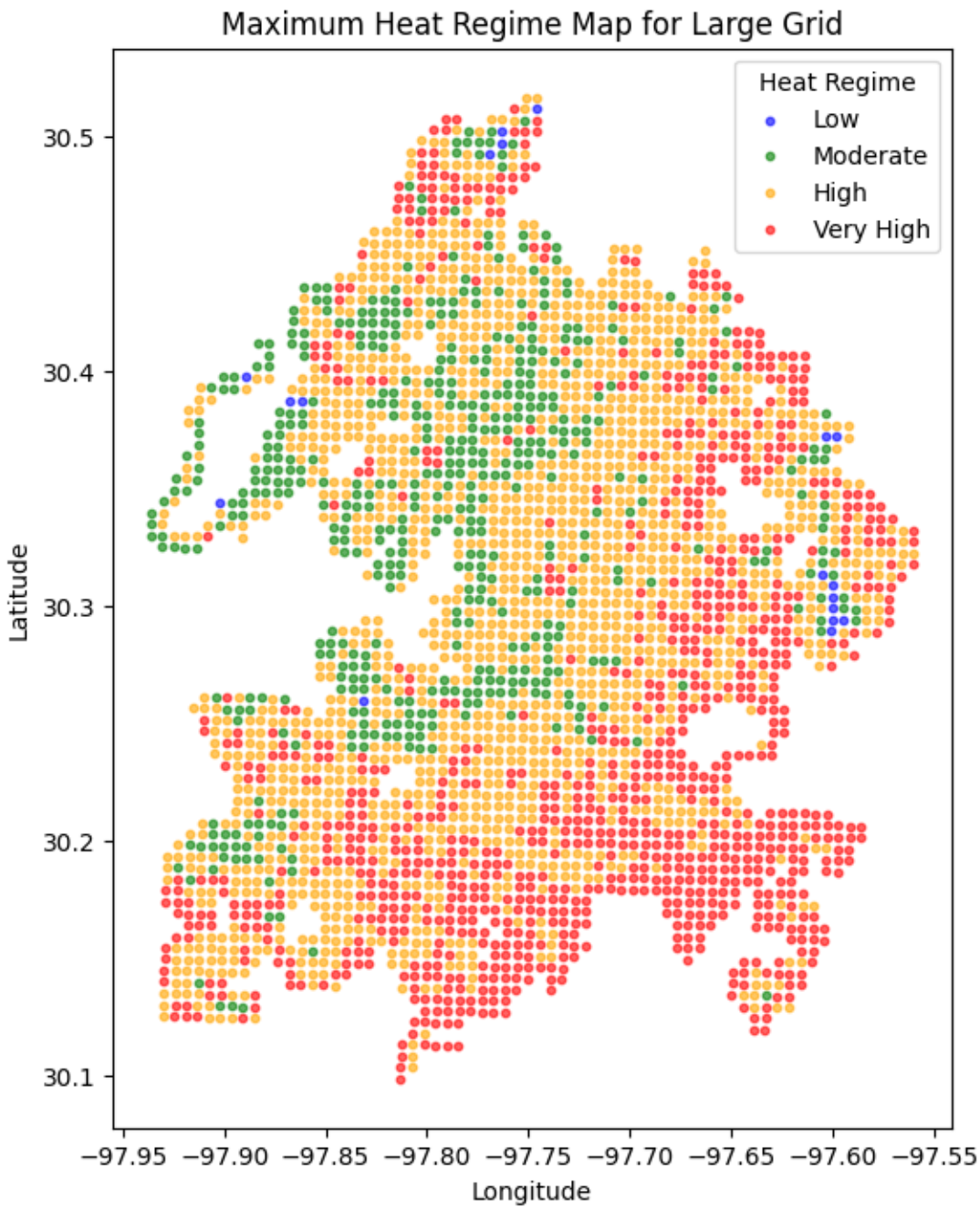

Figure 16. Heat regime distribution for the large scale throughout the city of Austin based on the maximum LST category.

In comparison to the small-scale map, the larger grid for the maximum LST heat regimes generalized the changes in temperature, showing a more uniform representation of

high (orange) and very high (red) heat regimes across the entire city (Fig. 30). However, instances of low (blue) and moderate (green) heat regimes are still appearing in the northwestern, central, southwestern portion of the city, though they are not as prominently seen as in the other LST heat regime.

5.3 Canopy Cover Correlations

This section details the Spearman's rho correlations for canopy cover and total removals to illustrate the relationships between total and development tree removals and levels of canopy cover for each LST heat regime.

Table 8. Canopy cover relationships with mean LST slope and total tree removals for the small and large scale.

		Small Grid	
Canopy Level	***N***	***Mean LST Slope***	***Correlation with Total Removals***
Low (<25%)	2532	0.4467	-0.0723
Medium (25-54%)	2532	0.4553	-0.0495
High (>54%)	2532	0.4209	0.0294
		Large Grid	
Canopy Level	***N***	***Mean LST Slope***	***Correlation with Total Removals***
Low (<25%)	607	0.4532	-0.1575
Medium (25-54%)	607	0.4556	-0.0581
High (>54%)	607	0.4051	0.0328

At the small scale, areas with low canopy cover showed the highest mean LST slope (0.4467), followed by medium canopy cover (0.4553), and high canopy cover (0.4209; Table 8). The correlation values show a weak negative relationship between total tree removals and LST slope in low (-0.0723) and medium (-0.0495) canopy areas, while a weak positive correlation (0.0294) was observed in areas with high canopy. At the large scale, low canopy

cover areas experienced the highest mean LST slope (0.4532), followed by medium canopy areas (0.4556), and high canopy areas (0.4051). Correlations at the large scale were stronger in low-canopy areas (-0.1575), showing a greater negative association between removals and LST slope. Medium-canopy areas showed a weaker negative correlation (-0.0581). In high-canopy areas, the correlation was weakly positive (0.0328).

Table 9: Canopy cover relationships with mean LST slope and total tree removals for the small and large scale.

		Small Grid	
Canopy Level	***N***	***Mean LST Slope***	***Correlation with Development Removals***
Low (<25%)	1565	0.4427	-0.0173
Medium (25-54%)	1565	0.4413	0.0162
High (>54%)	1565	0.4141	0.0616
		Large Grid	
Canopy Level	***N***	***Mean LST Slope***	***Correlation with Development Removals***
Low (<25%)	464	0.4599	-0.0876
Medium (25-54%)	464	0.4463	-0.1143
High (>54%)	465	0.3951	0.0452

At the small scale, areas with low canopy cover showed the highest mean LST slope (0.4427), followed closely by medium canopy cover (0.4413), and then high canopy cover (0.4141). The correlation values show a weak negative relationship between development tree removals and LST slope in low canopy areas (-0.0173). Medium (0.0162) and high (0.0616) canopy areas show a weak positive correlation with development related tree removals. At the large scale, low canopy cover areas experienced the highest mean LST slope (0.4599), followed by medium canopy level (0.4463), and high canopy level (0.3951). Correlations at the large scale were strongest in the medium-canopy areas (-0.1143), showing

a greater negative association between removals and LST slope. Low-canopy areas showed a weaker negative correlation (-0.0876). In high-canopy areas, the correlation was weakly positive (0.0452).

Table 10. Canopy cover relationships with minimum LST slope and total removals for the small and large scale

		Small Grid	
Canopy Level	***N***	***Mean LST Slope***	***Correlation with Total Removals***
Low (<25%)	2532	0.3549	-0.0754
Medium (25-54%)	2531	0.3783	-0.0555
High (>54%)	2532	0.3416	0.0283
		Large Grid	
Canopy Level	***N***	***Mean LST Slope***	***Correlation with Total Removals***
Low (<25%)	607	0.2410	-0.0702
Medium (25-54%)	607	0.2769	0.0235
High (>54%)	607	0.2426	0.0314

At the small scale, areas with medium canopy cover showed the highest mean LST slope (0.3783), followed low canopy cover (0.3549), and then high canopy cover (0.3416; Table 10). The correlation values show a weak negative relationship between total tree removals and LST slope in low canopy areas (-0.0754) and medium canopy areas (-0.0555). High canopy areas (0.0283) show a weak positive correlation with development related tree removals. At the large scale, medium canopy cover areas showed the highest mean LST slope (0.2769), followed by high canopy level (0.2426), and low canopy level (0.2410). Correlations at the large scale were strongest in the low-canopy areas (-0.0702). This correlation shows a negative association between total removals and LST slope. High-canopy areas showed a weaker positive correlation (0.0314), followed by medium canopy areas (0.0235).

Table 11. Canopy cover relationships with minimum LST slope and development removals for the small and large scale

Canopy Level	*N*	*Small Grid* *Mean LST Slope*	*Correlation with Development Removals*
Low (<25%)	1565	0.3496	-0.0194
Medium (25-54%)	1565	0.3633	0.0089
High (>54%)	1565	0.3335	0.0707
Canopy Level	*N*	*Large Grid* *Mean LST Slope*	*Correlation with Development Removals*
Low (<25%)	464	0.2397	-0.0656
Medium (25-54%)	464	0.2867	-0.0010
High (>54%)	465	0.2298	0.0332

At the small scale, areas with medium canopy cover showed the highest mean LST slope (0.3633), followed low canopy cover (0.3496), and then high canopy cover (0.3335; Table 11). The correlation values indicate a weak negative relationship between development tree removals and LST slope in low canopy areas (-0.0194). High canopy areas (0.0707) and medium canopy areas (0.0089) show weak positive correlations between the mean LST slope and development tree removals. At the large scale, medium canopy cover areas experienced the highest mean LST slope (0.2867), followed by low canopy level (0.2397), and high canopy level (0.2298). Correlations at this scale were strongest in the high-canopy areas (0.0332). Low-canopy areas showed a weak negative correlation (-0.0656). In high-canopy areas, the correlation was weakly negative (-0.0010).

Table 12. Canopy cover relationships with maximum LST slope and total removals for the small and large scale

Small Grid			
Canopy Level	***N***	***Mean LST Slope***	***Correlation with Total Removals***
Low (<25%)	2532	0.5406	-0.054
Medium (25-54%)	2531	0.538	-0.0453
High (>54%)	2532	0.5074	0.0285
Large Grid			
Canopy Level	***N***	***Mean LST Slope***	***Correlation with Total Removals***
Low (<25%)	607	0.6741	-0.1622
Medium (25-54%)	607	0.693	-0.178
High (>54%)	607	0.5977	-0.0532

At the small scale, areas with low canopy cover had the highest mean LST slope (0.5406), followed by medium canopy cover (0.538), and then high canopy cover (0.5074; Table 12). The correlation values indicate a weak negative relationship between total tree removals and LST slope in low canopy areas (-0.054) and medium canopy areas (-0.0453). High canopy areas (0.0285) show a weak positive correlation between the mean LST slope and total tree removals. At the large scale, low medium cover areas experienced the highest mean LST slope (0.693), followed by the low canopy level (0.6741), and then the high canopy level (0.5977). Correlations between total tree removals and mean LST slope at the large scale were strongest in the medium-canopy areas (-0.178). Low-canopy areas also showed a strong negative correlation (-0.178). In high-canopy areas, the correlation was weakly negative (-0.0532).

Table 13. Canopy cover relationships with maximum LST slope and development removals for the small and large scale

Canopy Level	*N*	*Small Grid* *Mean LST Slope*	*Correlation with Development Removals*
Low (<25%)	1565	0.5385	0.0006
Medium (25-54%)	1565	0.5245	0.0096
High (>54%)	1565	0.5023	0.0521
Canopy Level	*N*	*Large Grid* *Mean LST Slope*	*Correlation with Development Removals*
Low (<25%)	464	0.6734	-0.1684
Medium (25-54%)	464	0.6759	-0.0976
High (>54%)	464	0.5824	-0.0234

At the small scale, areas with low canopy cover had the highest mean LST slope (0.5385), followed by medium canopy cover (0.5245), and then high canopy cover (0.5023; Table 13). All correlation values indicate a weak positive relationship between development tree removals and LST slope in low canopy areas (0.0006), medium canopy areas (0.0096), and high canopy areas (0.0521). At the large scale, medium canopy cover areas experienced the highest mean LST slope (0.6759), followed by the low canopy areas (0.6734), and then the high canopy areas (0.5824). Correlations between development tree removals and mean LST slope at the large scale strongest in the low-canopy areas (-0.1684). Medium-canopy areas (-0.0976) and high canopy areas (-0.0234) showed weaker negative correlations between development removals and mean LST slope.

5.4 Slope Regime Summary Statistics

This section details the summary statistics for each slope regime for each LST category, quantifying the mean total or development related removals, mean canopy, mean LST slope, and the proportion of grid cells that each regime corresponds to.

Table 14. Slope Regime summary statistics for the mean LST heat regime, total removals and canopy cover for the small and large scale

				Small Grid				
Slope Regime	***Mean Total Removal***	***Total Removals SD***	***Mean Canopy Cover***	***Canopy Cover SD***	***Mean LST Slope***	***LST Slope SD***	***Total Count***	***Regime Proportion***
Low	6.237907	8.76503	0.402157	0.236	0.2785	0.0679	1013	0.1334
Moderate	9.041392	11.17284	0.444765	0.193	0.3985	0.0306	3334	0.4389
High	8.456225	11.02595	0.408295	0.17	0.5003	0.0348	2490	0.3278
Very High	4.996042	7.454573	0.350319	0.166	0.65	0.1063	758	0.098
				Large Grid				
Slope Regime	***Mean Total Removal***	***Total Removals SD***	***Mean Canopy Cover***	***Canopy Cover SD***	***Mean LST Slope***	***LST Slope SD***	***Total Count***	***Regime Proportion***
Low	20.65086	27.079386	0.450866	0.21877	0.2809	0.0490	746	0.127403
Moderate	39.41689	61.917691	0.454407	0.2059	0.3907	0.0268	746	0.409665
High	36.74826	56.732331	0.389241	0.16625	0.4832	0.0304	576	0.31631
Very High	15.77154	25.427404	0.336113	0.14915	0.6089	0.0732	267	0.146623

For the small grid, areas classified as having a very high LST slope exhibit the highest mean LST slope (0.65) and the lowest mean canopy cover (0.350319; Table 14). These areas also have the lowest mean total removals (4.99) and account for 9.98% of the total grid cells. To contrast, areas with of moderate LST slope contain the largest proportion of grid cells (43.90%) and show a mean LST slope of 0.3985, with the highest mean total removals (9.04). At the large grid scale, a similar trend is seen, as areas classified under the very high LST slope regime have the highest mean LST slope (0.6089) and the lowest mean canopy cover (0.336). These areas also show the lowest mean total removals (15.77) and

make up14.66% of the total grid cells. The moderate LST slope category again makes up the largest proportion of grid cells (40.97%) and has the highest mean total removals (39.42).

Table 15. Slope Regime summary statistics for the mean LST heat regime, development removals, and canopy cover for the small and large scale.

Slope Regime	*Mean Development Removals*	*Development Removals SD*	*Mean Canopy Cover*	*Small Grid Canopy Cover SD*	*Mean LST Slope*	*LST Slope SD*	*Total Count*	*Regime Proportion*
Low	7.164151	9.077748	0.453033	0.220956	0.307386	0.065053	1060	0.225772
Moderate	9.975117	10.892895	0.468228	0.177272	0.427121	0.033932	2572	0.547817
High	7.948919	9.712451	0.406893	0.163712	0.555307	0.054315	1018	0.216826
Very High	4.711111	4.341252	0.272524	0.194179	0.930991	0.208371	45	0.009585
Slope Regime	*Mean Development Removals*	*Development Removals SD*	*Mean Canopy Cover*	*Large Grid Canopy Cover SD*	*Mean LST Slope*	*LST Slope SD*	*Total Count*	*Regime Proportion*
Low	18.528662	24.384095	0.474928	0.214916	0.270765	0.050284	157	0.112706
Moderate	33.939292	51.935378	0.474574	0.196024	0.388323	0.027442	593	0.4257
High	32.966887	50.382925	0.397046	0.156358	0.478082	0.02923	453	0.325197
Very High	12.810526	23.943847	0.360201	0.134581	0.604478	0.077734	190	0.136396

For the small grid, areas with a very high LST slope show the highest mean LST slope (0.93) and the lowest mean canopy cover (27.25%; Table 15). These areas also have the lowest mean total removals (4.34) and make up 9.96 % of the total grid cells. Areas of moderate LST slope contain the largest proportion of grid cells (54.7%) with the highest mean total removals (10.9). These areas also have the highest mean canopy cover (46.8%). At the large grid scale, a similar trend is seen, with areas under the very high LST slope regime having the highest mean LST slope (0.604) and the lowest mean canopy cover (13.5%). These areas also have the lowest mean total removals (23.94) and make up 13.64% of the total grid cells. The moderate LST slope category again makes up the largest proportion of grid cells (42.57%) and has the highest mean total removals (33.94). However, the low LST slope regime shows the highest canopy cover (47.49%), followed very closely by the moderate LST slope regime (47.45%).

Table 16. Slope Regime summary statistics for the minimum LST heat regime, total removals, and canopy cover for the small and large scale

Slope Regime	*Mean Total Removals*	*Total Removals SD*	*Mean Canopy Cover*	*Small Grid Canopy Cover SD*	*Mean LST Slope*	*LST Slope SD*	*Total Count*	*Regime Proportion*
Low	7.692937	9.984461	0.424853	0.215701	0.256675	0.082504	3058	0.402899
Moderate	9.519923	11.990122	0.429315	0.17652	0.38851	0.031384	3112	0.410013
High	5.925806	8.004598	0.383788	0.160187	0.497008	0.034499	1240	0.163373
Very High	4.372222	5.741188	0.336447	0.173342	0.625588	0.081318	180	0.023715
Slope Regime	*Mean Total Removals*	*Total Removals SD*	*Mean Canopy Cover*	*Large Grid Canopy Cover SD*	*Mean LST Slope*	*LST Slope SD*	*Total Count*	*Regime Proportion*
Low	34.171852	55.086065	0.427252	0.201746	0.208249	0.110806	1350	0.744622
Moderate	31.708763	52.242579	0.390650	0.161422	0.380833	0.030740	388	0.214010
High	14.486486	15.175000	0.365375	0.146567	0.484407	0.030187	74	0.040816
Very High	1.000000	NaN	0.001428	NaN	0.665953	NaN	1	0.000552

For the small grid, areas with a very high LST slope show the highest mean LST slope (0.626) and the lowest mean canopy cover (33.6%; Table 16). These areas also have the lowest mean total removals (5.74) and encompass 0.024% % of the total grid cells. Areas for the moderate LST slope contain the largest proportion of grid cells (41%) with the highest mean total removals (11.99). These areas also have the highest mean canopy cover (42%), followed by the low LST slope regime (42.4%). At the large grid scale, a similar trend is seen, with areas under the very high LST slope regime having the highest mean LST slope (0.6659). Low LST slope regime areas had the highest canopy cover (42.73%). These areas also have the highest mean total removals (34.17) and make up 74.46% of the total grid cells. The very high LST slope regime areas had insufficient data, as there was only one grid of very high temperature based on the minimum LST slope regime natural breaks.

Table 17. Slope Regime summary statistics for the minimum LST heat regime, development removals, and canopy cover for the small and large scale

Slope Regime	*Mean Total Removals*	*Total Removals SD*	*Mean Canopy Cover*	*Small Grid Canopy Cover SD*	*Mean LST Slope*	*LST Slope SD*	*Total Count*	*Regime Proportion*
Low	8.675686	10.191865	0.461898	0.199406	0.280542	0.084687	2661	0.567015
Moderate	9.688389	10.676526	0.444759	0.168461	0.415801	0.033022	1688	0.359685
High	6.191617	8.550457	0.387261	0.161814	0.543247	0.04306	334	0.07117
Very High	3.6	2.91357	0.116367	0.153256	0.857431	0.153722	10	0.002131
Slope Regime	*Mean Total Removals*	*Total Removals SD*	*Mean Canopy Cover*	*Large Grid Canopy Cover SD*	*Mean LST Slope*	*LST Slope SD*	*Total Count*	*Regime Proportion*
Low	31.322005	48.231170	0.443358	0.188921	0.224892	0.114541	1177	0.847983
Moderate	17.216495	36.134816	0.382317	0.142673	0.411876	0.032601	194	0.139769
High	9.529412	15.021308	0.400630	0.140202	0.521151	0.020036	17	0.012248
Very High	NaN	NaN	NaN	NaN	NaN	NaN	0	0.00

For the small grid, areas with a very high LST slope show the highest mean LST slope (0.154) and the lowest mean canopy cover (11.6%; Table 17). These areas also have the lowest mean development removals (2.9) and encompass 0.021% of the total grid cells. Areas for the low LST slope contain the largest proportion of grid cells (56.7%) with the highest mean development removals (10.68). These areas also have the highest mean canopy cover (46.2%), followed by the moderate LST slope regime (44.5%). At the large grid scale, there is insufficient data across all variables, as there were no grids of very high temperature based on the minimum LST slope regime natural breaks that had development related removals.

Table 18. Slope Regime summary statistics for total removals, maximum LST, and canopy cover for the small and large scale.

				Small Grid				
Slope Regime	***Mean Total Removals***	***Total Removals SD***	***Mean Canopy Cover***	***Canopy Cover SD***	***Mean LST Slope***	***LST Slope SD***	***Total Count***	***Regime Proportion***
Low	5.135678	6.749986	0.350025	0.230818	0.28678	0.050622	199	0.026212
Moderate	7.21546	9.579074	0.438106	0.210811	0.408982	0.028359	1643	0.216412
High	9.321507	11.542293	0.434252	0.183699	0.508372	0.034822	3636	0.478925
Very High	6.873226	9.651868	0.380143	0.17948	0.677656	0.12439	2114	0.278451
				Large Grid				
Slope Regime	***Mean Total Removals***	***Total Removals SD***	***Mean Canopy Cover***	***Canopy Cover SD***	***Mean LST Slope***	***LST Slope SD***	***Total Count***	***Regime Proportion***
Low	2	1.414214	0.529981	0.45311	0.308569	0.039893	2	0.0011
Moderate	19.766234	29.020817	0.493916	0.208749	0.418512	0.025778	77	0.042331
High	38.022581	55.125993	0.474403	0.200679	0.520563	0.032283	620	0.340847
Very High	30.772321	53.629242	0.378192	0.177584	0.744049	0.176324	1120	0.615723

For the small grid, areas with a very high LST slope show the highest mean LST slope (0.677) and the lowest mean canopy cover (38%). Areas with the low LST slope regime have the lowest mean total removals (6.7) and encompass 2.62% % of the total grid cells. Areas for the high LST slope contain the largest proportion of grid cells (47.89%) with the highest mean development removals (11.54). At the large grid scale, areas under the very high LST slope regime have the highest mean LST slope (0.744) and the lowest mean canopy cover (37.8%). These area also take up 61.57% of the grid cells. Areas in the high LST slope regime have the highest mean total removals (38.02). The low LST slope category has the highest canopy cover (53%).

Table 19. Slope Regime summary statistics for total removals, maximum LST, and canopy cover for the small and large scale.

Slope Regime	*Mean Development Removals*	*Development Removals SD*	*Mean Canopy Cover*	*Small Grid Canopy Cover SD*	*Mean LST Slope*	*LST Slope SD*	*Total Count*	*Regime Proportion*
Low	5.950673	10.139224	0.386753	0.226369	0.314423	0.052234	223	0.047528
Moderate	8.37208	9.371329	0.476058	0.19466	0.442297	0.032745	1841	0.39237
High	9.686802	10.989533	0.444571	0.17276	0.567527	0.059154	2417	0.515132
Very High	6.611374	8.612873	0.347772	0.190688	0.891987	0.179151	211	0.04497
Slope Regime	*Mean Development Removals*	*Development Removals SD*	*Mean Canopy Cover*	*Large Grid Canopy Cover SD*	*Mean LST Slope*	*LST Slope SD*	*Total Count*	*Regime Proportion*
Low	3.666667	2.804758	0.295374	0.138229	0.345104	0.032787	6	0.004313
Moderate	24.313725	37.249244	0.52058	0.203512	0.453804	0.029245	153	0.109993
High	33.609244	51.921467	0.442259	0.181419	0.595497	0.065758	952	0.6844
Very High	16.632143	25.936171	0.361062	0.156149	0.909754	0.191762	280	0.201294

For the small grid, areas with a very high LST slope show the highest mean LST slope (0.89) and the lowest mean canopy cover (34.8%; Table 19). Areas with the low LST slope regime have the lowest mean development removals (5.95) and encompass 4.7% of the total grid cells. Areas for the high LST slope contain the largest proportion of grid cells (51.51%) with the highest mean development removals (9.68). At the large grid scale, areas under the very high LST slope regime have the highest mean LST slope (0.910). The low LST regime exhibits the lowest mean canopy cover (29.54%), and the moderate regime shows the highest canopy cover (44.235%). Areas in the high LST slope regime have the highest mean total removals (33.6).

5.4 Multinomial Logistic Regression Results for Total Removals

The multinomial logistic regression assesses the relationship between total removals, canopy cover, an interaction term between canopy cover and removals, and each heat regime that we created for our analysis (moderate, high, and very high). The reference category is low.

Table 20. Multinomial Logistic Regression for the Mean LST Heat Regime and Total Removals. Reference category is the Low Heat Regime. Asterisk indicates significance at the 0.01 level and lower.

Heat Regime	*Variable*	*Coefficient (B)*	*Exp(B)*	*Small Grid Std. Err.*	*z*	*P>|z|*	*[0.025*	*0.975]*
Moderate	Constant	0.5992	1.8205	0.11	5.46	0	0.384	0.814
	Removals	0.0239	1.0242	0.014	1.683	0.092	-0.004	0.052
	Total Canopy Cover	0.9173	2.5020	0.242	3.793	0*	0.443	1.391
	Removals x Canopy	0.0074	1.0074	0.029	0.26	0.795	-0.049	0.063
High	Constant	0.7881	2.1993	0.112	7.062	0	0.569	1.007
	Removals	0.0151	1.0152	0.015	1.039	0.299	-0.013	0.043
	Total Canopy Cover	-0.17	0.8440	0.25	-0.679	0.497	-0.661	0.321
	Removals x Canopy	0.022	1.0222	0.029	0.751	0.452	-0.035	0.079
Very High	Constant	0.3351	1.3980	0.139	2.417	0.016	0.063	0.607
	Removals	-0.023	0.9773	0.021	-1.076	0.282	-0.065	0.019
	Total Canopy Cover	-1.3701	0.2542	0.33	-4.155	0*	-2.016	-0.724
	Removals x Canopy	0.0079	1.0079	0.045	0.174	0.862	-0.081	0.096
Pseudo r^2		0.01551						

				Large Grid				
Heat Regime	***Variable***	***Coefficient (B)***	***Exp (B)***	***Std. Err.***	***z***	***P>|z|***	***[0.025***	***0.975]***
Moderate	Constant	0.6122	1.8445	0.222	2.754	0.006	0.177	1.048
	Removals	0.0272	1.0276	0.008	3.438	0.001*	0.012	0.043
	Total Canopy Cover	0.6038	1.8295	0.441	1.368	0.171	-0.261	1.469
	Removals × Canopy	-0.0362	0.9644	0.015	-2.490	0.013	-0.065	-0.008
High	Constant	1.1343	3.1093	0.224	5.061	0.000	0.695	1.574
	Removals	0.0276	1.0280	0.008	3.434	0.001*	0.012	0.043
	Total Canopy Cover	-1.2161	0.2963	0.465	-2.616	0.009*	-2.127	-0.305
	Removals × Canopy	-0.0380	0.9627	0.015	-2.531	0.011	-0.067	-0.009
Very High	Constant	1.3666	3.9212	0.246	5.558	0.000	0.885	1.849
	Removals	-0.0031	0.9969	0.011	-0.292	0.770	-0.024	0.018
	Total Canopy Cover	-2.9913	0.0502	0.550	-5.434	0.000*	-4.070	-1.912
	Removals × Canopy	0.0003	1.0003	0.021	0.016	0.987	-0.041	0.041
Pseudo r^2		0.03746						

5.4.1 Total Removals

In the moderate heat regime, total removals have a small positive effect on LST (B = 0.0239, exp (B) = 1.0242, p = 0.092; Table 19) in the smaller grid but a statistically significant positive effect in the larger grid (B = 0.0272, exp (B) = 1.0276 p = 0.001; Table 19). In the high heat regime, total removals remain positive and significant for the large grid (B = 0.0276, exp (B) =1.0280 p = 0.001; Table 19) but not for the smaller grid (B = 0.7881, exp (B) =1.0152, p = 0.299; Table 19). In the very high heat regime, removals are not significant in the small grid (B = -0.023, exp (B) =0.9773, p = 0.282; Table 19) or the large grid (B = -0.0031, exp (B) = 0.9969, p = 0.770; Table 19) and show a negative relationship in both grids.

5.4.2 Canopy Cover

In the moderate heat regime, canopy cover is positive and significant in the smaller grid (B = 0.9173, exp (B) =2.5020, p < 0.001; Table 21) but is not significant in the larger grid (B =0.6038, exp (B) =1.8295, p = 0.171; Table 21). In the high heat regime, canopy cover has a negative and significant effect in the larger grid (B = -1.2161, exp (B) = 0.2963, p = 0.009; Table 21), but is insignificant with a negative relationship in the small grid (B = -0.17, exp (B) = 0.8440, p = 0.497). In the very high heat regime, canopy cover shows a strong negative relationship with LST across both grid sizes (B = -1.3701, exp (B) = 0.2542, p < 0.001 in the smaller grid, B = -2.9913, exp (B) = 0.0502, p < 0.001 in the larger grid), with the negative relationship being stronger in the large grid.

5.4.3 Interaction between Removals and Canopy Cover:

In the moderate heat regime for the small grid, the interaction term for total removals and canopy cover shows a positive relationship with LST change and is not significant (B =0.0074 , exp (B) =1.0074 , p = 0.013; Table 19). In the moderate regime for the large grid,

the interaction term for total removals and canopy cover shows a negative relationship with LST change and is not significant B = -0.0362, exp (B)= p = 0.013; Table 19). In the high heat regime for the large grid, the interaction is also negative and insignificant (B = -0.038, exp (B) = 0.9627, p = 0.011; Table 19). However, for the high heat regime in the small grid, the relationship is positive and insignificant (B = 0.022, exp (B) = 1.0222, p = 0.452; Table 19). In the very high heat regime, the interaction is not significant in either grid (B = 0.0079 , exp (B) = 1.0079, p = 0.862 for the small grid, B = 0.0003, exp (B) = 1.0003, p = 0.987 for the large grid; Table 19).

5.4.4 Model Fit

The pseudo r^2 for these multinomial logistic regressions measure the explanatory power or the fit of the models to the data. For the small grid for total removals, the pseudo r^2 = 0.0155. The suggests moderate explanatory power. Approximately 1.55% of the variations present within LST change can be explained by the model. For the large grid for total removals, the pseudo r^2 = 0.03746, also suggesting moderate explanatory power. Approximately 3.75% of the variations within LST change can be explained by the model.

5.5 Multinomial Logistic Regression Results for Development Removals

The multinomial logistic regression assesses the relationship between development removals, canopy cover, an interaction term between canopy cover and removals, and each heat regime that we created for our analysis (moderate, high, and very high). The reference category is low.

Table 21. Logistic Regression for the Mean LST Heat Regime and Development Removals. Asterisk indicates significance.

				Small Grid				
Heat Regime	***Variable***	***Coefficient (B)***	***Exp (B)***	***Std. Err.***	***z***	***P>|z|***	***[0.025***	***0.975]***
Moderate	Constant	0.5725	1.7725	0.127	4.511	0	0.324	0.821
	Development Removals	0.023	1.0233	0.015	1.537	0.124	-0.006	0.052
	Canopy Cover	0.1399	1.1501	0.26	0.539	0.59	-0.369	0.649
	Removals x Canopy	0.0136	1.0137	0.029	0.47	0.639	-0.043	0.07
High	Constant	0.4772	1.6113	0.144	3.313	0.001	0.195	0.76
	Development Removals	0.0121	1.0122	0.018	0.691	0.49	-0.022	0.046
	Canopy Cover	-1.4745	0.2292	0.311	-4.735	0*	-2.085	-0.864
	Removals x Canopy	0.007	1.0070	0.035	0.202	0.84	-0.061	0.075
Very High	Constant	-1.5513	0.2121	0.388	-3.996	0	-2.312	-0.79
	Development Removals	0.0758	1.0788	0.056	1.364	0.173	-0.033	0.185
	Canopy Cover	-3.7258	0.0240	1.211	-3.078	0.002*	-6.099	-1.353
	Removals x Canopy	-0.3375	0.7135	0.188	-1.799	0.072	-0.705	-0.03
Pseudo r^2		0.01924						

				Large Grid				
Heat Regime	***Variable***	***Coefficient (B)***	***Exp (B)***	***Std. Err.***	***z***	***P>|z|***	***[0.025***	***0.975]***
Moderate	Constant	0.7269	2.0689	0.286	2.537	0.011	0.165	1.288
	Development Removals	0.0376	1.0383	0.011	3.309	0.001*	0.015	0.06
	Canopy Cover	0.7106	2.0352	0.558	1.274	0.203	-0.383	1.804

	Removals x Canopy	-0.0536	0.9478	0.02	-2.685	0.007*	-0.093	-0.014
High	Constant	1.5575	4.7434	0.288	5.41	0.00	0.993	2.122
	Development	0.0362	1.0369	0.012	3.149	0.002*	0.014	0.059
	Removals Canopy Cover	-1.8274	0.1612	0.587	-3.111	0.002*	-2.979	-0.676
	Removals x Canopy	-0.0504	0.9509	0.021	-2.454	0.014	-0.091	-0.01
Very High	Constant	1.4553	4.2847	0.322	4.525	0.000	0.825	2.086
	Development	0.0099	1.0100	0.016	0.632	0.527	-0.021	0.041
	Removals Canopy Cover	-2.8634	0.0571	0.703	-4.075	0.00*	-4.241	-1.486
	Removals x Canopy	-0.0322	0.9683	0.032	-1.017	0.309	-0.094	0.03
Pseudo r^2		0.04267						

5.5.1 Development Removals

In the moderate heat regime, development removals have a positive but not significant relationship with LST in the smaller grid (B = 0.023, exp (B) = 1.0233, p = 0.124; Table 20) but are significant in the larger grid (B = 0.0376, exp (B) = 2.0689 p = 0.001; Table 20). In the high heat regime, development removals are positive but not significant in the smaller grid (B = 0.0121, exp (B) = 1.0122, p = 0.49; Table 20), but are significant in the larger grid (B = 0.0362, exp (B) = 1.0369, p = 0.002; Table 20). In the very high heat regime, development removals are positive but not significant in either grid (B = 0.0758, exp (B) = 1.0788, p = 0.173 for the small grid, B = 0.0099, exp (B) = 1.0100, p = 0.527 for the large grid; Table 20).

5.5.2 Canopy Cover

In the moderate heat regime, canopy cover is positive and not significant in either grid size (B = 0.1399, exp (B) = 1.1501, p = 0.59 for the small grid, B = 0.7106, exp (B) = 2.3052, p = 0.203 for the large grid; Table 20). In the high heat regime, canopy cover has a strong negative and significant relationship with LST in both grids (B = -1.4745, exp (B) = 0.2292, p = 0 in the small grid, B = -1.8274, exp (B) = 0.1612, p = 0.002 in the large grid; Table 21). In the very high heat regime, canopy cover has an even more significant and negative relationship with LST in both grids (B = -3.7258, exp (B) = 0.0240, p = 0.002 in the small grid, B = -2.8634, exp (B) = 0.0571, p = 0 in the large grid; Table 20).

5.5.3 Interaction between Development Removals and Canopy Cover

In the moderate heat regime for the small, the interaction term for development removals and canopy cover is positive and insignificant (B = 0.0136, exp (B) = 1.0137, p =0.0639; Table 21), but is negative and significant for the large grid (B = -0.0536, exp (B) = 0.9478, p = 0.007; Table 21). In the high heat regime for the large grid, the interaction term is also

negative and insignificant (B = -0.0504, exp (B) = 0.9509, p = 0.014). For the small grid, the interaction term was positive and insignificant in the high regime (B = 0.007, exp (B) = 1.0070, p = 0.84; Table 20). In the very high heat regime, the interaction term is negative and insignificant at both grid sizes (B = -0.3375, exp (B) =0.7135, p =0.072 for the small grid, B =-0.0322, exp (B)= 0.9683 , p = 0.309 for the large grid; Table 20).

5.5.4 Model Fit

The pseudo r^2 for these multinomial logistic regressions measure the explanatory power or the fit of the models to the data. For the small grid for development removals, the pseudo $r^2 = 0.01924$. The suggests moderate explanatory power. Approximately 1.9% of the variations present within LST change can be explained by the model. For the large grid for development removals, the pseudo $r^2 = 0.04267$, which also suggests moderate explanatory power. Approximately 4.3% of the variations within LST change can be explained by the model.

6. Discussion

6.1 Canopy Cover Correlations with LST, Scales of Interest, Tree Removals, and Heat Regimes

6.1.1 Canopy Cover and LST

Across all heat regimes, low canopy areas consistently showed the highest mean LST slope values. In contrast, high-canopy areas showed the lowest mean LST slope values. These results are similar to those from related studies, supporting the notion that low canopy areas are more susceptible to higher temperatures than areas of moderate or high canopy (Howe et al. 2017; Wang et al. 2023). High-canopy areas showed weak positive correlations with tree removals, and low-canopy areas showed stronger negative correlations with tree removals, most notably at the small scale. The stronger negative correlations between tree removals and LST slope in the presence of low canopy cover suggest that, while low canopy areas experience notably higher changes in LST, tree removals are not strongly correlated with these temperature changes. This may be because low canopy areas have already experienced a significant reduction in canopy over time, and in turn, tree removals over the last decade do not play a significant role in increasing LST. In contrast, the positive correlations between tree removals in high canopy areas suggest that, while the LST change in these areas is lower, the removal of trees has a more significant impact.

6.1.2 Scales of Interest

The differences in correlation strength between the small and large grids emphasize the importance of spatial scale in studying and understanding urban temperature dynamics (Karanja and Kiage 2021). Correlations between total tree removals and LST slope were stronger at the large scale, particularly in low-canopy areas, which exhibited the strongest

negative correlations. This suggests that low-canopy areas at the neighborhood scale are less prone to LST changes in the presence of removals. The small scale, however, showed more positive correlations between tree removals and LST across all canopy levels. This suggests that small scale tree removal patterns, even in areas of already reduced canopy cover, have a stronger positive relationship with increased LST than large scale removal patterns.

6.1.3 Total vs Development-related Tree Removals

The results showed a difference between total tree removals and development removals in relation to canopy cover. While both removal types showed negative correlations with LST slope in low and medium canopy areas, total removals generally had a stronger relationship, particularly at the large scale. These strong negative relationships may indicate that routine removals, whether for maintenance, hazard reduction, or natural loss, do not have as strong of an impact on temperature trends in association with canopy cover. Development related removals show stronger positive relationships with LST in high canopy areas than total removals, indicating that development related removals have a stronger relationship with LST change in high canopy areas than total removals.

6.1.4 Heat Regime Variability

The analysis of minimum and maximum LST slopes along with the mean LST slope was critical for this research, as temperature trends may vary throughout the city and may also be dependent on the scale of interest (Howe et al. 2017; Karanja and Kiage 2021). The maximum LST slope showed the strongest negative correlations with tree removals, specifically at the large scale. The maximum LST heat regimes represent the highest LST slope values in each grid block. These strong, negative correlations with tree removals suggests that tree removals do not play a strong role in increasing temperatures in areas that

are already experiencing high changes in temperature. In contrast, minimum LST slopes showed more positive correlations with both total and development removals, suggesting that removals influence temperature trends more strongly in areas that are experiencing stable or relatively low rates of change in LST.

6.2 Heat Regimes, Tree Removals, and Scales of Interest

6.2.1 Heat Regime Variability

By categorizing LST slope values from maximum, mean, and minimum LST measurements into low, moderate, high, and very high heat regimes, areas in higher slope regimes were found to be more closely associated with substantial tree removals. The maximum LST slope regimes in relation to both total and development tree removals showed higher removal counts than the mean LST slope heat regimes and the minimum LST slope heat regimes. Even more so, the high and very high heat regime categories within the mean, maximum, and minimum LST slope generally show higher counts of both total and development related removals, suggesting that urban modifications, particularly those involving vegetation or tree loss, increase temperature. The low heat regimes across the mean LST regimes, the minimum LST regimes, and the maximum LST regimes show the highest mean canopy cover values, suggesting that present tree canopy cover plays a role in reducing temperatures and keeping these low heat areas temperature stable. These results are similar to results from other studies examining the role that canopy cover and vegetation play in mitigating urban heat island effects (Howe et al. 2017; Wang et al. 2023; Wang & Akbari, 2016; Zhou et al. 2017).

6.2.2 Total vs. Development-Related Tree Removals

Overall the mean, minimum, and maximum heat regimes, development removals align with higher LST slope values. In other words, tree removals that are related to development are consistently seen in areas of higher LST change than total removals, which are consistent with results found in similar studies focused on land use change and LST (Fu and Weng 2016). Meanwhile, total removals, while still a sizable portion of canopy loss, include cases such as natural mortality, maintenance, or hazard mitigation, which may not always be associated with development or expansion.

6.2.3 Scales of Interest

The results show that heat regimes and tree removals vary by scale. At the small grid scale, areas of moderate or high LST slope consistently show the highest mean total removals. Across both grid scales, areas with a very high LST slope show a lower mean tree removal count compared to other slope regimes. This suggests that locations experiencing the highest increases in LST are also areas where fewer tree removals occur. This could indicate that these areas already had limited vegetation cover due to long-term urban development, leading to fewer tree removal opportunities. The mean LST slope is consistently higher at the large grid scale. This suggests that as spatial scale increases, temperature changes are more significant, which may be due to a combination of localized temperature effects such as expanded impervious surface cover, building microclimate conditions, and other activities related to urbanization (Fu and Weng 2016; Cheng et al. 2017). Areas with the highest mean total removals align closely with moderate LST slope regimes at both scales. This may be because tree removals occur more frequently in areas where urbanization or land use change

is occurring, such as new suburban developments (Morgenroth et al. 2017), but not necessarily in the regions experiencing the most extreme LST changes.

6.3 Multinomial Logistic Regression

This section of the discussion draws on the four multinomial regression models evaluating total removals, development-related removals, canopy cover, and the interaction between both sets of removals and canopy cover as a predictors of land surface temperature (LST) heat regimes. Specifically, we examined models using two different grid sizes—small and large—and conducted multinomial regressions separately for total tree removals and for development-related removals. In all models, the outcome variable was heat regime categories.

6.3.1 Heat Regimes and Total and Development-related Tree Removals

The analysis revealed that tree removals due to development contribute to an increase in LST, particularly in the moderate and high heat regimes and at the larger spatial scale. At the small scale, development-related tree removals were found to not be a significant predictor in any heat regime. Results, however, showed 2.3% and 1.2% increases in the odds of experiencing moderate and high LST change due to development-related tree removals compared to the low heat regime but not at a significant level. In the very high heat regime, development-related tree removals increase the odds of being in the very high heat regime by 7.9%, but again, this effect is not statistically significant. This suggests that other factors such as impervious cover or the built environment may play a larger role in changing LST at the small scale (Wang et al. 2021).

In the large grid for the moderate heat regime, the results suggest that, compared to the low heat regime, areas with development-related tree removals are twice as likely to fall

in the very high LST regime in the larger grid at a significant level. Similarly, in the high heat regime, the effect remains significant, indicating a 3.69% increase in the odds of development removals being in the high LST regime compared to the low heat regime. The significant positive coefficients for these regimes suggest that development-related tree removals influence urban heat, likely due to the loss of shade, evapotranspiration, and other cooling benefits provided by trees (Ziter et al. 2019, Liu et al. 2017). However, in the very high heat regime in the large grid, development removals are not significant, suggesting only a 1% increase in the odds of occurring in areas of very high LST change relative to low heat areas. This may be due to a variety of factors, including the concentration of impervious surfaces in very high heat areas, which reduces the additional warming effect from tree loss since temperatures are already maximized by extensive urbanization (Zhao et al. 2014).

Total tree removals, which include both development-related and other removals, showed a significance pattern similar to development. In the small grids, total tree removals were not found to be significant in any heat regimes. While the direction of the relationship is positive in the moderate and high regimes, showing a 2.4% and 1.5% increases in the odds of total removals occurring in those respective regimes , the lack of significance supports the idea that total removals at the smaller, neighborhood spatial scale are not the primary influence on LST change. In the very high heat regime the results suggest a 2.3% decrease in the odds of occurring in the very high heat regime relative to the low heat regime, though again, not statistically significant.

For the large grid in the moderate regime, results showed a 2.8% increase in the odds of total removals in areas of moderate LST change compared to low heat areas at a significant level. In the high regime, the odds are similar at 2.8%. However, total tree

removals are not significant in the very high heat regime, where the odds are slightly lower (0.3%) than in the low heat regime, although not meaningfully so. This again suggests that areas facing high heat are influenced by additional factors beyond tree removal.

Total and development removals' insignificant relationship with the very high LST heat regime not only suggest that high heat regimes are subject to more extensive factors that contribute to urban heat but are also consistent with the results from the canopy cover correlations. Areas that are subject to very high temperature changes have low canopy cover and do not have a strong relationship with tree removals. These areas have likely been subjected to urbanization and deforestation over multiple decades to the extent that tree removals no longer play a significant role in the change of LST.

6.3.2 Canopy Cover and LST Mitigation

Canopy cover consistently demonstrated a significant cooling effect, particularly in areas with higher LST slope. In the moderate heat regime, however, canopy cover did not show a significant relationship with LST at either grid size. For the smaller grid with the inclusion of total tree removals, canopy cover was a strong predictor (150%) of being in the moderate heat regime compared to the low heat regime. In comparison, for the larger grid, canopy cover was still a strong predictor (82.95%) of being in the moderate heat regime compared to the low heat regime. Similarly, at both the small and large grid scales with only development-related tree removals, results showed a 15% and 130% increase, respectively, in the odds of being in the moderate heat regime compared to the low regime, but neither were significant. These results suggests that in areas with lower heat, canopy cover may not be the primary form of temperature control. Other landscape or microclimate factors, such as proximity to water bodies, may play a role in temperature mitigation (Syafii 2021).

In contrast, areas with high canopy cover strongly reduces the chances of being in the high heat regime at both small and large grid scales. For the smaller grid with total tree removals, canopy cover was associated witha 15.6% decrease in the odds of being in the high heat regime relative to the low regime, although this effect is not statistically significant. In the larger grid with total tree removals, the effect of canopy cover was both stronger and significant with a 70.4% decrease in the odds of falling in the high heat regime compared to the low regime for each unit increase in canopy cover. For the models that considered development-related tree removals only, the impact of canopy cover is even more pronounced. In both the small and large grids, canopy cover accounted for 77.1% and 83.9% reductions in the odds of being in the high heat category, respectively.

In the very high heat regime, the cooling effect of canopy cover is even more significant at both scales. For the models with total removals, canopy cover has a strong and highly significant effect in both grids. The results showed a 74.6% and 94.98% reduction, respectively, in the odds of being in the very high LST heat regime compared to the low heat regime. For the models with development-related removals, the pattern is similar. Results indicated that canopy cover reduces the odds of being in the very high LST regime by 97.6% and 94.3%, respectively, highlighting the strong mitigating effect of canopy cover in areas with extreme heat change. These findings emphasize the critical role of tree cover in mitigating urban heat, particularly in areas already experiencing extreme temperature changes over time (Estoque et al. 2017; Wang & Akbari, 2016; Zhou et al. 2017).

6.3.3 Interaction between Development Removals and Canopy Cover

We also explored the interaction between canopy cover and tree removals to assess whether the combined influence of these factors predicts membership in LST heat regimes.

Interaction terms were tested in models using both small and large grids, and for both total and development-related removals.

The absence of a significant interaction effect at the smaller grid scale for both total and development-related removals suggests that tree removals in the cooling effects of canopy cover in the presence of total and development related removals in parcel or property sized projects may not directly influence LST. In the moderate regime, the interaction between total removals and canopy cover in the small grid demonstrate a 0.74% increase in the odds of being in the moderate regime compared to the low heat regime, while the interaction between development removals and canopy cover shows a 1.37% increase in the odds of being in the moderate regime. Neither of these effects are statistically significant. In the high heat regime for the interaction between total removals and canopy cover showed a 2.2% increase in the odd of occurring in the high heat regime, and the interaction between development removals and canopy cover displayed a 0.7% increase in the odd of occurring in the high heat regime. However, neither of these effects are statistically significant. For the interaction between total removals and canopy cover in the very high heat regime, the results showed a 0.79% increase in the odds of occurring in the very high heat regime, lacking statistical significance.. For the interaction between development removals and canopy cover, the results suggest a 28.65% reduction in the odds of being in the very high heat category compared to the low regime, although the effect is not statistically significant.

In the moderate regime, for the interaction between total removals and canopy cover in the large grid, the results indicate a 3.55% decrease in the odds of being in the moderate heat regime relative to the low heat regime. Similarly, for the interaction between

development removals and canopy cover in the large grid, the results show a 5.22% reduction in the odds of occurring in the moderate heat regime compared to the low heat regime. This is the only significant results for the interaction term. In the high heat regime for the larger grid, the interaction between total removals and canopy cover show a 3.73% decrease in the odds of being in the high heat regime, and the interaction between development removals and canopy cover show a 4.91% decrease in the odds of being in the high heat regime relative to the low regime. In the very high heat regime, the interaction between total removals and canopy cover in the larger grid shows a 0.03% increase in odds of being in the very high heat regime, indicating a negligible and non-significant increase in odds. For the interaction between development removals and canopy cover the results shows a 3.17% reduction in the odds of being in the very high heat category compared to the low regime, although this effect is statistically significant. These results suggest that while the interaction between removals and canopy cover has limited influence at the parcel level, it can be meaningful at broader spatial scales. Particularly in moderate and high heat regimes, the combined effects of development-related removals and canopy cover play a statistically significant role in predicting LST outcomes.

Together, these analyses emphasize the importance of both vegetation structure and spatial scale in predicting urban heat exposure. Canopy cover alone consistently emerges as a critical predictor of lower odds of being in high and very high LST regimes, especially at larger spatial scales. Meanwhile, tree removals—particularly those related to development—are shown to significantly increase the odds of moderate and high heat regime membership, but only at broader scales. At smaller scales, removals appear to have limited predictive power, likely due to local heterogeneity or the influence of surrounding land cover.

Importantly, interaction models reveal that while the combined effects of canopy and removals are minimal at the parcel level, they become statistically meaningful at neighborhood or district scales, particularly in moderate and high heat regimes. These findings collectively underscore that strategies to mitigate urban heat must account for both the presence of canopy and the spatial dynamics of tree loss, especially in areas undergoing active development. Urban heat adaptation efforts will benefit from scaling interventions appropriately and aligning them with the drivers of heat intensification in a given context.

7. Conclusion and Practical Applications

This research reveals that both tree canopy and removals influence urban heat, but their impacts vary significantly by spatial scale and development context. At larger grid scales, canopy cover significantly reduces the odds of falling into high and very high land surface temperature (LST) regimes, while development-related tree removals significantly increase them in the moderate and high regimes. Interaction effects between removals and canopy cover also become meaningful at broader spatial scales, emphasizing the importance of integrated green space planning. In contrast, at the parcel level, these predictors have less explanatory power—suggesting that interventions at small scales may not be sufficient in isolation.

The results of this research carry significant implications for urban planning, urban forest management, environmental policy, and climate adaptation strategies. With compelling evidence that tree removals contribute to rising urban temperatures, particularly in areas experiencing moderate to high levels of LST change, municipalities should make tree preservation and canopy conservation a central focus, especially in neighborhoods in Austin subject to future development. Given that effects were more pronounced at broader spatial scales, urban forest management strategies should consider neighborhood or district-level planning units when setting canopy conservation goals.

Cities such Los Angeles and Phoenix, which are already grappling with extreme heat, have implemented tree inventory programs and heat mitigation strategies (LA Sanitation and Environment n.d.; City of Phoenix n.d.). Programs like this can be expanded upon to focus more directly on preventing canopy loss due to construction. Strategic urban forestry policies

that minimize or restrict non-essential tree removals, especially those tied to new development, can play an important role in mitigating LST increases and reducing the adverse effects of the UHI. To address these issues, future development projects should prioritize nature-based solutions, such as the integration of tree planting initiatives, green infrastructure, and the conservation of existing natural spaces.

Programs such as New York City's MillionTrees NYC and Melbourne's Urban Forest Strategy demonstrate how large-scale urban forestry campaigns can improve microclimates, reduce surface temperatures, and create more resilient neighborhoods (The City of New York n.d.; City of Melbourne n.d.). These efforts not only reduce the heat stress on urban areas but also provide other benefits, such as improved air quality, stormwater management, carbon sequestration, and enhanced mental and physical well-being. In Austin, targeted interventions such as increasing shade trees along roadways, converting unused lots into mini urban forests, or preserving patches of tree canopy in fast-developing areas can provide substantial cooling benefits and improve the daily quality of life for residents.

This research also contributes to urban forestry practices by highlighting the importance of preserving trees most at risk of removal due to development pressures. These trees, once lost, may have disproportionate impacts on local microclimates and exacerbate temperature changes. Urban forest management should incorporate predictive models or assessments of development trends and proactively protect canopy cover before it's lost. Planners should consider integrating canopy conservation into development approvals and leveraging zoning incentives to retain mature trees.

Future studies should build on this research by examining the long-term effects of urban tree loss in combination with other environmental and social factors, such as air quality, increased surface runoff, and public health outcomes related to heat exposure. Expanding this research framework to include global cities can provide a broader understanding of how tree canopy influences urban heat resilience. These insights can inform climate-resilient urban design and development, guide green infrastructure investment, and enhance the sustainability of cities in an era of rapid environmental change. Ultimately, these insights can support sustainable development policies that prioritize canopy conservation as a frontline defense against extreme urban heat.

While this study provides valuable insights into the relationship between tree removals, canopy cover, and LST changes, several limitations should be acknowledged. First, this study relies on tree removal data from the past decade, but long-term urbanization and historical land cover changes were not accounted for in detail. Future research should incorporate historical datasets spanning multiple decades to assess long-term changes in LST. Second, while this study focuses on tree removals and canopy cover, additional environmental factors such as wind patterns, humidity, precipitation, and proximity to water bodies may also influence LST. Incorporating these variables in future studies may enhance the understanding of LST changes in urban areas. Third, this study uses remotely sensed LST data. This is effective but may be influenced by factors such as atmospheric conditions. Future studies could incorporate in-situ temperature measurements to validate remote sensing measurements. Finally, while the regression models used in this study account for multiple predictors, they do not explicitly address potential issues of spatial autocorrelation among

observations, which are common in spatial data. Future research should explore geostatistical or spatial regression techniques to test and control for spatial dependencies.

8. References

Austin Chamber. (2023). *Population Overview*. https://www.austinchamber.com/economic-development/austin-profile/population/overview

Bottalico, F., Chirici, G., Giannetti, F., de Marco, A., Nocentini, S., Paoletti, E., Salbitano, F., Sanesi, G., Serenelli, C., & Travaglini, D. (2016). Air Pollution Removal by Green Infrastructures and Urban Forests in the City of Florence. *Agriculture and Agricultural Science Procedia*, *8*, 243–251. https://doi.org/10.1016/j.aaspro.2016.02.099

Bowler, D. E., Buyung-Ali, L., Knight, T. M., & Pullin, A. S. (2010). Urban greening to cool towns and cities: A systematic review of the empirical evidence. In *Landscape and Urban Planning* (Vol. 97, Issue 3, pp. 147–155). Elsevier. https://doi.org/10.1016/j.landurbplan.2010.05.006

Chang, Y., Xiao, J., Li, X., Middel, A., Zhang, Y., Gu, Z., Wu, Y., & He, S. (2021). *Exploring diurnal thermal variations in urban local climate zones with ECOSTRESS land surface temperature data 2 3*.

City of Austin Development Services Department. (2022). *Tree Canopy 2022*.

City of Melbourne. (n.d.). *Urban Forest Strategy*.

City of Phoenix. (n.d.). *Tree Shade Programs*.

Clark, C., Ordóñez, C., & Livesley, S. J. (2020). Private tree removal, public loss: Valuing and enforcing existing tree protection mechanisms is the key to retaining urban trees on private land. *Landscape and Urban Planning*, *203*. https://doi.org/10.1016/j.landurbplan.2020.103899

Cole, J., Nowak, D. J., & Greenfield, E. J. (2021). Potential Hurricane Wind Risk to US Rural and Urban Forests. *Journal of Forestry*, *119*(4), 393–406. https://doi.org/10.1093/jofore/fvab018

Conway, T. M. (2016). Tending their urban forest: Residents' motivations for tree planting and removal. *Urban Forestry and Urban Greening*, *17*, 23–32. https://doi.org/10.1016/j.ufug.2016.03.008

Croeser, T., Ordóñez, C., Threlfall, C., Kendal, D., van der Ree, R., Callow, D., & Livesley, S. J. (2020). Patterns of tree removal and canopy change on public and private land in the City of Melbourne. *Sustainable Cities and Society*, *56*. https://doi.org/10.1016/j.scs.2020.102096

Dai, J. ping, Qin, J. zheng, Zhou, T., Qin, X. jian, Zhu, K., & Peng, J. song. (2023). Study on the influence of urban tree canopy on thermal environment in Luoping County. *Scientific Reports*, *13*(1). https://doi.org/10.1038/s41598-023-40449-2

DiDonato, G. T., Stewart, J. R., Sanger, D. M., Robinson, B. J., Thompson, B. C., Holland, A. F., & van Dolah, R. F. (2009). Effects of changing land use on the microbial water quality of tidal creeks. *Marine Pollution Bulletin*, *58*(1), 97–106. https://doi.org/10.1016/j.marpolbul.2008.08.019

Ebi, K. L., Capon, A., Berry, P., Broderick, C., de Dear, R., Havenith, G., Honda, Y., Kovats, R. S., Ma, W., Malik, A., Morris, N. B., Nybo, L., Seneviratne, S. I., Vanos, J., & Jay, O. (2021). Hot weather and heat extremes: health risks. In *The Lancet* (Vol. 398, Issue 10301, pp. 698–708). Elsevier B.V. https://doi.org/10.1016/S0140-6736(21)01208-3

Ermida, S. L., Soares, P., Mantas, V., Gottsche, F. M., & Trigo, I. F. (2020). Google Earth Engine open-source code for Land Surface Temperature estimation from the Landsat series. *MDPI Remote Sensing*, *12*(9).

ESRI. (n.d.). *Introduction to ArcGIS Pro*.

ESRI. (n.d.). *Use snapping*.

Estoque, R. C., Murayama, Y., & Myint, S. W. (2017). Effects of landscape composition and pattern on land surface temperature: An urban heat island study in the megacities of Southeast Asia. *Science of the Total Environment*, *577*, 349–359. https://doi.org/10.1016/j.scitotenv.2016.10.195

Fan, C., Myint, S. W., & Zheng, B. (2015). Measuring the spatial arrangement of urban vegetation and its impacts on seasonal surface temperatures. *Progress in Physical Geography*, *39*(2), 199–219. https://doi.org/10.1177/0309133314567583

Gerrish, E., & Watkins, S. L. (2017). *The relationship between urban forests and income: A meta-analysis*.

Google. (n.d.). *Platform-Google Earth Engine*.

Google Earth Engine. (n.d.). *Resampling and Reducing Resolution*.

Grant, A., Millward, A. A., Edge, S., Roman, L. A., & Teelucksingh, C. (2022). Where is environmental justice? A review of US urban forest management plans. *Urban Forestry and Urban Greening*, *77*. https://doi.org/10.1016/j.ufug.2022.127737

Greene, C. S., & Millward, A. A. (2017). Getting closure: The role of urban forest canopy density in moderating summer surface temperatures in a large city. *Urban Ecosystems*, *20*(1), 141–156. https://doi.org/10.1007/s11252-016-0586-5

Guo, A., He, T., Yue, W., Xiao, W., Yang, J., Zhang, M., & Li, M. (2023). Contribution of urban trees in reducing land surface temperature: Evidence from china's major cities. *International*

Journal of Applied Earth Observation and Geoinformation, *125*. https://doi.org/10.1016/j.jag.2023.103570

Guo, T., Morgenroth, J., & Conway, T. (2018). Redeveloping the urban forest: The effect of redevelopment and property-scale variables on tree removal and retention. *Urban Forestry and Urban Greening*, *35*, 192–201. https://doi.org/10.1016/j.ufug.2018.08.012

Guo, T., Morgenroth, J., & Conway, T. (2019). To plant, remove, or retain: Understanding property owner decisions about trees during redevelopment. *Landscape and Urban Planning*, *190*. https://doi.org/10.1016/j.landurbplan.2019.103601

Harvey, C. A., Medina, A., Sánchez, D. M., Vílchez, S., Hernández, B., Saenz, J. C., Maes, J. M., Casanoves, F., & Sinclair, F. L. (2006). Patterns of animal diversity in different forms of tree cover in agricultural landscapes. *Ecological Applications*, *16*(5), 1986–1999. https://doi.org/10.1890/1051-0761(2006)016[1986:POADID]2.0.CO;2

Howe, D. A., Hathaway, J. M., Ellis, K. N., & Mason, L. R. (2017). Spatial and temporal variability of air temperature across urban neighborhoods with varying amounts of tree canopy. *Urban Forestry and Urban Greening*, *27*, 109–116. https://doi.org/10.1016/j.ufug.2017.07.001

Hsu, A., Sheriff, G., Chakraborty, T., & Manya, D. (2021a). Disproportionate exposure to urban heat island intensity across major US cities. *Nature Communications*, *12*(1). https://doi.org/10.1038/s41467-021-22799-5

Jackson, K. (2023, July 19). *Austin is now the 10th Largest City in the U.S.*

Jiguet, F., Devictor, V., Julliard, R., & Couvet, D. (2012). French citizens monitoring ordinary birds provide tools for conservation and ecological sciences. *Acta Oecologica*, *44*, 58–66. https://doi.org/10.1016/j.actao.2011.05.003

Karanja, J., & Kiage Lawrence. (2021). Perspectives on spatial representation of urban heat vulnerability. *Science of the Total Environment*, *774*.

Khandelwal, S., Goyal, R., Kaul, N., & Mathew, A. (2018). Assessment of land surface temperature variation due to change in elevation of area surrounding Jaipur, India. *Egyptian Journal of Remote Sensing and Space Science*, *21*(1), 87–94. https://doi.org/10.1016/j.ejrs.2017.01.005

Kirkpatrick, J. B., Davison, A., & Daniels, G. D. (2012). Resident attitudes towards trees influence the planting and removal of different types of trees in eastern Australian cities. *Landscape and Urban Planning*, *107*(2), 147–158. https://doi.org/10.1016/j.landurbplan.2012.05.015

Koeser, A. K., Hauer, R. J., Andreu, M., Northrop, R., & Hilbert, D. R. (2023). Attitudes towards tree protections, development, and urban forest incentives among Florida (United States) residents. *Urban Forestry and Urban Greening*, *86*. https://doi.org/10.1016/j.ufug.2023.128032

Kowarik, I., Hiller, A., Planchuelo, G., Seitz, B., Lippe, M. von der, & Buchholz, S. (2019). Emerging urban forests: Opportunities for promoting the wild side of the urban green infrastructure. *Sustainability (Switzerland)*, *11*(22). https://doi.org/10.3390/su11226318\

LA Sanitation and Environment. (n.d.). *Trees*.

Lavy, B. L., & Hagelman, R. R. (2017). Spatial and Temporal Patterns Associated with Permitted Tree Removal in Austin, Texas, 2002–2011. *Professional Geographer*, *69*(4), 539–552. https://doi.org/10.1080/00330124.2016.1266953

Lavy, B. L., & Hagelman, R. R. (2019). Protecting the urban forest: Variations in standards and sustainability dimensions of municipal tree preservation ordinances. *Urban Forestry and Urban Greening*, *44*. https://doi.org/10.1016/j.ufug.2019.126394

Lee, S. J., Longcore, T., Rich, C., & Wilson, J. P. (2017). Increased home size and hardscape decreases urban forest cover in Los Angeles County's single-family residential neighborhoods. *Urban Forestry and Urban Greening*, *24*, 222–235. https://doi.org/10.1016/j.ufug.2017.03.004

Lindsey, R., & Dahlman, L. (2024, January 18). *Climate Change: Global Temperature*. National Oceanic and Atmospheric Administration.

Liu, X., Li, X. X., Harshan, S., Roth, M., & Velasco, E. (2017). Evaluation of an urban canopy model in a tropical city: The role of tree evapotranspiration. *Environmental Research Letters*, *12*(9). https://doi.org/10.1088/1748-9326/aa7ee7

Liu, Z., He, C., & Wu, J. (2016). The relationship between habitat loss and fragmentation during urbanization: An empirical evaluation from 16 world cities. *PLoS ONE*, *11*(4). https://doi.org/10.1371/journal.pone.0154613

Meyers, L., Gamst, G., & Guarino, A. J. (2017). *Applied Multivariative Research: Design and Interpretation* (L. Fargotstein, O. Weber-Stenis, & C. West, Eds.; 3rd ed.). SAGE.

Morgenroth, J., O'Neil-Dunne, J., & Apiolaza, L. A. (2017). Redevelopment and the urban forest: A study of tree removal and retention during demolition activities. *Applied Geography*, *82*, 1–10. https://doi.org/10.1016/j.apgeog.2017.02.011

Multi-Resolution Land Characteristics Consortium. (n.d.). *National Land Cover Database Class Legend and Description*.

Nowak, D. J., & Greenfield, E. J. (2021). *The increase of impervious cover and decrease of tree cover within urban areas globally (2012–2017)*. https://www.sciencedirect.com/science/article/pii/S161886671930295X

Nowak, D. J., & Greenfield, E. J. (2018a). *Declining Urban and Community Tree Cover in the United States*.

Nowak, D. J., & Greenfield, E. J. (2018b). US urban forest statistics, values, and projections. *Journal of Forestry*, *116*(2), 164–177. https://doi.org/10.1093/jofore/fvx004

Nuruzzaman, Md. (2015a). Urban Heat Island: Causes, Effects and Mitigation Measures - A Review. *International Journal of Environmental Monitoring and Analysis*, *3*(2), 67. https://doi.org/10.11648/j.ijema.20150302.15

Oh, B., Lee, K. J., Zaslawski, C., Yeung, A., Rosenthal, D., Larkey, L., & Back, M. (2017). Health and well-being benefits of spending time in forests: Systematic review. In *Environmental Health and Preventive Medicine* (Vol. 22, Issue 1). BioMed Central Ltd. https://doi.org/10.1186/s12199-017-0677-9

Oleson, K. W., Monaghan, A., Wilhelmi, O., Barlage, M., Brunsell, N., Feddema, J., Hu, L., & Steinhoff, D. F. (2015). Interactions between urbanization, heat stress, and climate change. *Climatic Change*, *129*(3–4), 525–541. https://doi.org/10.1007/s10584-013-0936-8

Paerl, H. W., & Scott, J. T. (2010). Throwing fuel on the fire: Synergistic effects of excessive nitrogen inputs and global warming on harmful algal blooms. In *Environmental Science and Technology* (Vol. 44, Issue 20, pp. 7756–7758). https://doi.org/10.1021/es102665e

Pinho, R. C., Miller, R. P., & Alfaia, S. S. (2012). Agroforestry and the improvement of soil fertility: A view from amazonia. In *Applied and Environmental Soil Science* (Vol. 2012). https://doi.org/10.1155/2012/616383

Qin, Y. (2020a). Urban flooding mitigation techniques: A systematic review and future studies. In *Water (Switzerland)* (Vol. 12, Issue 12). MDPI AG. https://doi.org/10.3390/w12123579

Rendon, P., Love, N., Pawlak, C., Yost, J., Ritter, M., & Doremus, J. (2024). Street tree diversity and urban heat. *Urban Forestry and Urban Greening*, *91*. https://doi.org/10.1016/j.ufug.2023.128180

Riley, C. B., & Gardiner, M. M. (2020). Examining the distributional equity of urban tree canopy cover and ecosystem services across United States cities. *PLoS ONE*, *15*(2). https://doi.org/10.1371/journal.pone.0228499

Roman, L. A., Fristensky, J., Lundgren, R., Cerwinka, C., & Lubar, J. (2022). Construction and Proactive Management Led to Tree Removals on an Urban College Campus. *Forests*, *13*(6). https://doi.org/10.3390/f13060871

Schwarz, K., Fragkias, M., Boone, C. G., Zhou, W., McHale, M., Grove, J. M., O'Neil-Dunne, J., McFadden, J. P., Buckley, G. L., Childers, D., Ogden, L., Pincetl, S., Pataki, D., Whitmer, A., & Cadenasso, M. L. (2015). Trees grow on money: Urban tree canopy cover and environmental justice. *PLoS ONE*, *10*(4). https://doi.org/10.1371/journal.pone.0122051

Seabold, S., & Perktold, J. (2010). Statsmodels: Econometric and Statistical Modeling with Python. *PYTHON IN SCIENCE CONF*.

Stangierska, D., Fornal-Pieniak, B., Szumigała, P., Widera, K., Żarska, B., & Szumigała, K. (2023a). Green Physical Activity Indicator: Health, Physical Activity and Spending Time Outdoors Related to Residents Preference for Greenery. *International Journal of Environmental Research and Public Health*, *20*(2). https://doi.org/10.3390/ijerph20021242

Syafii, N. I. (2021). Promoting Urban Water Bodies as a Potential Strategy to Improve Urban Thermal Environment. *Geographica Pannonica*, *25*(2), 113–120. https://doi.org/10.5937/gp25-30431

Sun, Q., Wu, Z., & Tan, J. (2012). The relationship between land surface temperature and land use/land cover in Guangzhou, China. *Environmental Earth Sciences*, *65*(6), 1687–1694. https://doi.org/10.1007/s12665-011-1145-2

The City of New York. (n.d.). *MillionTreesNYC*.

Tubby, K. v., & Webber, J. F. (2010). Pests and diseases threatening urban trees under a changing climate. *Forestry*, *83*(4), 451–459. https://doi.org/10.1093/forestry/cpq027

Ulmer, J. M., Wolf, K. L., Backman, D. R., Tretheway, R. L., Blain, C. J., O'Neil-Dunne, J. P., & Frank, L. D. (2016). Multiple health benefits of urban tree canopy: The mounting evidence for a green prescription. *Health and Place*, *42*, 54–62. https://doi.org/10.1016/j.healthplace.2016.08.011

United Nations. (2018, July 16). *68% of the world population projected to live in urban areas by 2050, says UN*.

United States Census Bureau. (2022, December 29). *Nation's Urban and Rural Populations Shift Following 2020 Census*.

University of Michigan Center for Sustainable Systems. (2023). *Built Environment*.

Upreti, R., Wang, Z.-H., & Yang, J. (2017). Radiative shading effect of urban trees on cooling the regional built environment. *Urban Forestry and Urban Greening*, *26*.

Vailshery, L. S., Jaganmohan, M., & Nagendra, H. (2013). Effect of street trees on microclimate and air pollution in a tropical city. *Urban Forestry and Urban Greening*, *12*(3), 408–415. https://doi.org/10.1016/j.ufug.2013.03.002

Vicedo-Cabrera, A. M., Scovronick, N., Sera, F., Royé, D., Schneider, R., Tobias, A., Astrom, C., Guo, Y., Honda, Y., Hondula, D. M., Abrutzky, R., Tong, S., Coelho, M. de S. Z. S., Saldiva, P. H. N., Lavigne, E., Correa, P. M., Ortega, N. V., Kan, H., Osorio, S., … Gasparrini, A. (2021). The burden of heat-related mortality attributable to recent human-induced climate change. *Nature Climate Change*, *11*(6), 492–500. https://doi.org/10.1038/s41558-021-01058-x

Wang, H., Cai, Y., Deng, W., Li, C., Dong, Y., Zhou, L., Sun, J., Li, C., Song, B., Zhang, F., & Zhou, G. (2023). The Effects of Tree Canopy Structure and Tree Coverage Ratios on Urban Air Temperature Based on ENVI-Met. *Forests*, *14*(1). https://doi.org/10.3390/f14010080

Wang, Q. (2018). Urbanization and Global Health: The Role of Air Pollution. In *Iran J Public Health* (Vol. 47, Issue 11). http://ijph.tums.ac.ir

Wang, Y., & Akbari, H. (2016). The effects of street tree planting on Urban Heat Island

Wang, Z., Meng, Q., Allam, M., Hu, D., Zhang, L., & Menenti, M. (2021). Environmental and anthropogenic drivers of surface urban heat island intensity: A case-study in the Yangtze River Delta, China. *Ecological Indicators*, *128*. https://doi.org/10.1016/j.ecolind.2021.107845

Wolf, K. L., Lam, S. T., McKeen, J. K., Richardson, G. R. A., Bosch, M. van den, & Bardekjian, A. C. (2020). Urban trees and human health: A scoping review. In *International Journal of Environmental Research and Public Health* (Vol. 17, Issue 12, pp. 1–30). MDPI AG. https://doi.org/10.3390/ijerph17124371

Wu, J., Wang, Y., Qiu, S., & Peng, J. (2019). Using the modified i-Tree Eco model to quantify air pollution removal by urban vegetation. *Science of the Total Environment*, *688*, 673–683. https://doi.org/10.1016/j.scitotenv.209.05.437

Xu, H. (2010). Analysis of Impervious Surface and its Impact on Urban Heat Environment using the Normalized Difference Impervious Surface Index (NDISI). *Photogrammetric Engineering & Remote Sensing*, *76*(5).

Zhang, Y., Li, Y., Chen, Y., Liu, S., & Yang, Q. (2022). Spatiotemporal Heterogeneity of Urban Land Expansion and Urban Population Growth under New Urbanization: A Case Study of Chongqing. *International Journal of Environmental Research and Public Health*, *19*(13). https://doi.org/10.3390/ijerph19137792

Zhao, L., Lee, X., Smith, R. B., & Oleson, K. (2014). *Strong contributions of local background climate to urban heat islands.* Nature, 511(7508), 216–219.

Zhou, W., Wang, J., & Cadenasso, M. L. (2017). Effects of the spatial configuration of trees on urban heat mitigation: A comparative study. *Remote Sensing of Environment, 195*.

Ziter, C. D., Pedersen, E. J., Kucharik, C. J., & Turner, M. G. (2019). Scale-dependent interactions between tree canopy cover and impervious surfaces reduce daytime urban heat during summer. *Proceedings of the National Academy of Sciences of the United States of America*, *116*(15), 7575–7580. https://doi.org/10.1073/pnas.1817561116

Zolch, T., Maderspacher, J., Wamsler, C., & Pauleit, S. (2016). Using green infrastructure for urban climate-proofing: An evaluation of heat mitigation measures at the micro-scale. *Urban Forestry and Urban Greening*, *20*.

Appendix A: LST Maps

08-31-2013

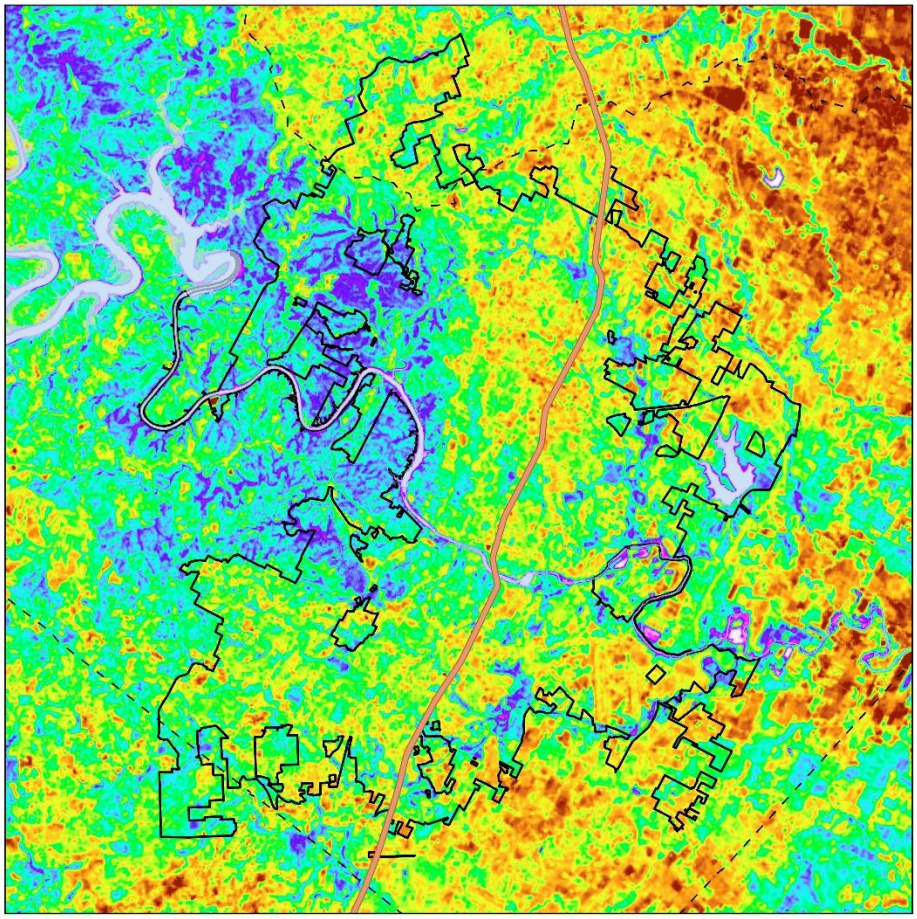

07-20-2015

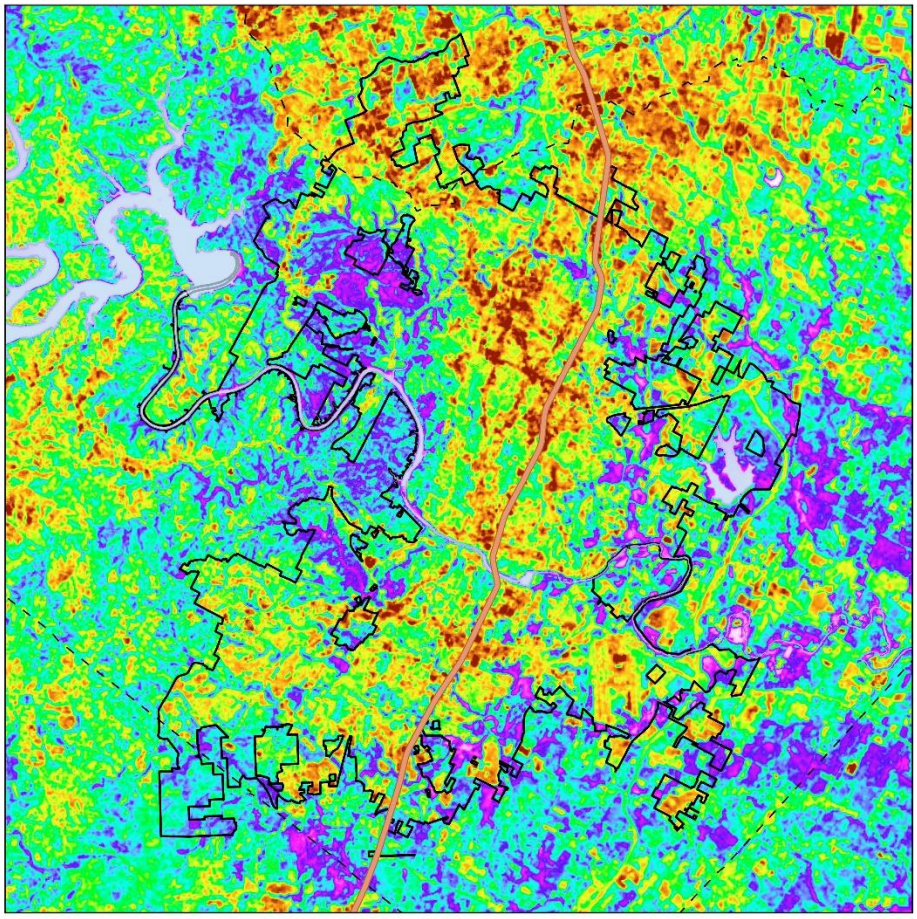
Legend
Land Surface Temperature (°C)
55.70
27.20
Interstate 35
County Boundaries
Austin City Limits
Water
N
0 2.5 5 10 Kilometers

07-22-2016

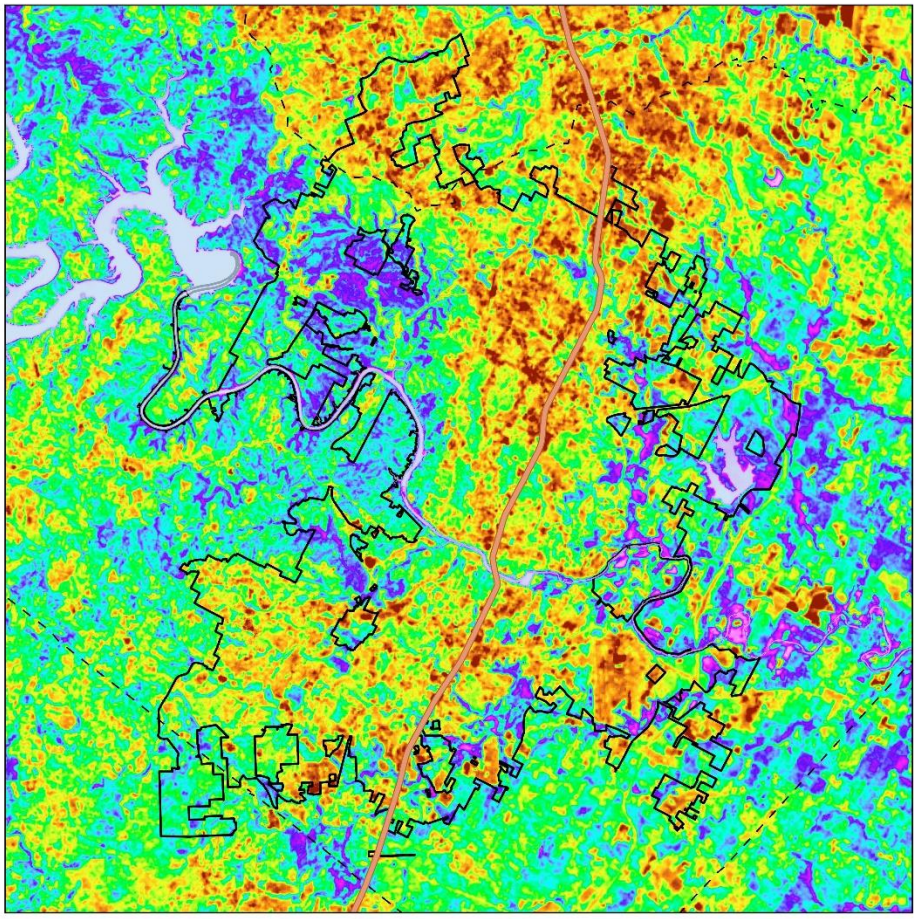

Legend

Land Surface Temperature (°C)

58.14

29.26

Interstate 35

County Boundaries

Austin City Limits

Water

N

0 2.5 5 10 Kilometers

08-11-2023

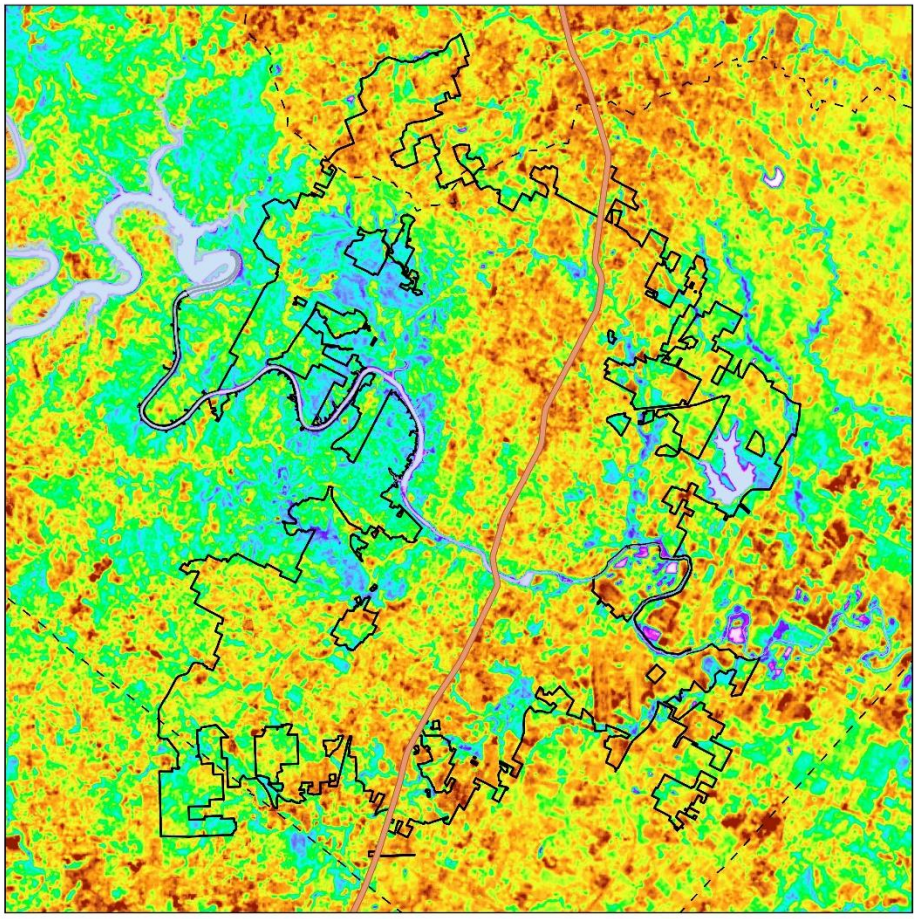

Legend

Land Surface Temperature (°C)

59.8854

30.8512

Interstate 35

County Boundaries

Austin City Limits

Water

N

0 2.5 5 10 Kilometers

08-18-2020

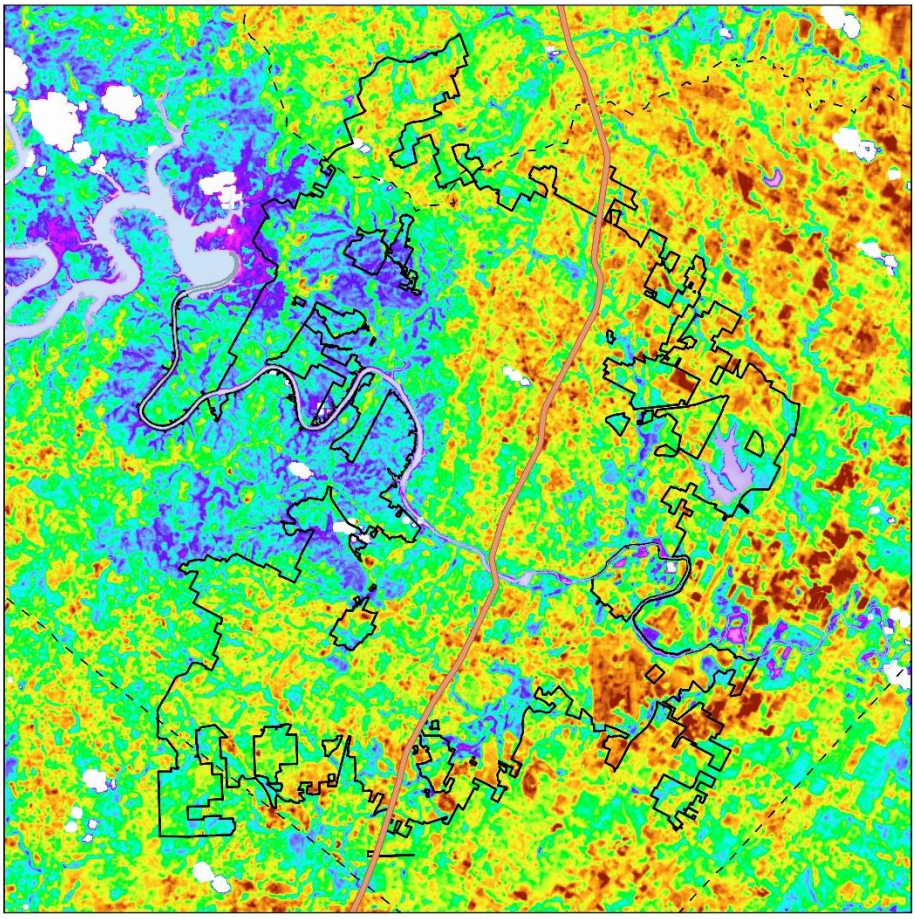

Legend

Land Surface Temperature (°C)

53.54

20.97

Interstate 35

County Boundaries

Austin City Limits

Water

N

0 2.5 5 10 Kilometers

07-09-2017

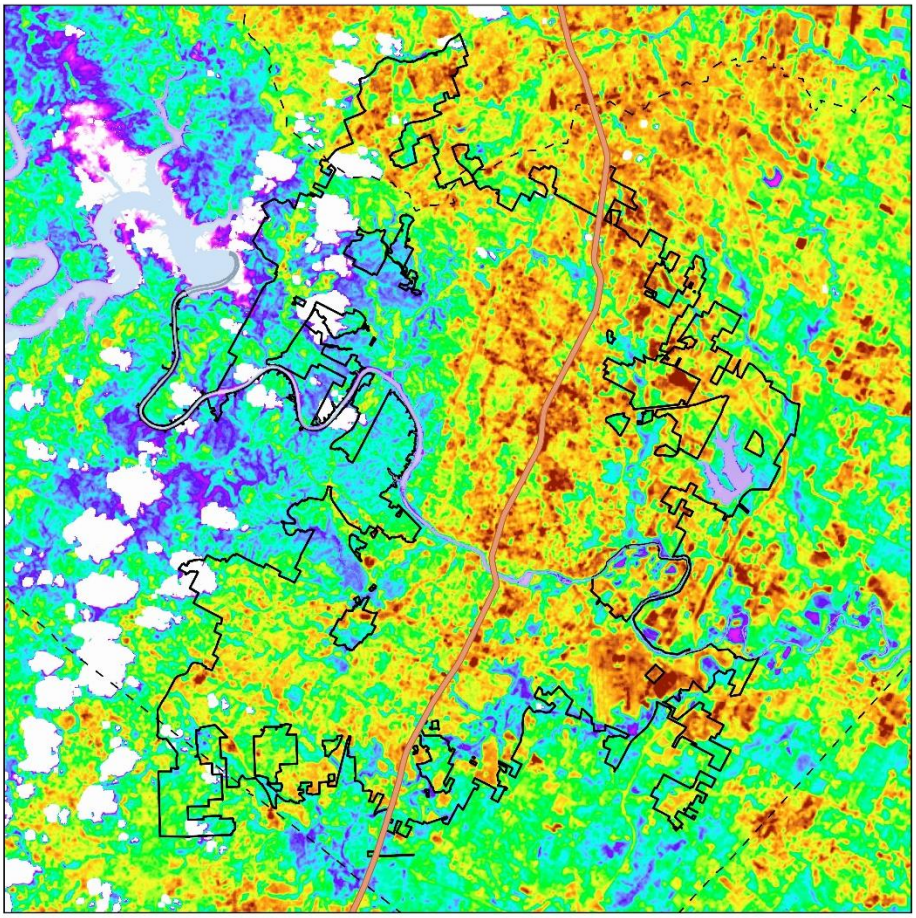

Legend

Land Surface Temperature (°C)

57.98

15.18

Interstate 35

County Boundaries

Austin City Limits

Water

N

0 2.5 5 10 Kilometers

08-29-2018

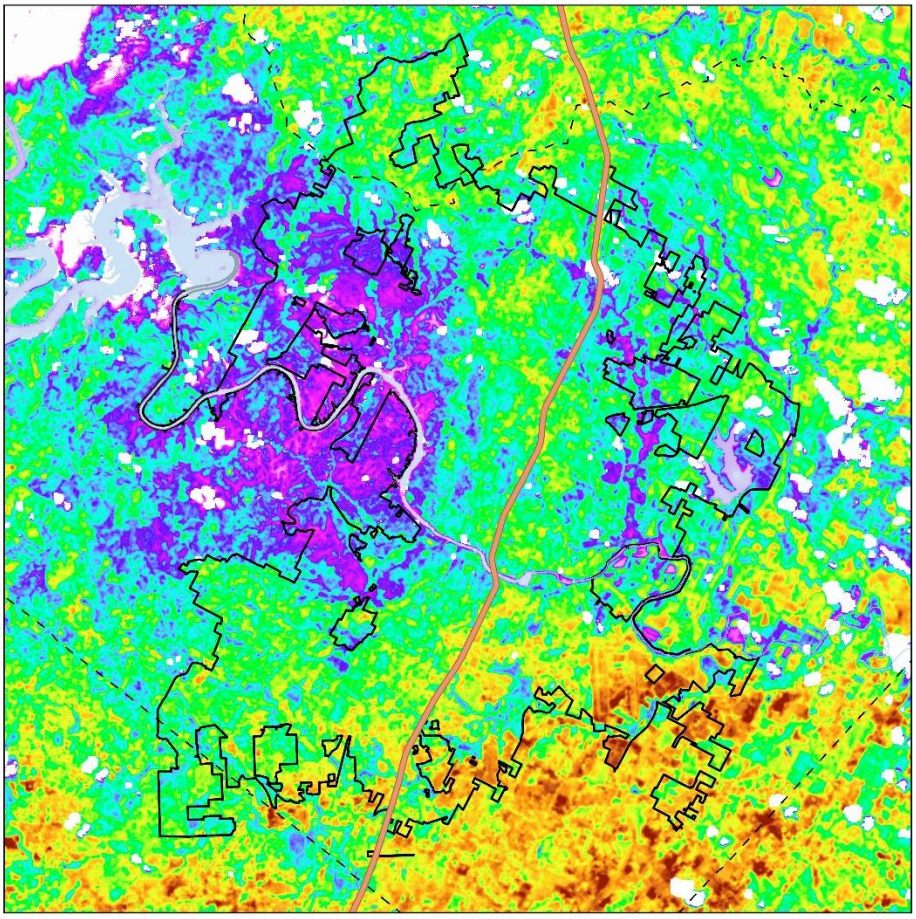

Legend

Land Surface Temperature (°C)

51.48

-1.81

Interstate 35

County Boundaries

Austin City Limits

Water

N

0 2.5 5 10 Kilometers

08-16-2019

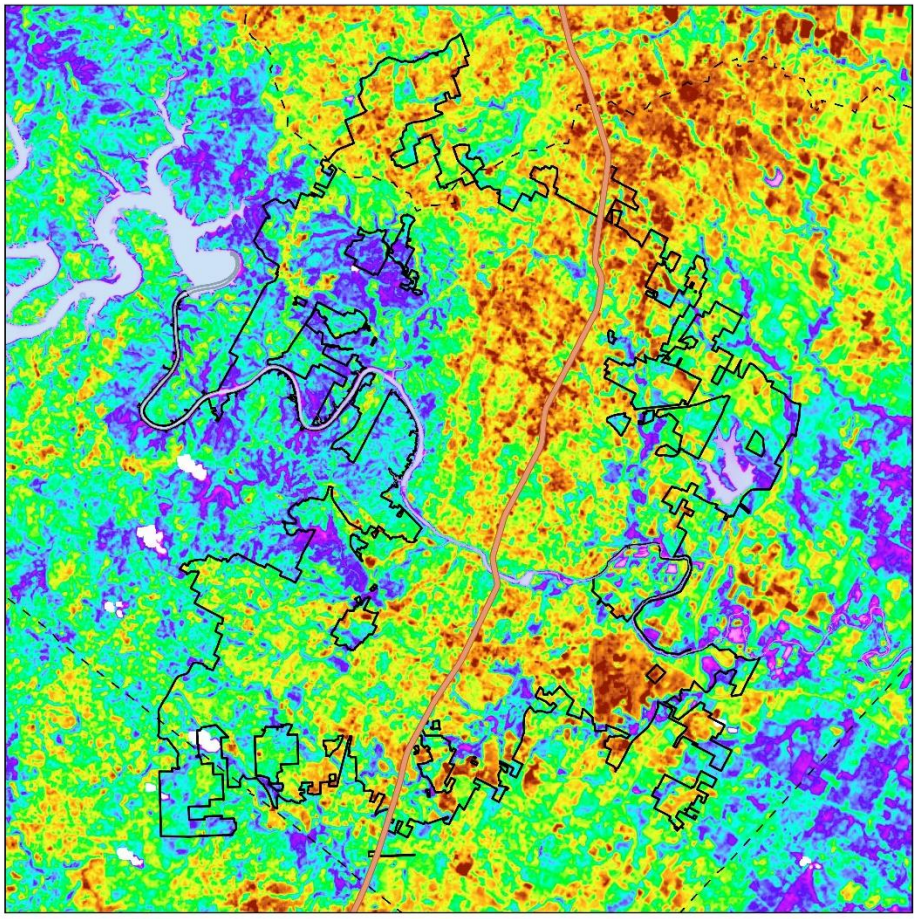
Legend
Land Surface Temperature (°C)
58.19
25.61
Interstate 35
County Boundaries
Austin City Limits
Water
N
0 2.5 5 10 Kilometers

08-11-2023

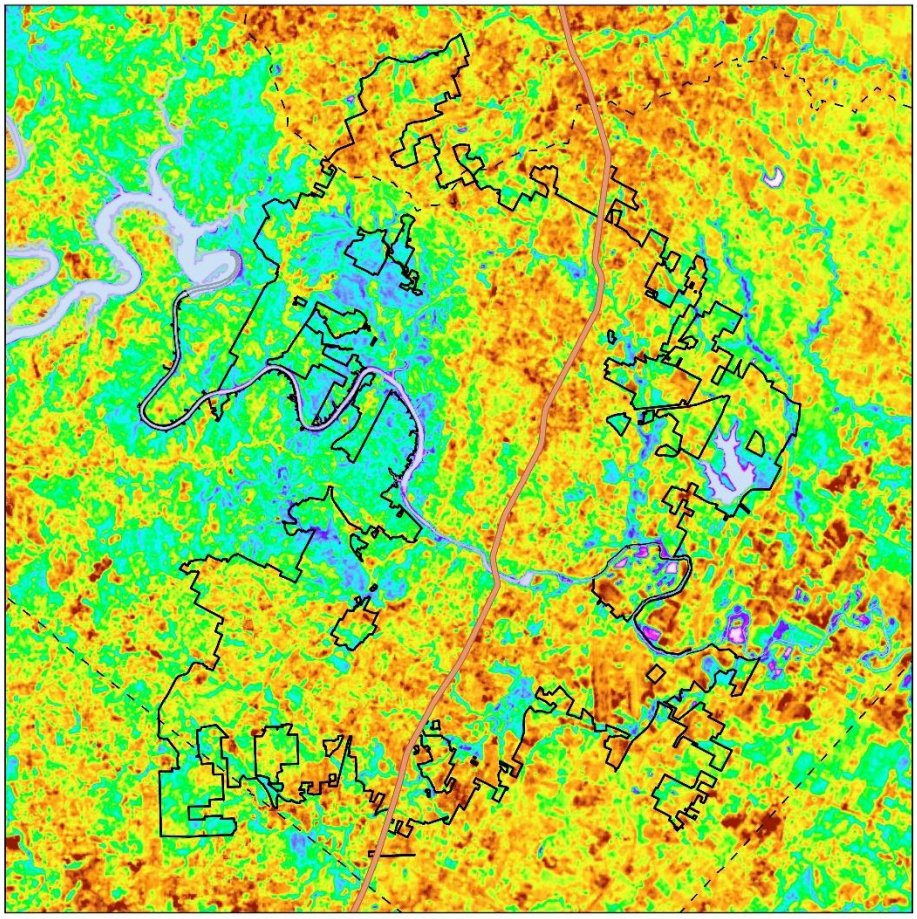

Legend

Land Surface Temperature (°C)

59.8854

30.8512

Interstate 35

County Boundaries

Austin City Limits

Water

N

0 2.5 5 10 Kilometers

Appendix B: Scale Maps

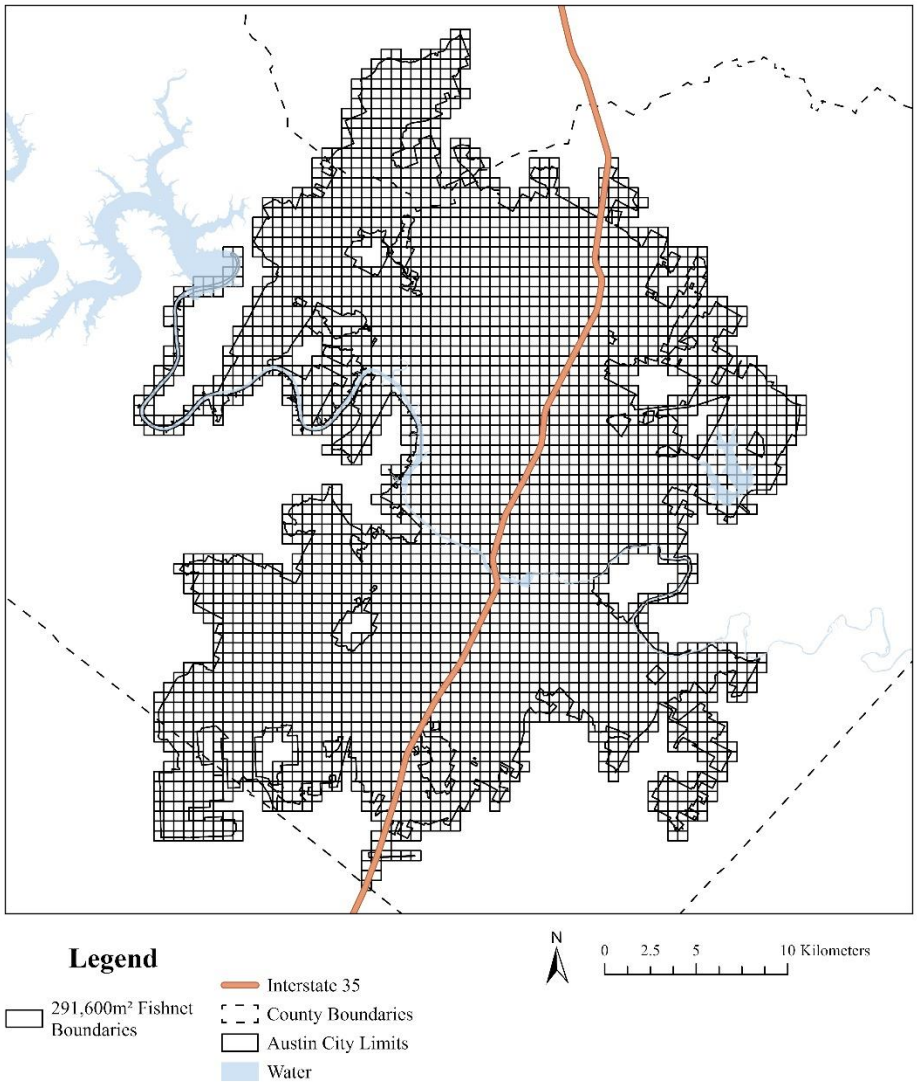

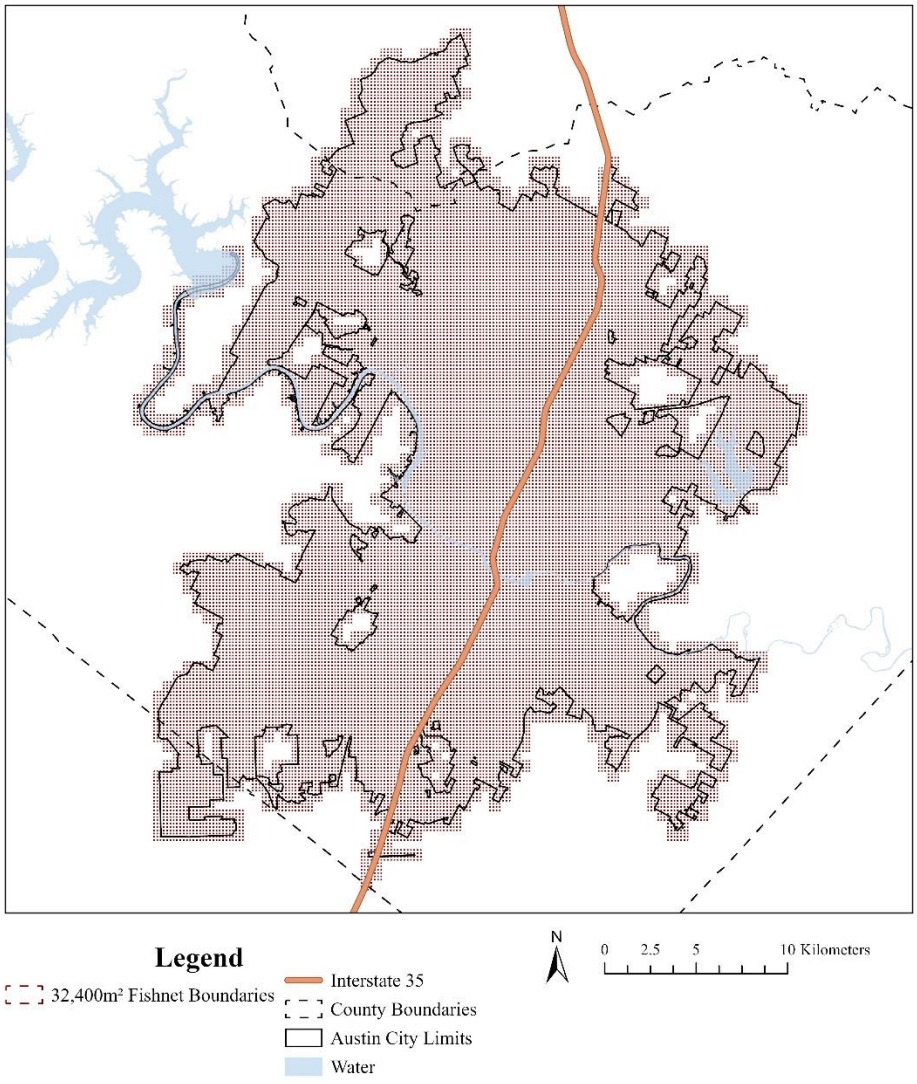
Legend
32,400m² Fishnet Boundaries
Interstate 35
County Boundaries
Austin City Limits
Water
N
0 2.5 5 10 Kilometers

Appendix C: LST Slope Map

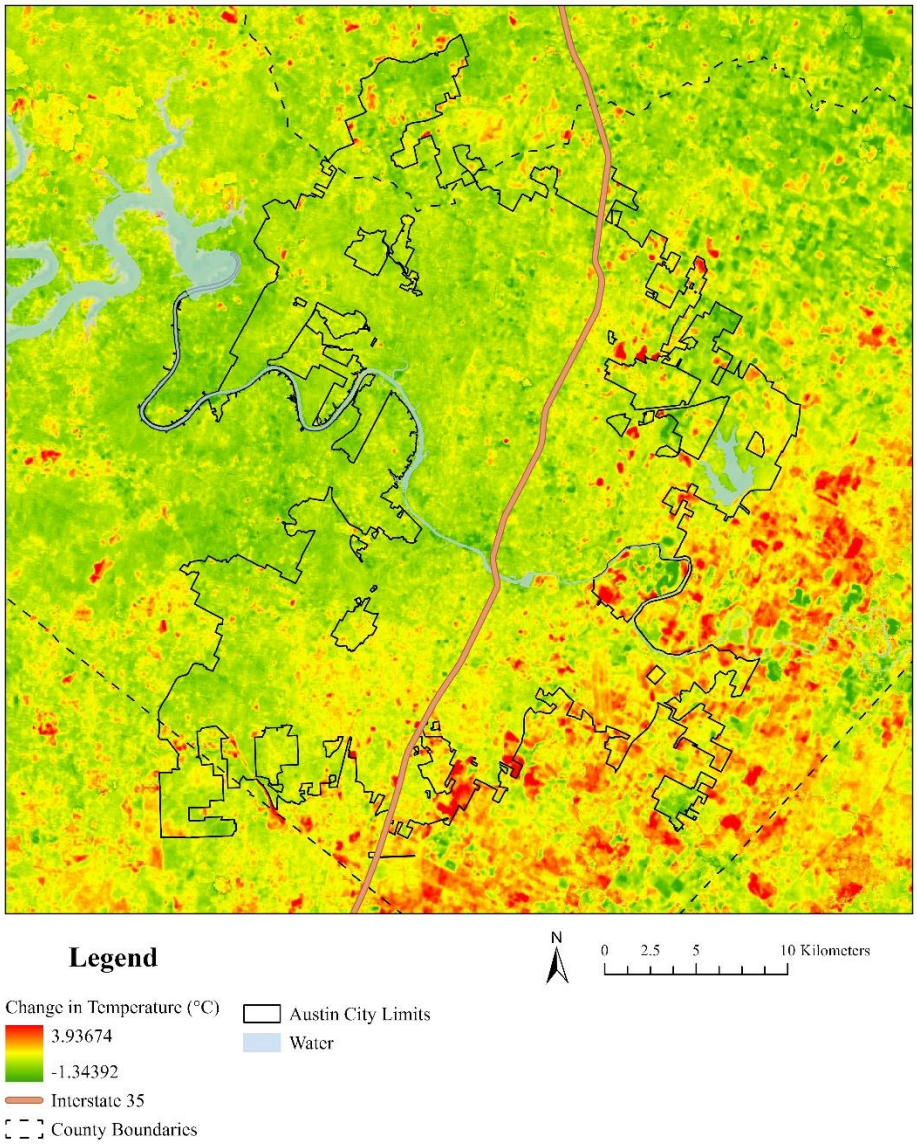

Appendix D: Tree removal maps

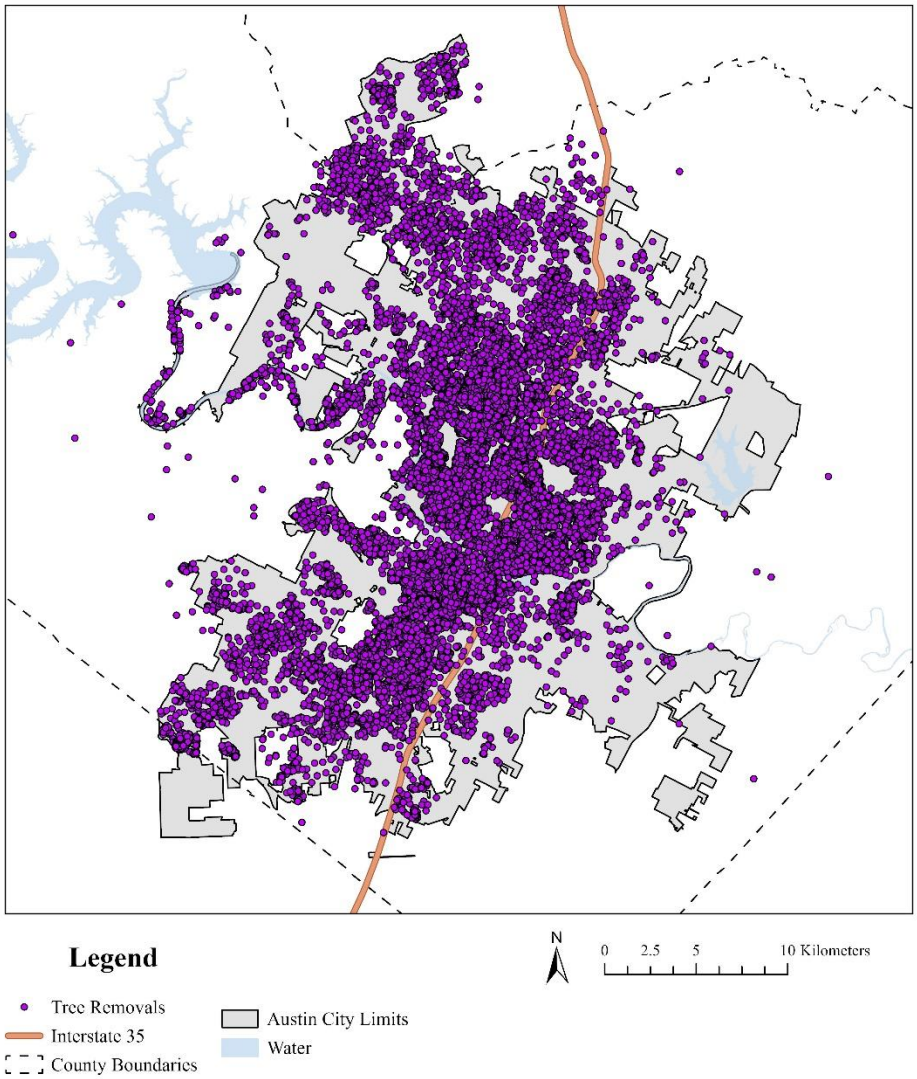

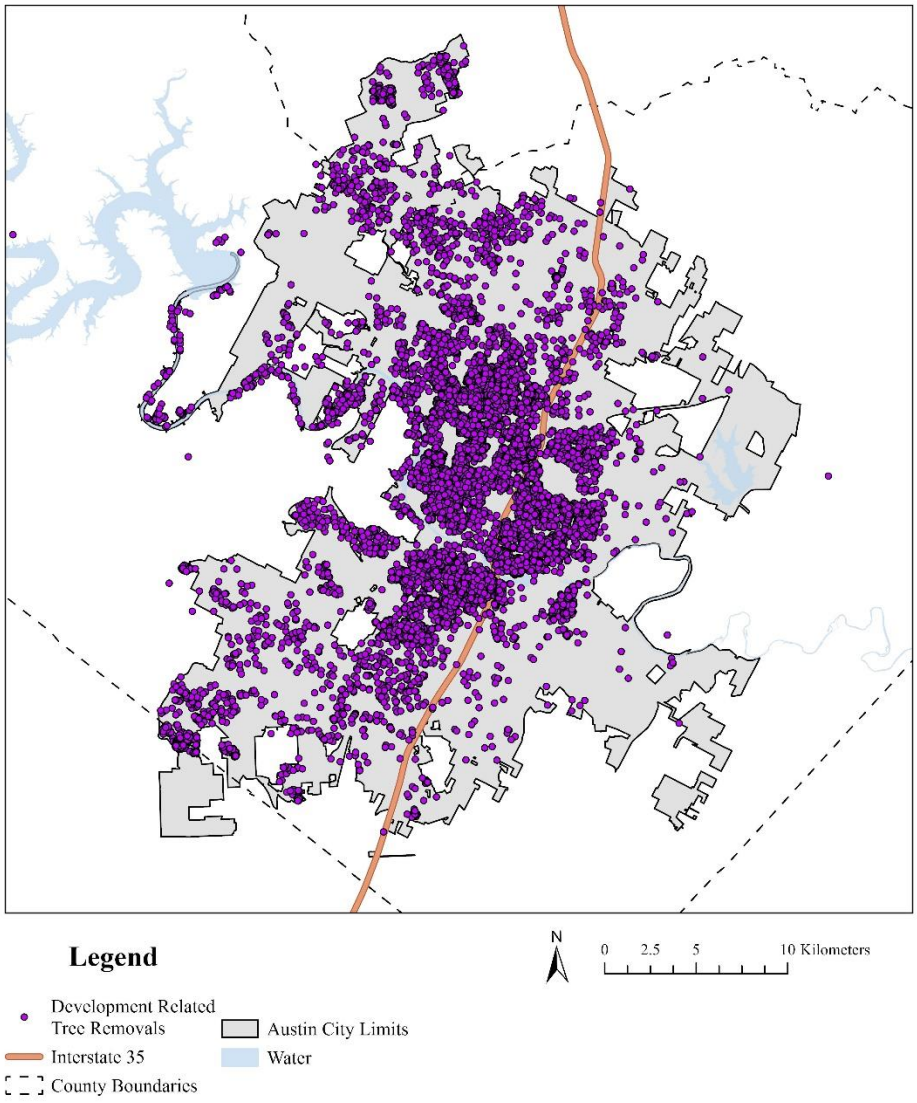
Legend
Development Related Tree Removals
Interstate 35
County Boundaries
Austin City Limits
Water
N
0 2.5 5 10 Kilometers

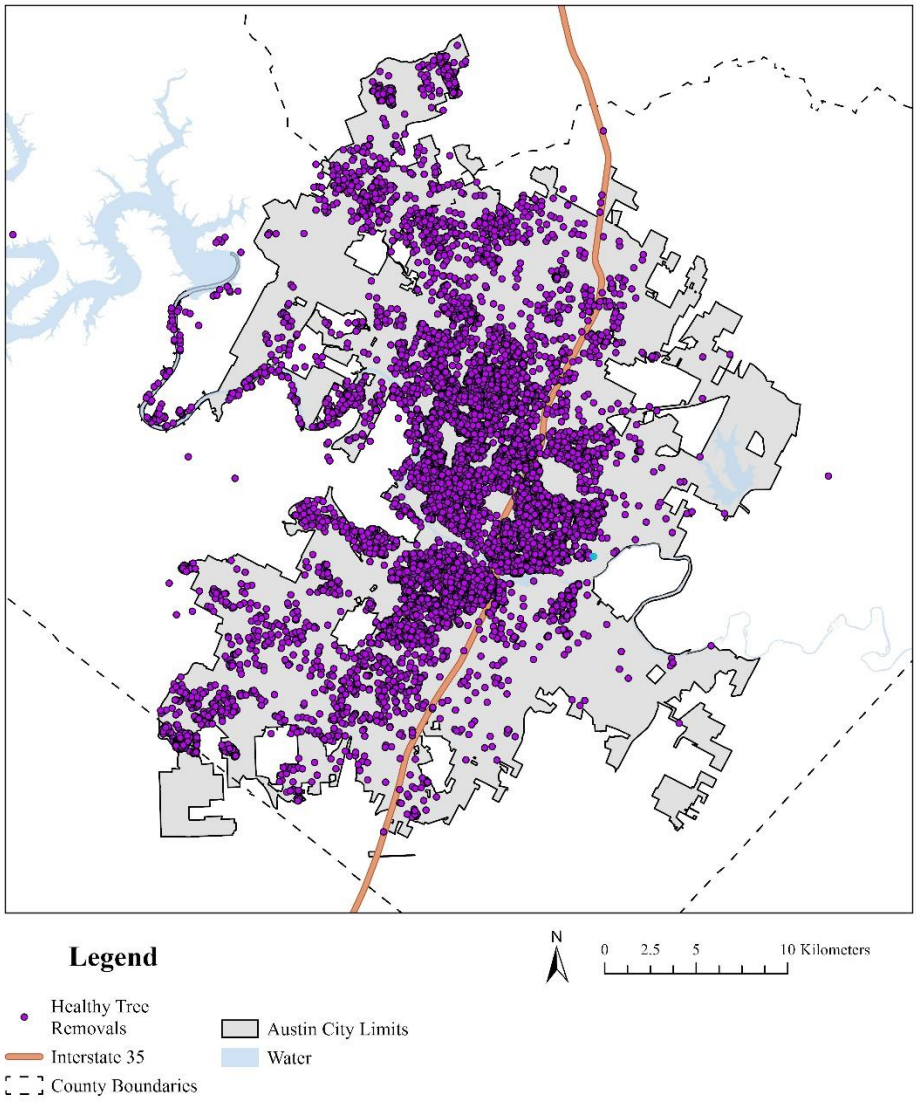
Legend
Healthy Tree Removals
Interstate 35
County Boundaries
Austin City Limits
Water
N
0 2.5 5 10 Kilometers

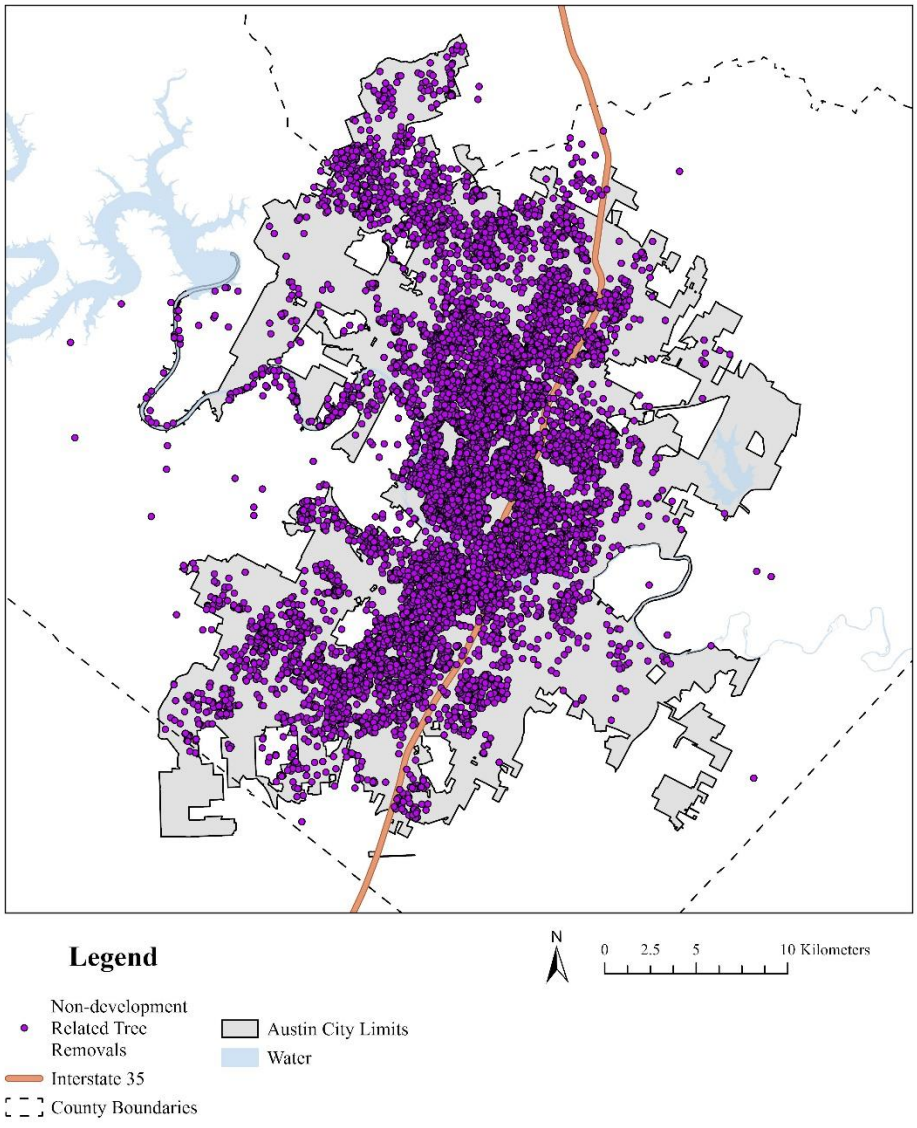
Legend
Non-development Related Tree Removals
Interstate 35
County Boundaries
Austin City Limits
Water
N
0 2.5 5 10 Kilometers

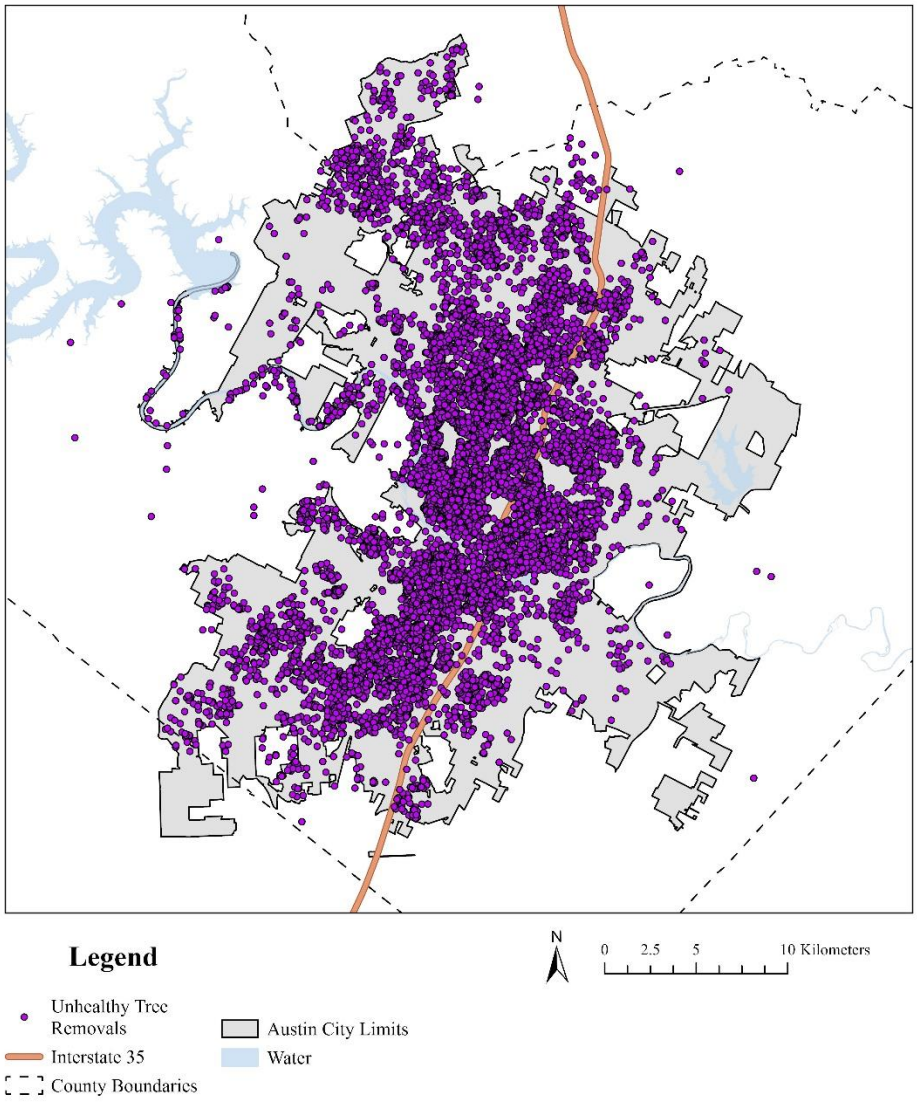
Legend
Unhealthy Tree Removals
Interstate 35
County Boundaries
Austin City Limits
Water
N
0 2.5 5 10 Kilometers

Appendix E: Tree Removal Distribution Maps

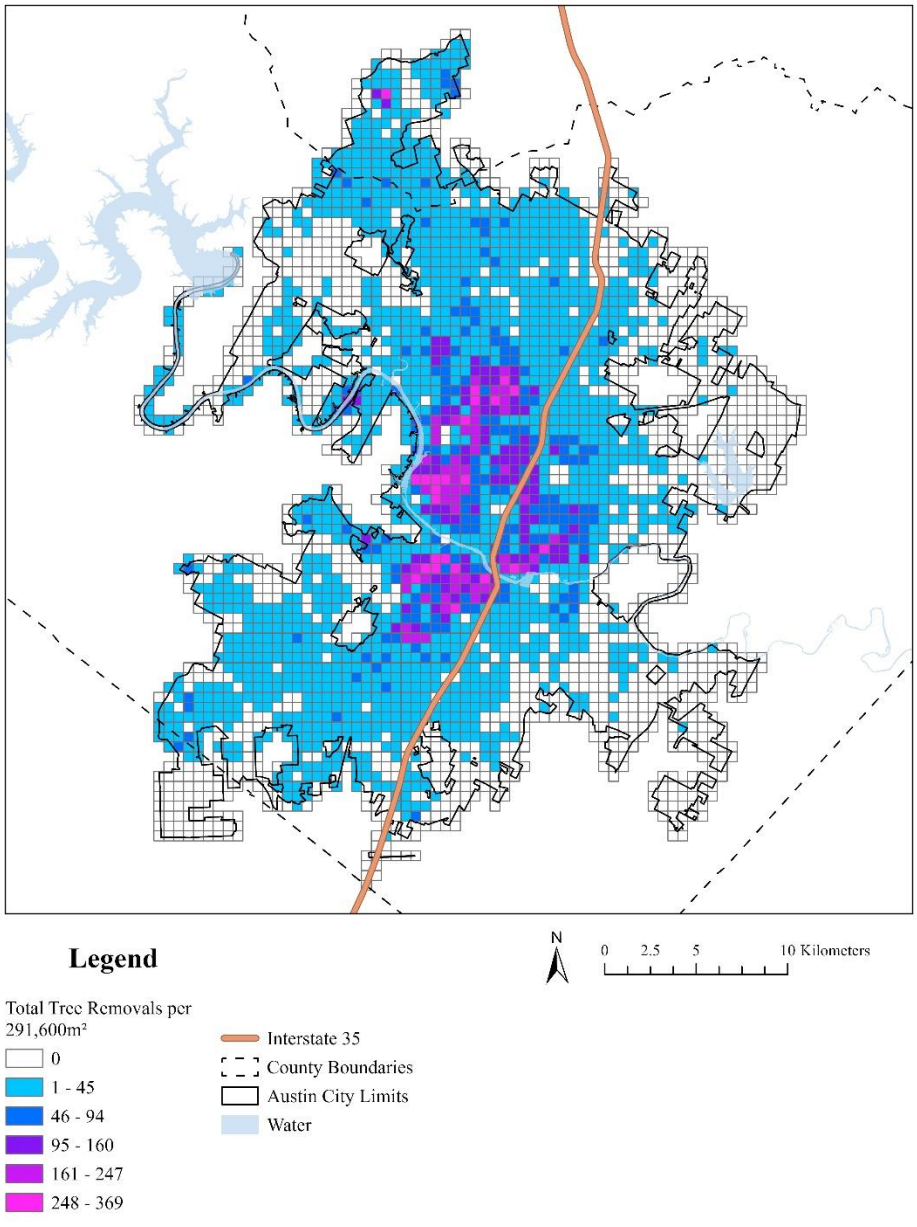

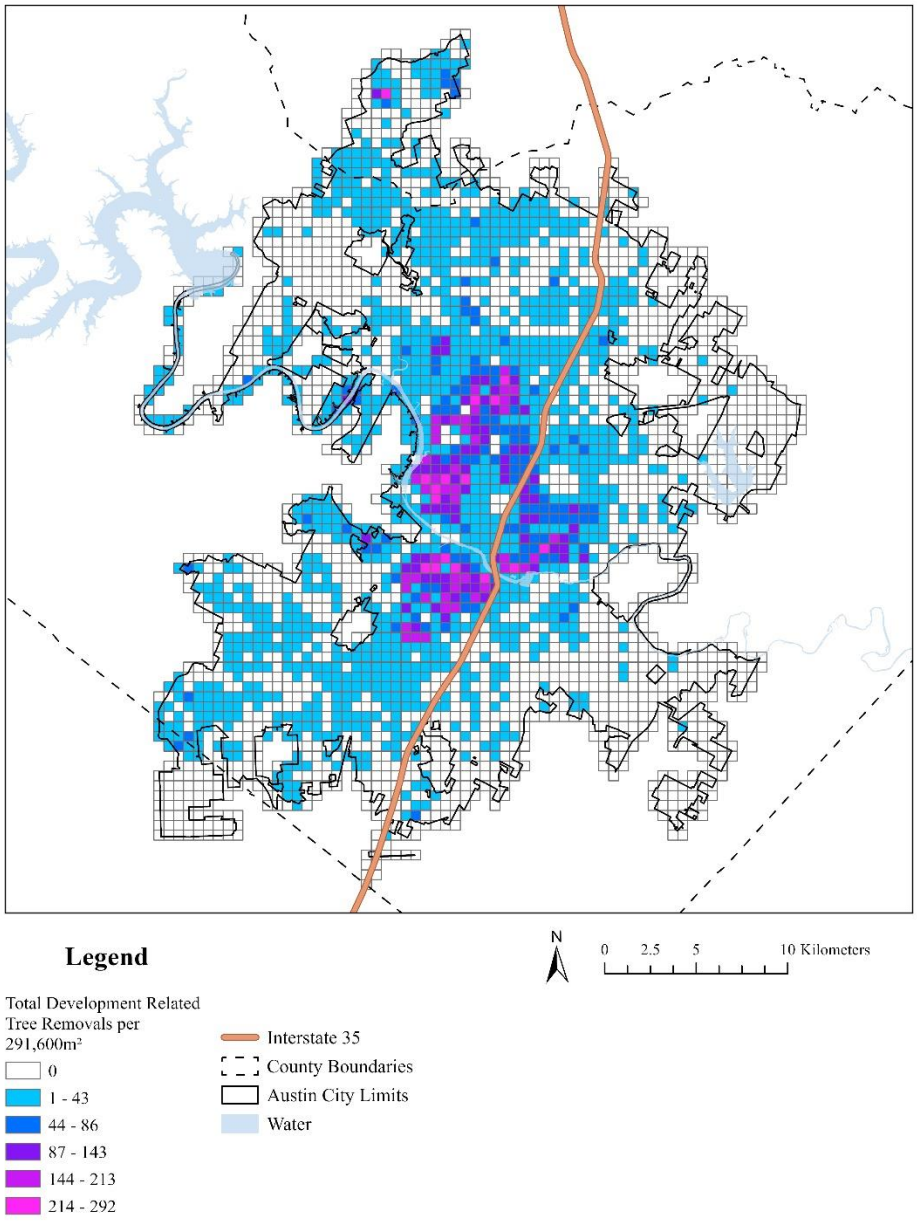
Legend
Total Development Related
Tree Removals per
291,600m²
0
1 - 43
44 - 86
87 - 143
144 - 213
214 - 292
Interstate 35
County Boundaries
Austin City Limits
Water
N
0 2.5 5 10 Kilometers

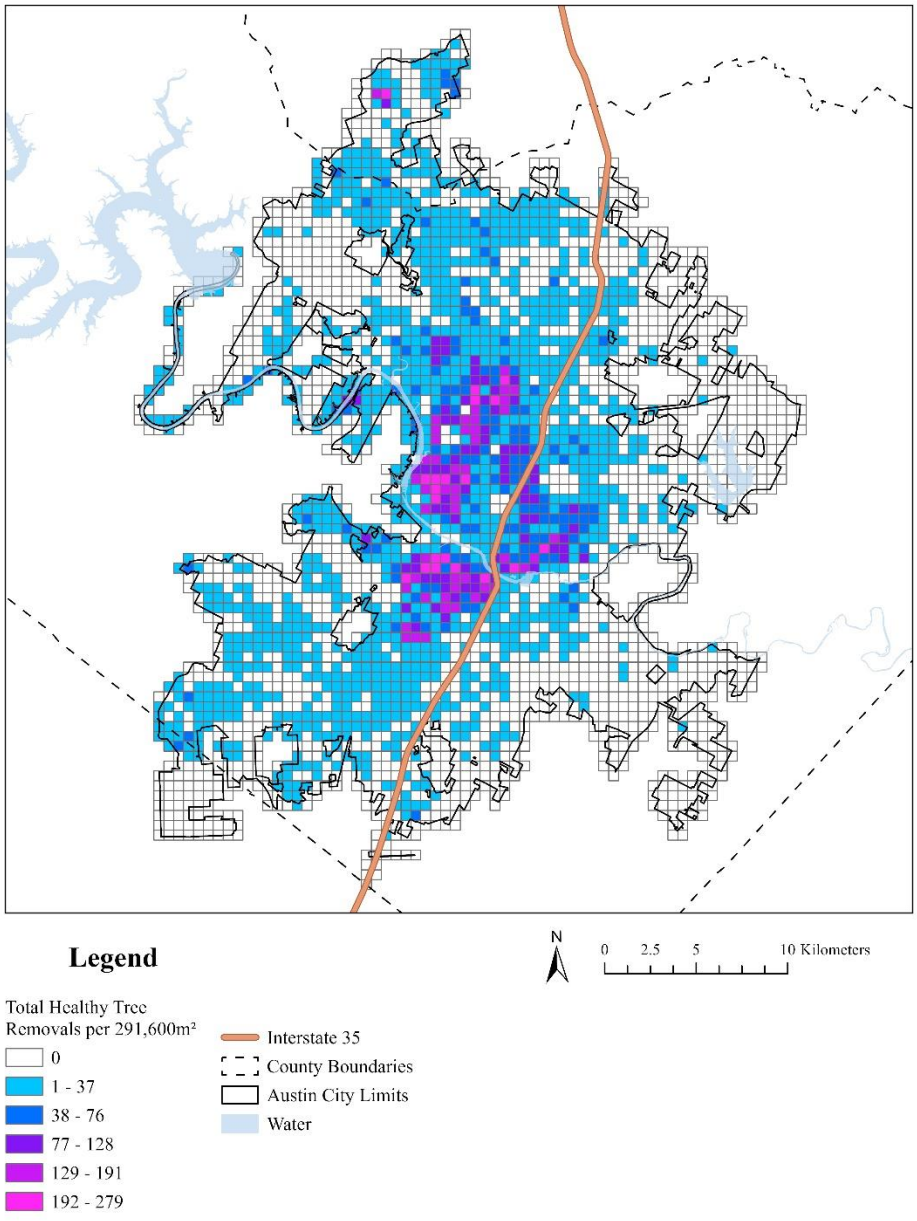
Legend
Total Healthy Tree Removals per 291,600m²
0
1 - 37
38 - 76
77 - 128
129 - 191
192 - 279
Interstate 35
County Boundaries
Austin City Limits
Water
N
0 2.5 5 10 Kilometers

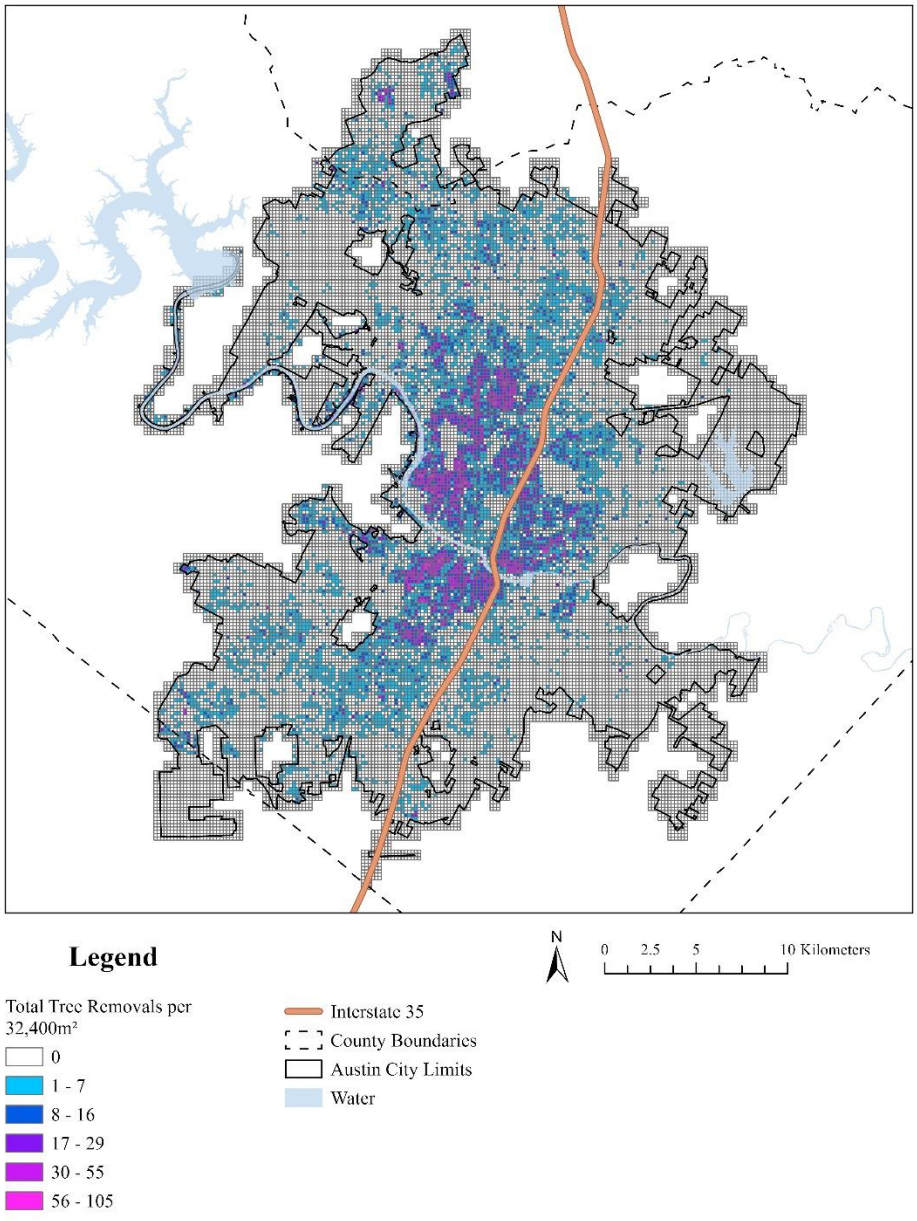
Legend
Total Tree Removals per 32,400m²
0
1 - 7
8 - 16
17 - 29
30 - 55
56 - 105
Interstate 35
County Boundaries
Austin City Limits
Water
N
0 2.5 5 10 Kilometers

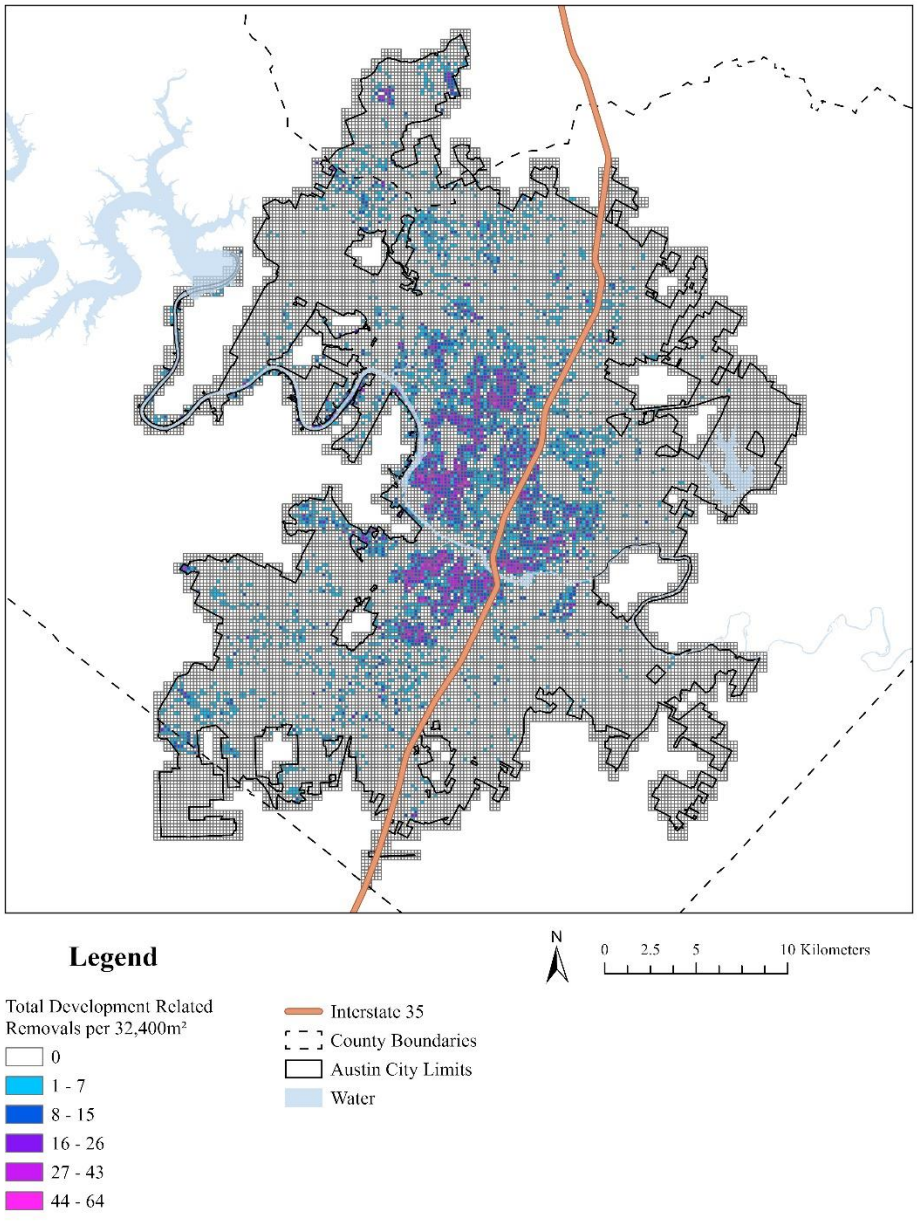
Legend
Total Development Related Removals per 32,400m²
0
1 - 7
8 - 15
16 - 26
27 - 43
44 - 64
Interstate 35
County Boundaries
Austin City Limits
Water
N
0 2.5 5 10 Kilometers

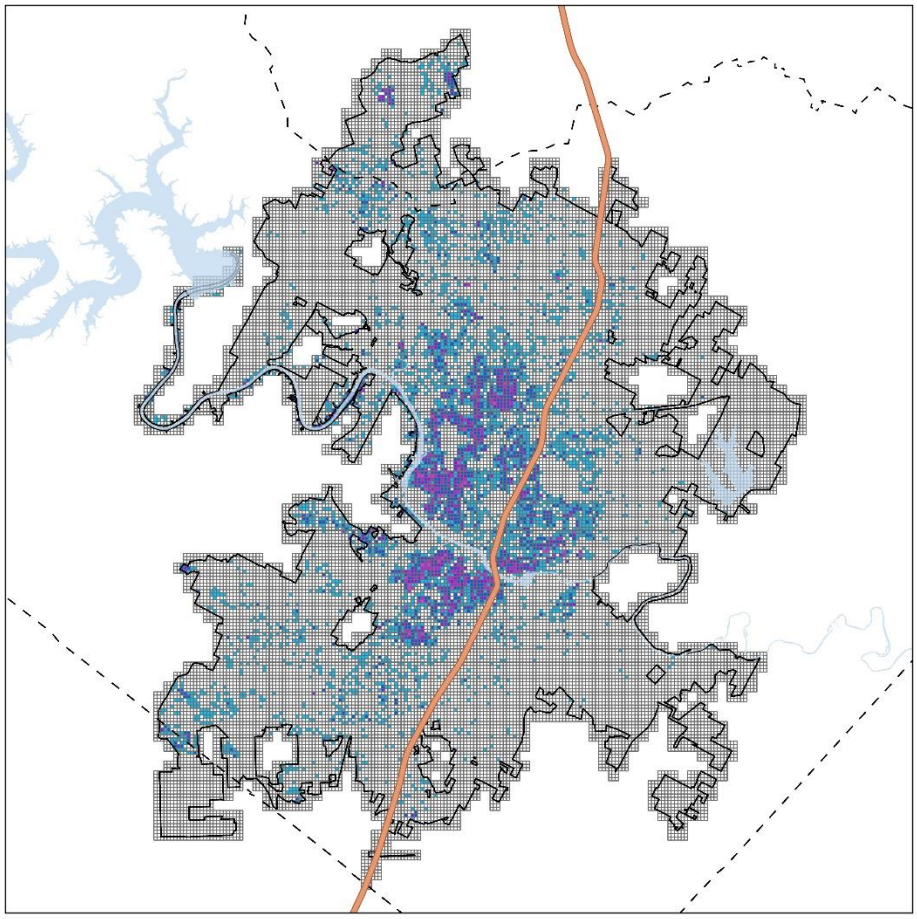

Legend

Total Healthy Tree Removals per 32,400m²

- 0
- 1 - 8
- 9 - 17
- 18 - 28
- 29 - 43
- 44 - 66

- Interstate 35
- County Boundaries
- Austin City Limits
- Water

N

0 2.5 5 10 Kilometers

Appendix F: Canopy Cover Distribution Maps

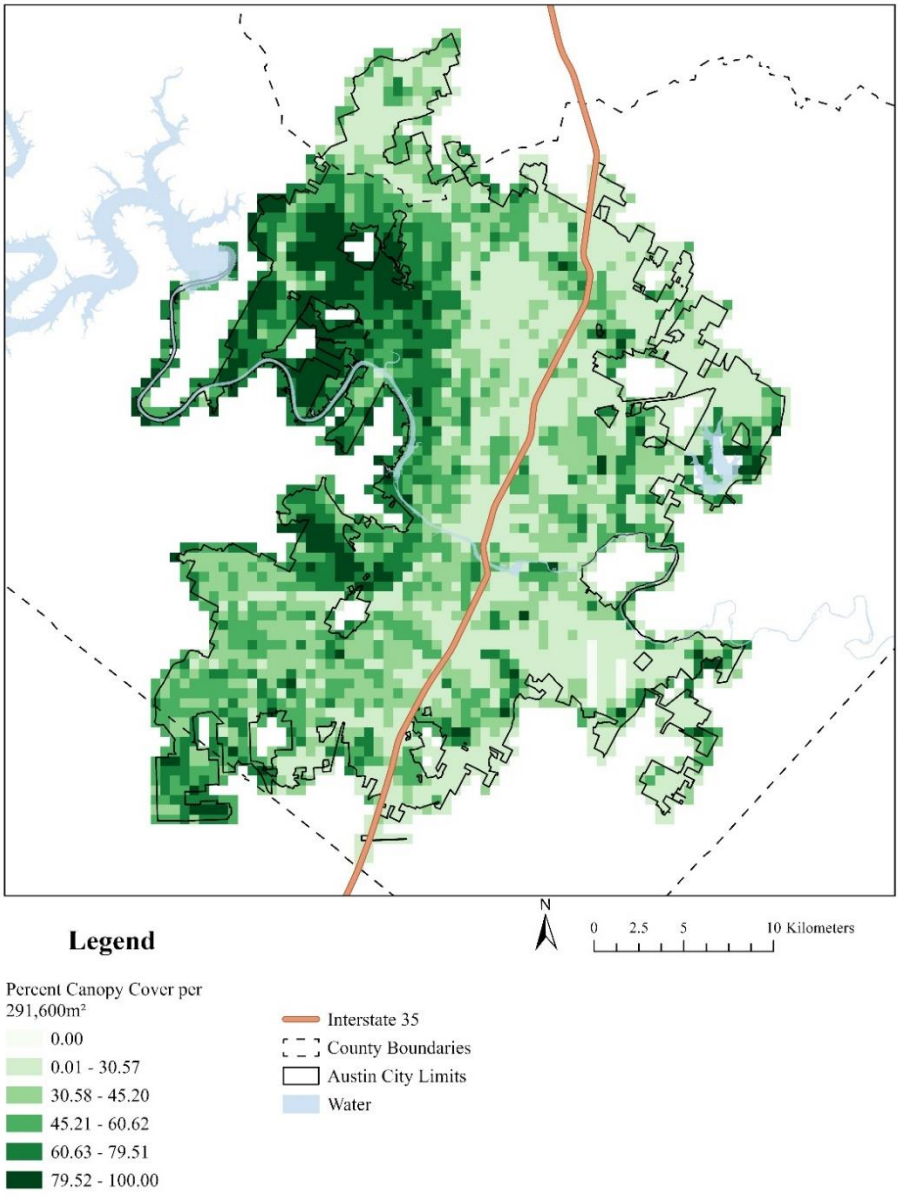

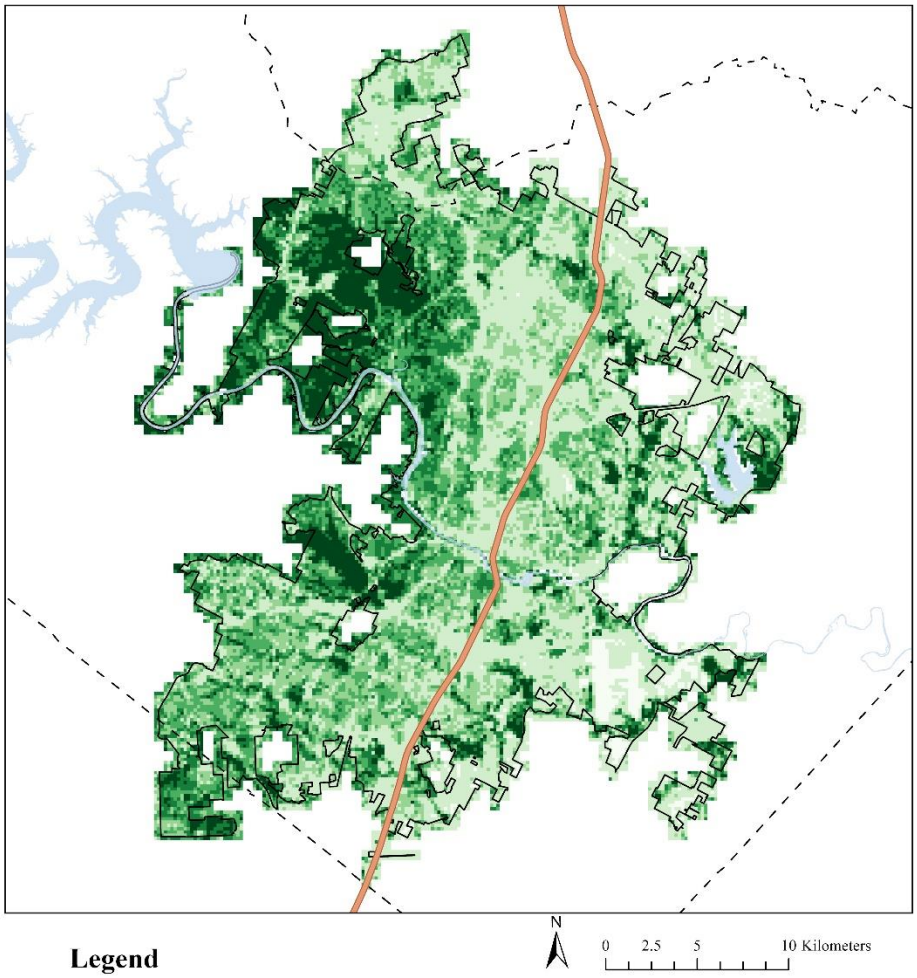
N
0 2.5 5 10 Kilometers
Legend
Percent Canopy Cover per 32,400m²
0.00
0.01 - 28.47
28.48 - 44.56
44.57 - 62.07
62.08 - 82.94
82.95 - 100.00
Interstate 35
County Boundaries
Austin City Limits
Water

Appendix F: Impervious cover classification distribution maps

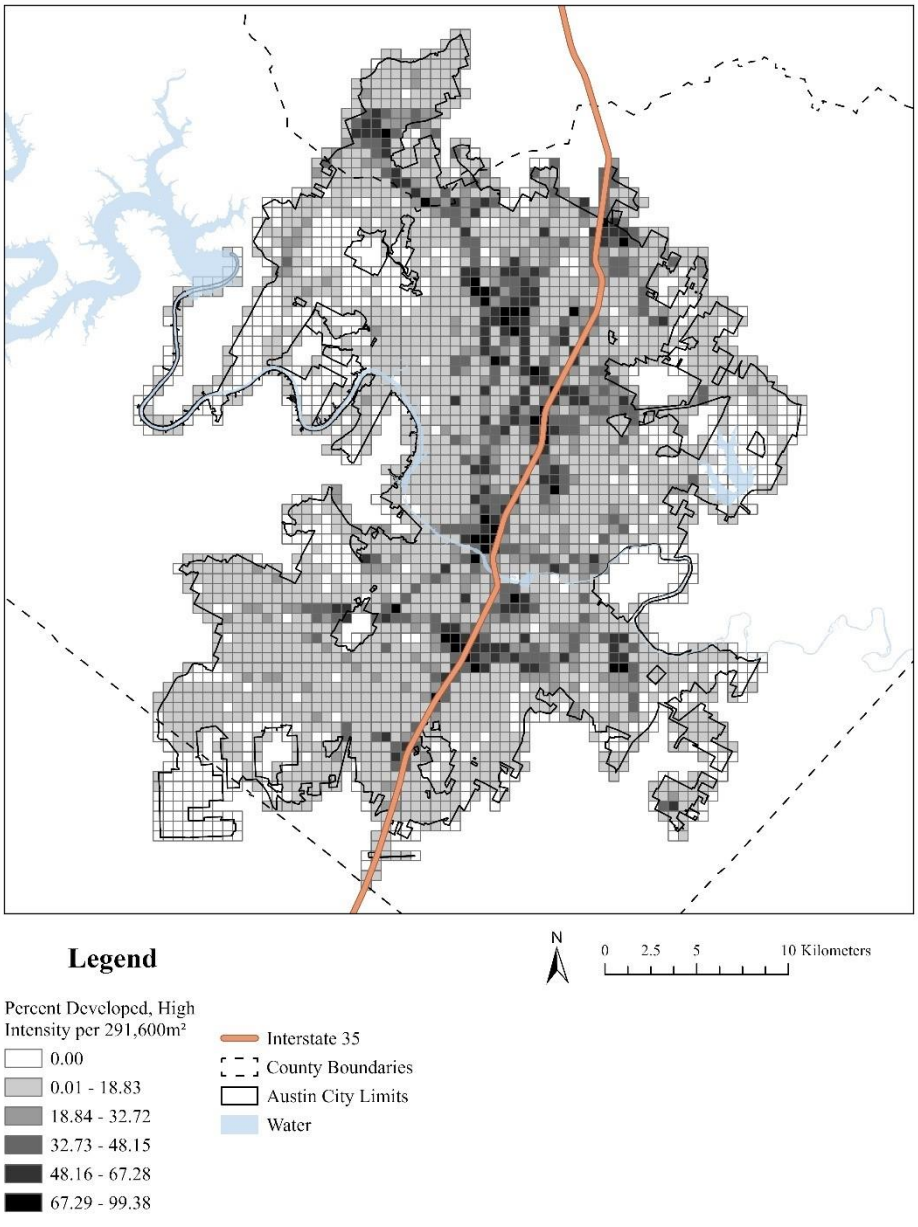

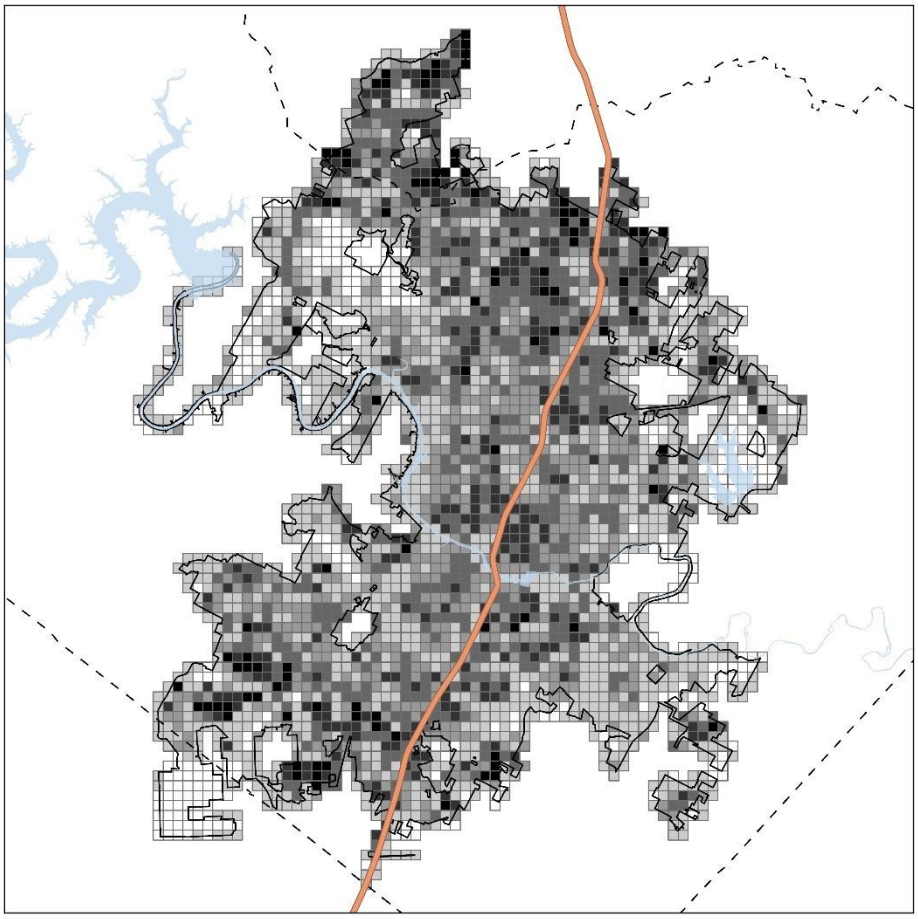
Legend
Percent Developed, Medium Intensity per 291,600m²
0.00
0.01 - 18.21
18.22 - 28.09
28.10 - 38.27
38.28 - 51.23
51.24 - 81.17
Interstate 35
County Boundaries
Austin City Limits
Water
N
0 2.5 5 10 Kilometers

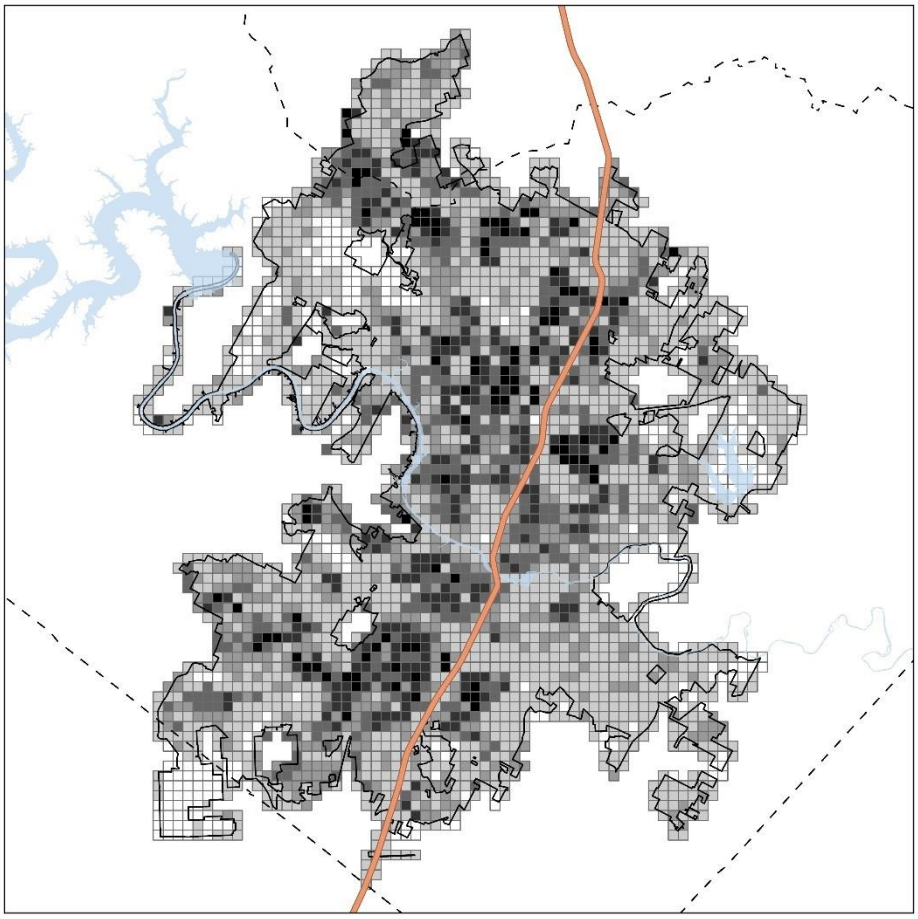

Legend

Percent Developed, Low Intensity per 291,600m²

- 0.00
- 0.01 - 15.12
- 15.13 - 25.00
- 25.01 - 36.11
- 36.12 - 49.38
- 49.39 - 72.53

- Interstate 35
- County Boundaries
- Austin City Limits
- Water

N

0 2.5 5 10 Kilometers

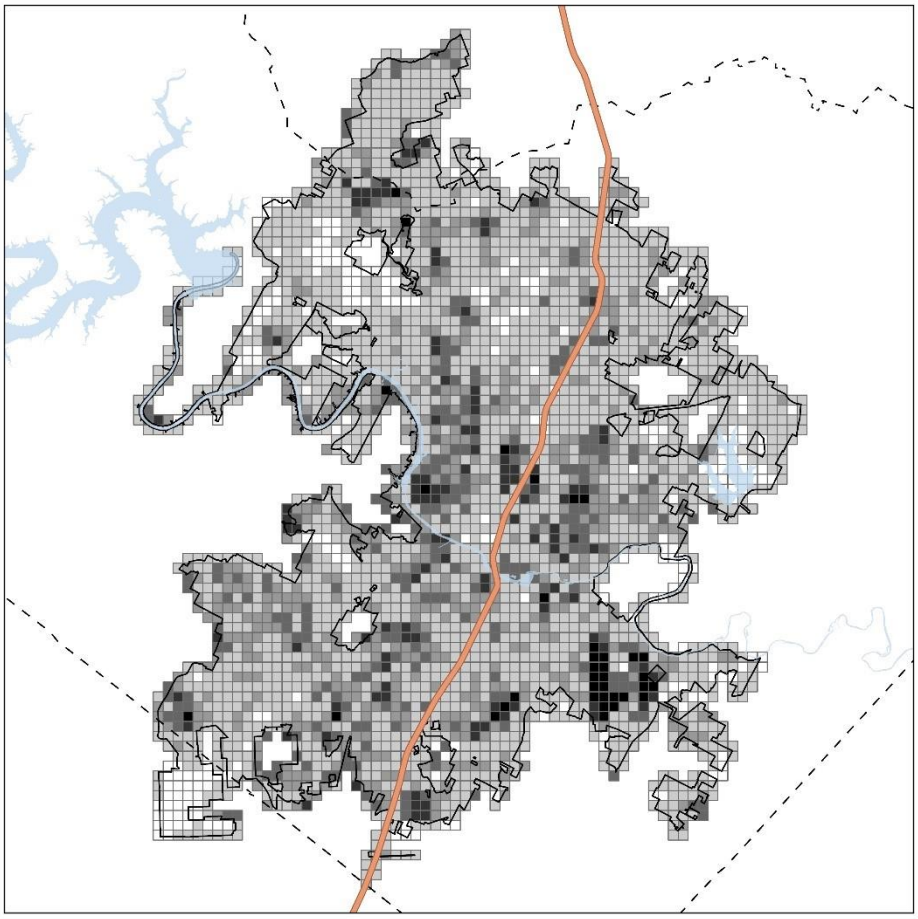
Legend
Percent Developed, Open Space per 291,600m²
0.00
0.01 - 12.65
12.66 - 21.60
21.61 - 33.64
33.65 - 53.09
53.10 - 92.59
Interstate 35
County Boundaries
Austin City Limits
Water
N
0 2.5 5 10 Kilometers

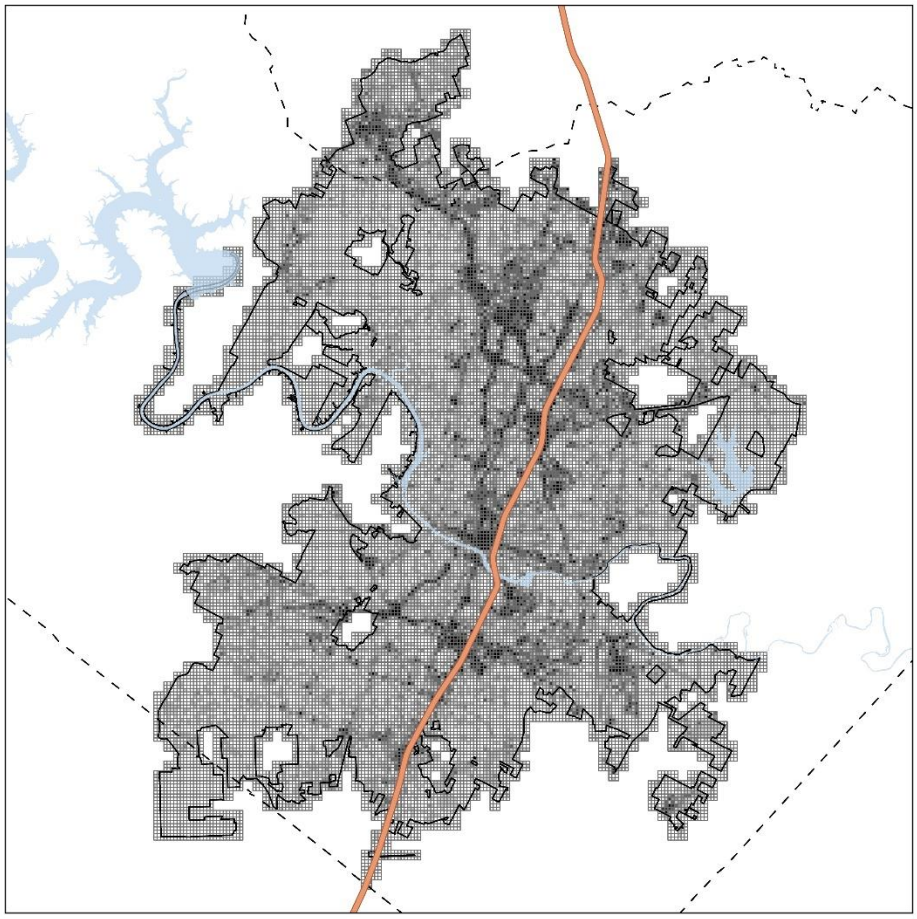
Legend
Percent Developed, High Intensity 32,400m²
0.00
0.01 - 22.22
22.23 - 41.67
41.68 - 61.11
61.12 - 80.56
80.57 - 100.00
Interstate 35
County Boundaries
Austin City Limits
Water
N
0 2.5 5 10 Kilometers

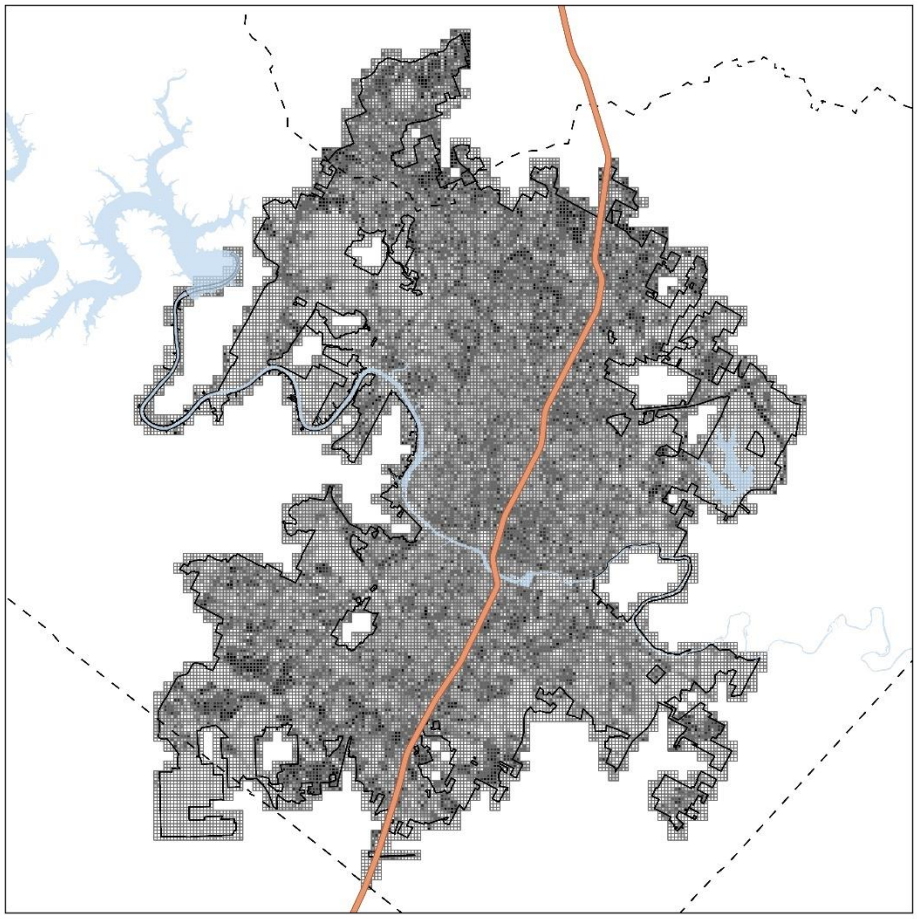

Legend

Percent Developed, Medium Intensity per 32,400m²

- 0.00
- 0.01 - 22.22
- 22.23 - 38.89
- 38.90 - 55.56
- 55.57 - 72.22
- 72.23 - 97.22

- Interstate 35
- County Boundaries
- Austin City Limits
- Water

N

0 2.5 5 10 Kilometers

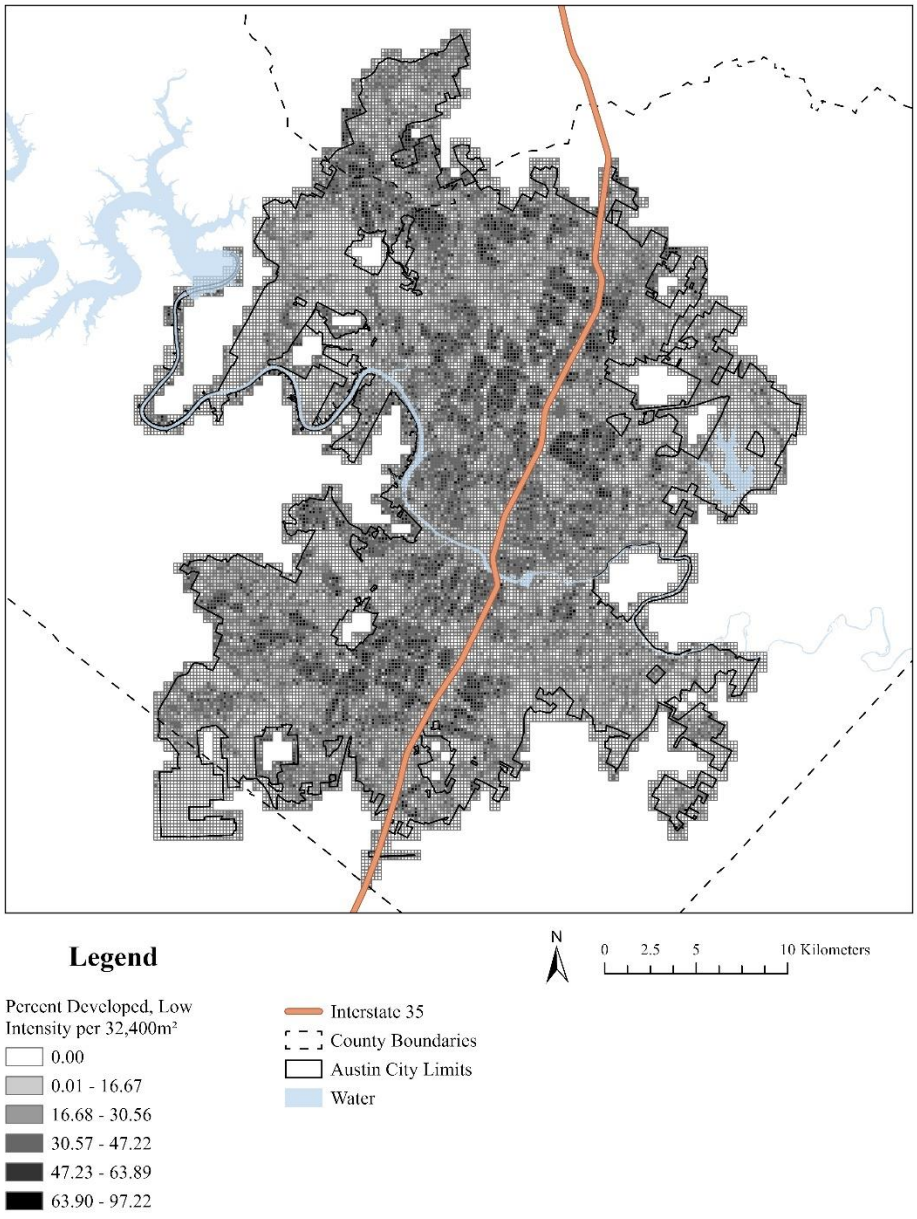
Legend
Percent Developed, Low Intensity per 32,400m²
0.00
0.01 - 16.67
16.68 - 30.56
30.57 - 47.22
47.23 - 63.89
63.90 - 97.22
Interstate 35
County Boundaries
Austin City Limits
Water
N
0 2.5 5 10 Kilometers

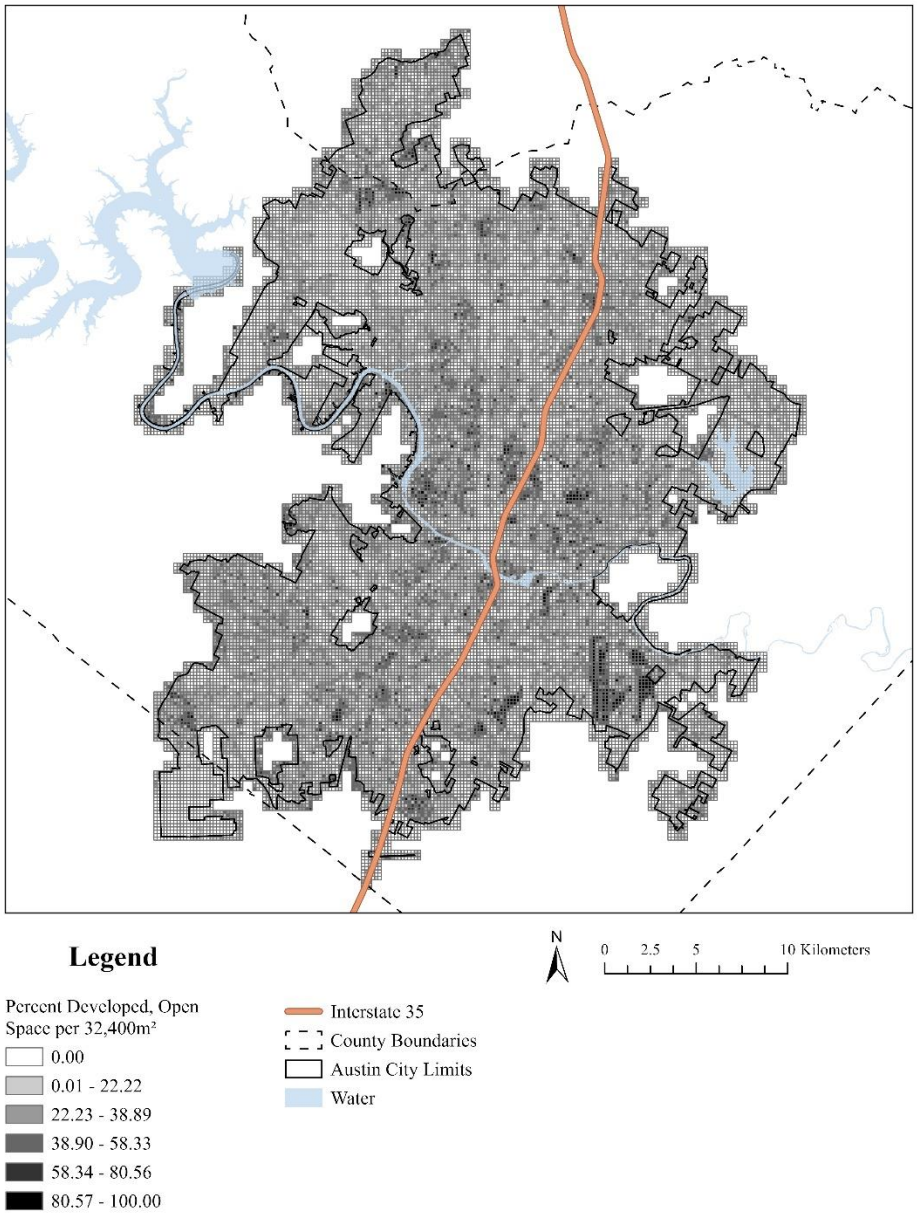
Legend
Percent Developed, Open Space per 32,400m²
0.00
0.01 - 22.22
22.23 - 38.89
38.90 - 58.33
58.34 - 80.56
80.57 - 100.00
Interstate 35
County Boundaries
Austin City Limits
Water
N
0 2.5 5 10 Kilometers

Appendix G: LST Slope Distribution maps

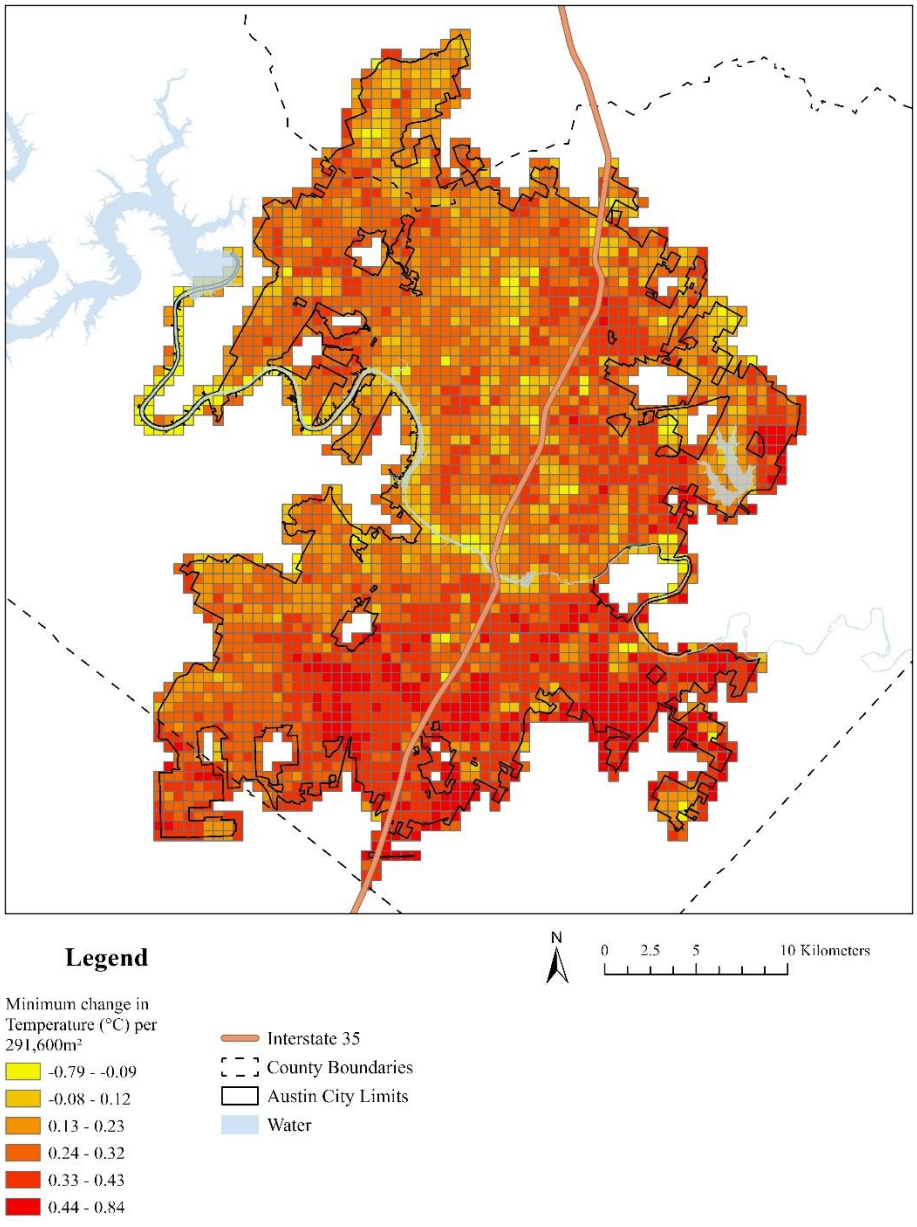

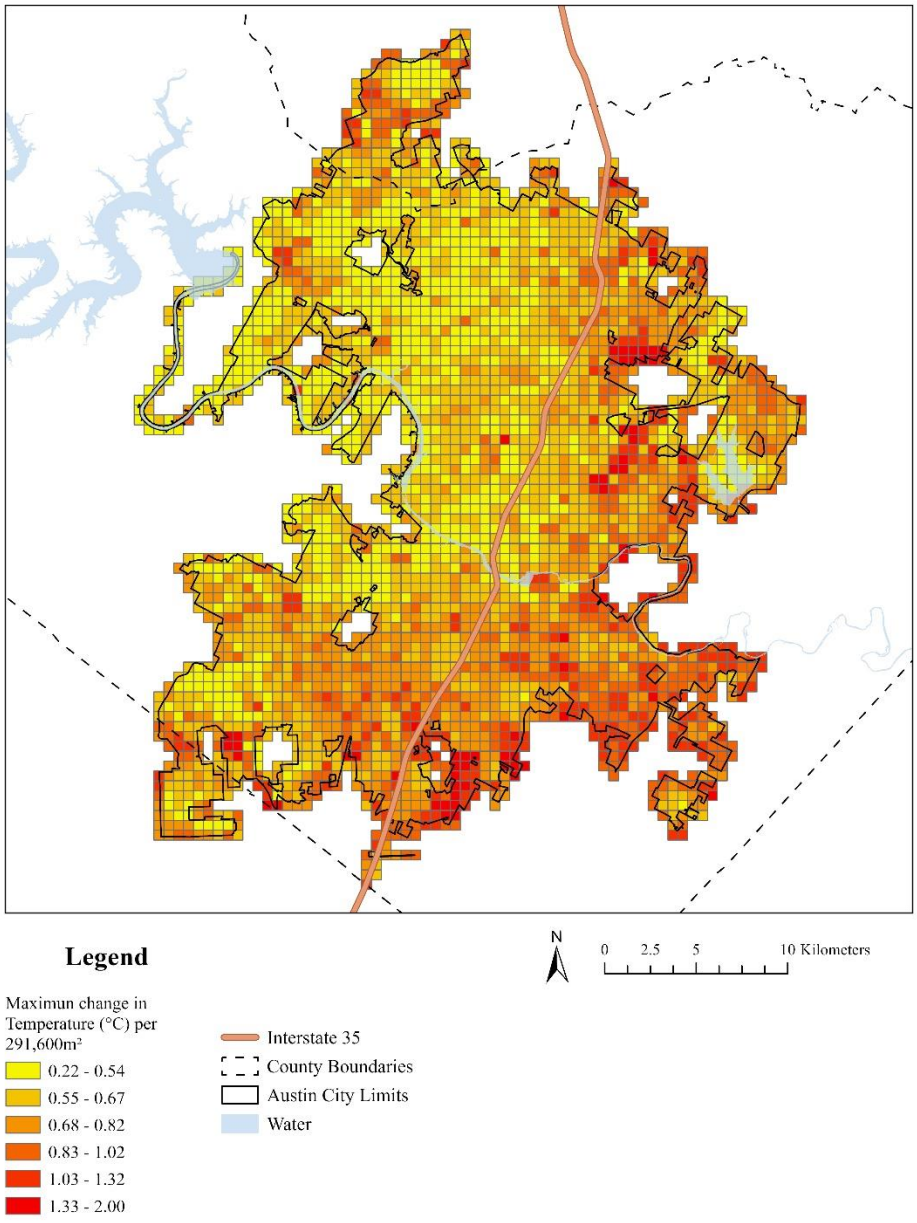
Legend
Maximun change in Temperature (°C) per 291,600m²
0.22 - 0.54
0.55 - 0.67
0.68 - 0.82
0.83 - 1.02
1.03 - 1.32
1.33 - 2.00
Interstate 35
County Boundaries
Austin City Limits
Water
N
0 2.5 5 10 Kilometers

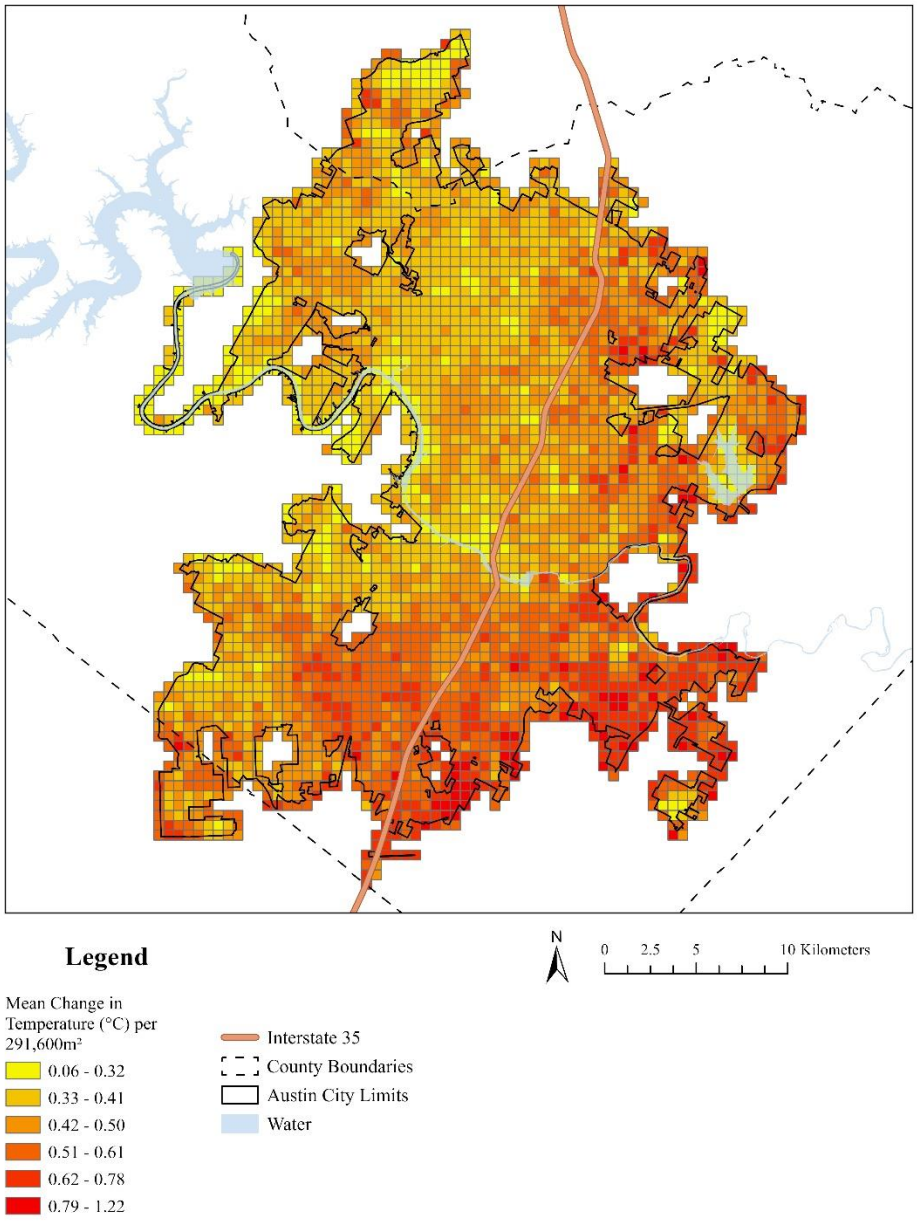
Legend
Mean Change in Temperature (°C) per 291,600m²
0.06 - 0.32
0.33 - 0.41
0.42 - 0.50
0.51 - 0.61
0.62 - 0.78
0.79 - 1.22
Interstate 35
County Boundaries
Austin City Limits
Water
N
0 2.5 5 10 Kilometers

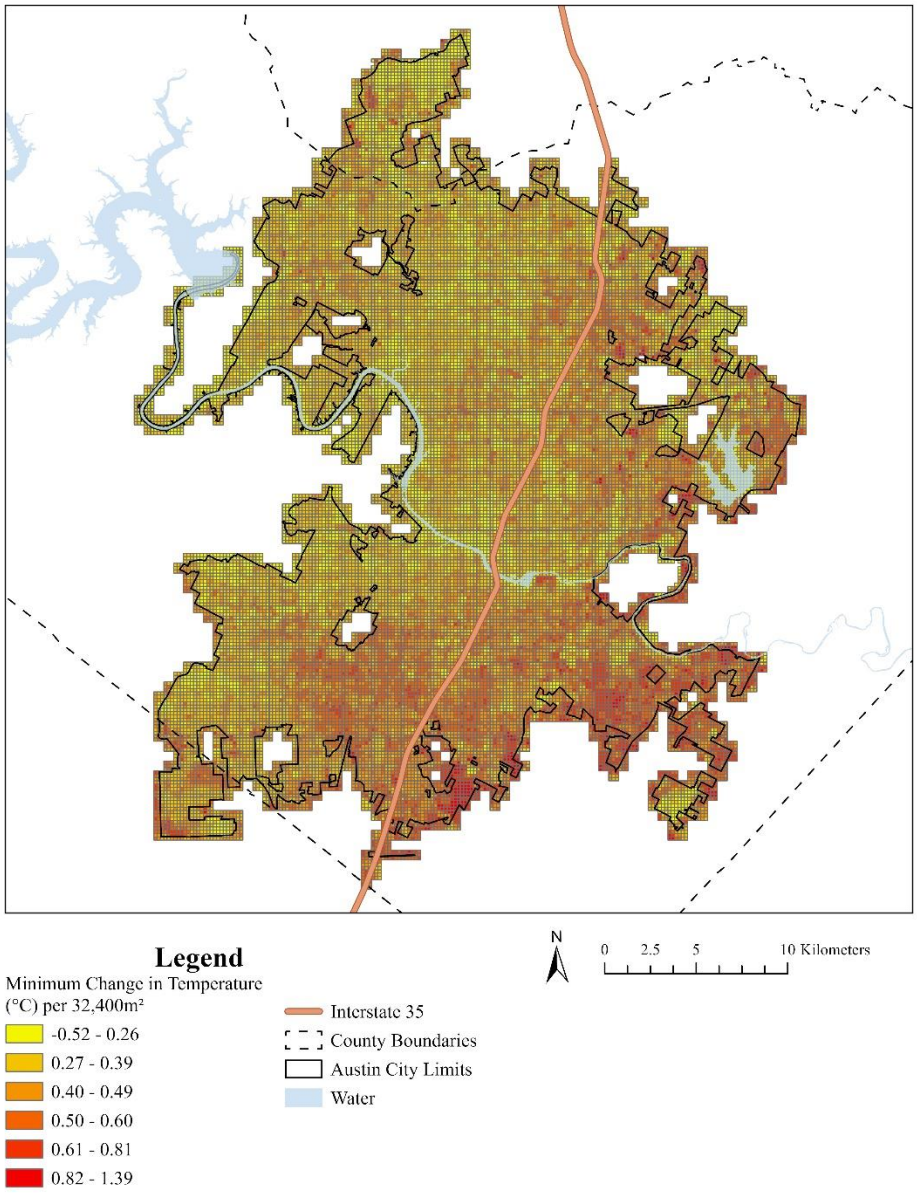
Legend
Minimum Change in Temperature
(°C) per 32,400m²
-0.52 - 0.26
0.27 - 0.39
0.40 - 0.49
0.50 - 0.60
0.61 - 0.81
0.82 - 1.39
Interstate 35
County Boundaries
Austin City Limits
Water
N
0 2.5 5 10 Kilometers

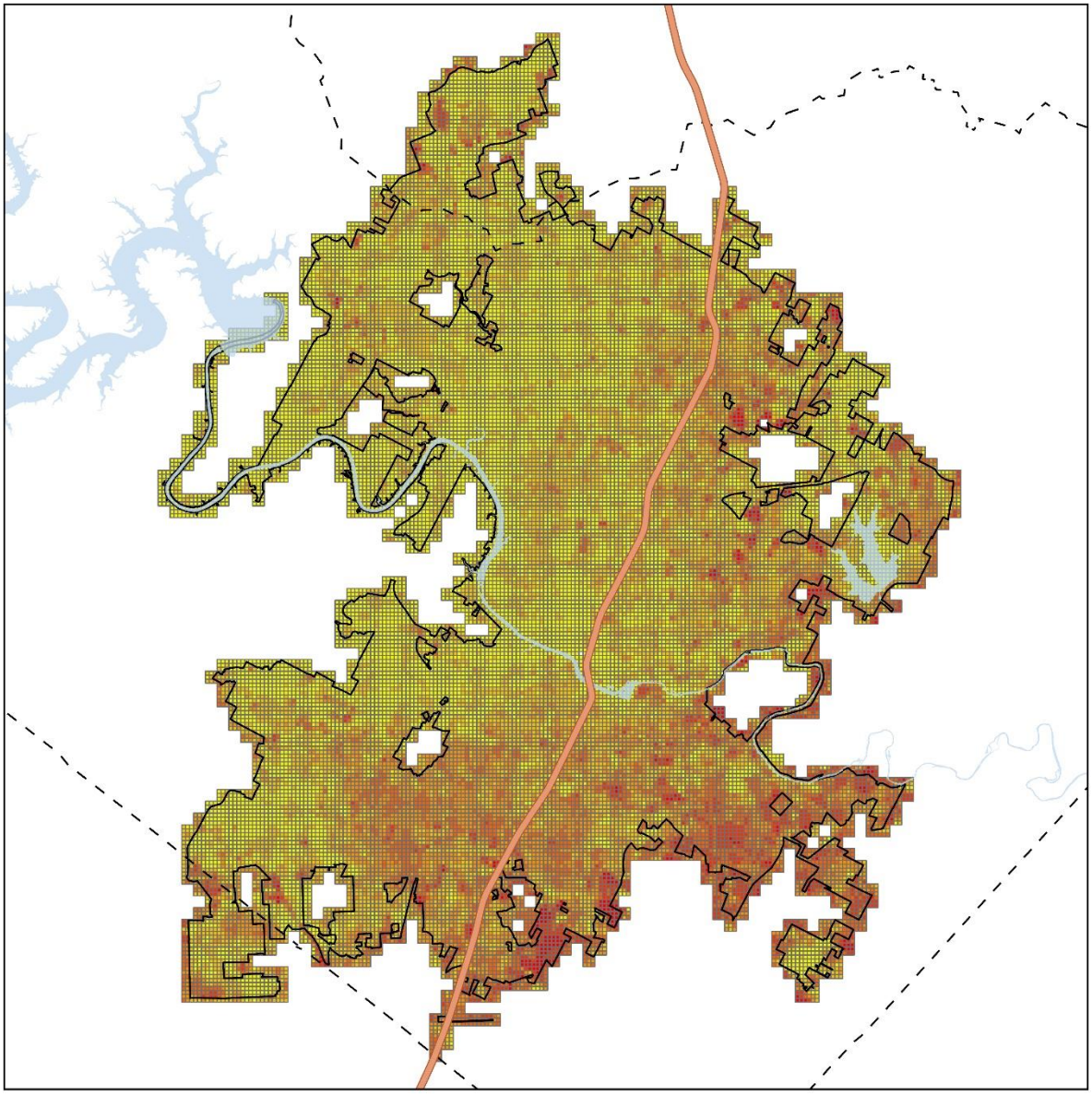
Legend
Mean Change in Temperature
(°C) per 32,400m²
-0.22 - 0.41
0.42 - 0.51
0.52 - 0.61
0.62 - 0.75
0.76 - 0.99
1.00 - 1.52
Interstate 35
County Boundaries
Austin City Limits
Water
N
0 2.5 5 10 Kilometers

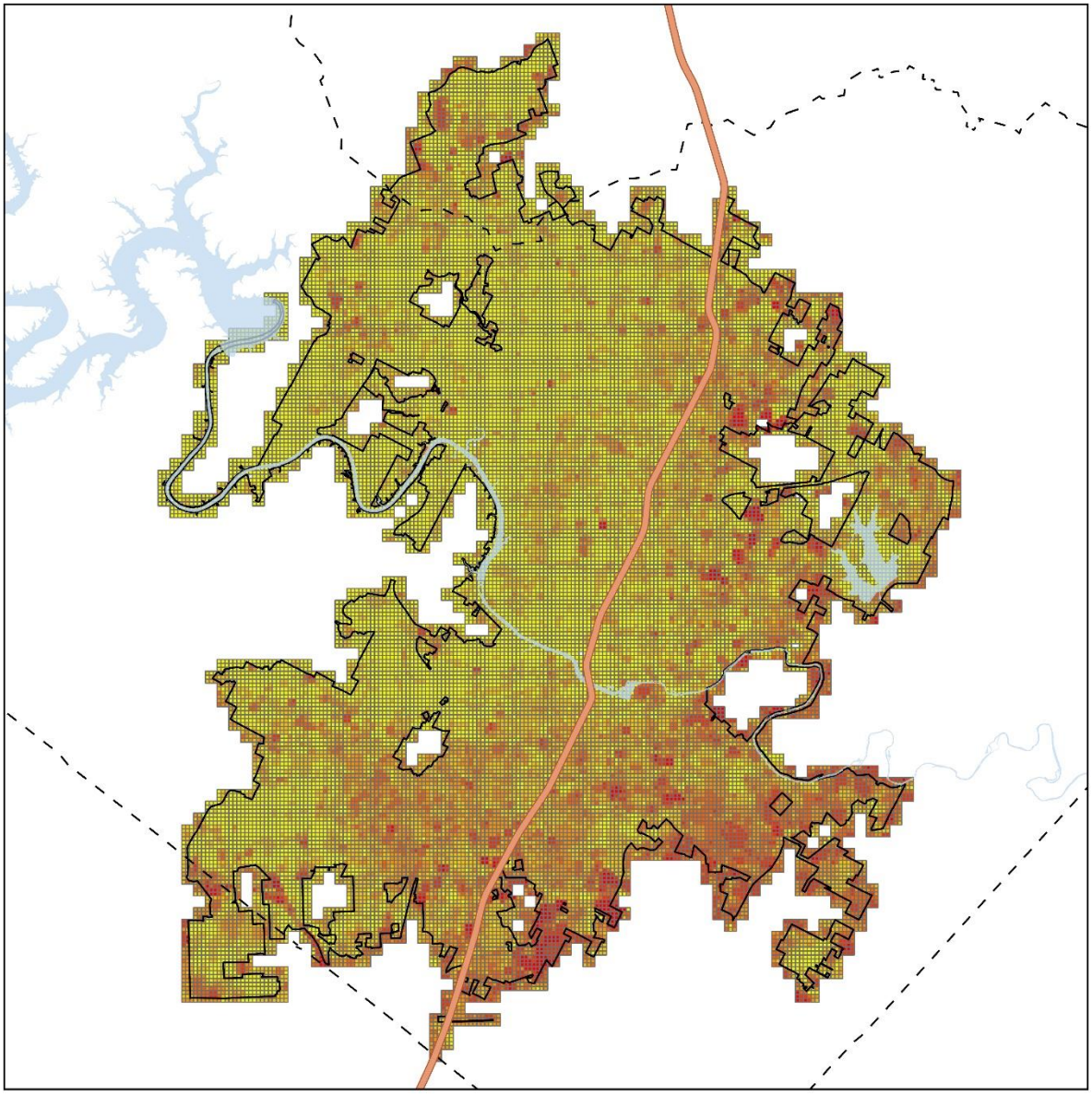
Legend
Maximum Change in Temperature
(°C) per 32,400m²
0.10 - 0.50
0.51 - 0.62
0.63 - 0.74
0.75 - 0.91
0.92 - 1.19
1.20 - 1.76
Interstate 35
County Boundaries
Austin City Limits
Water
N
0 2.5 5 10 Kilometers

Appendix H: Q-Q Plots for Normality

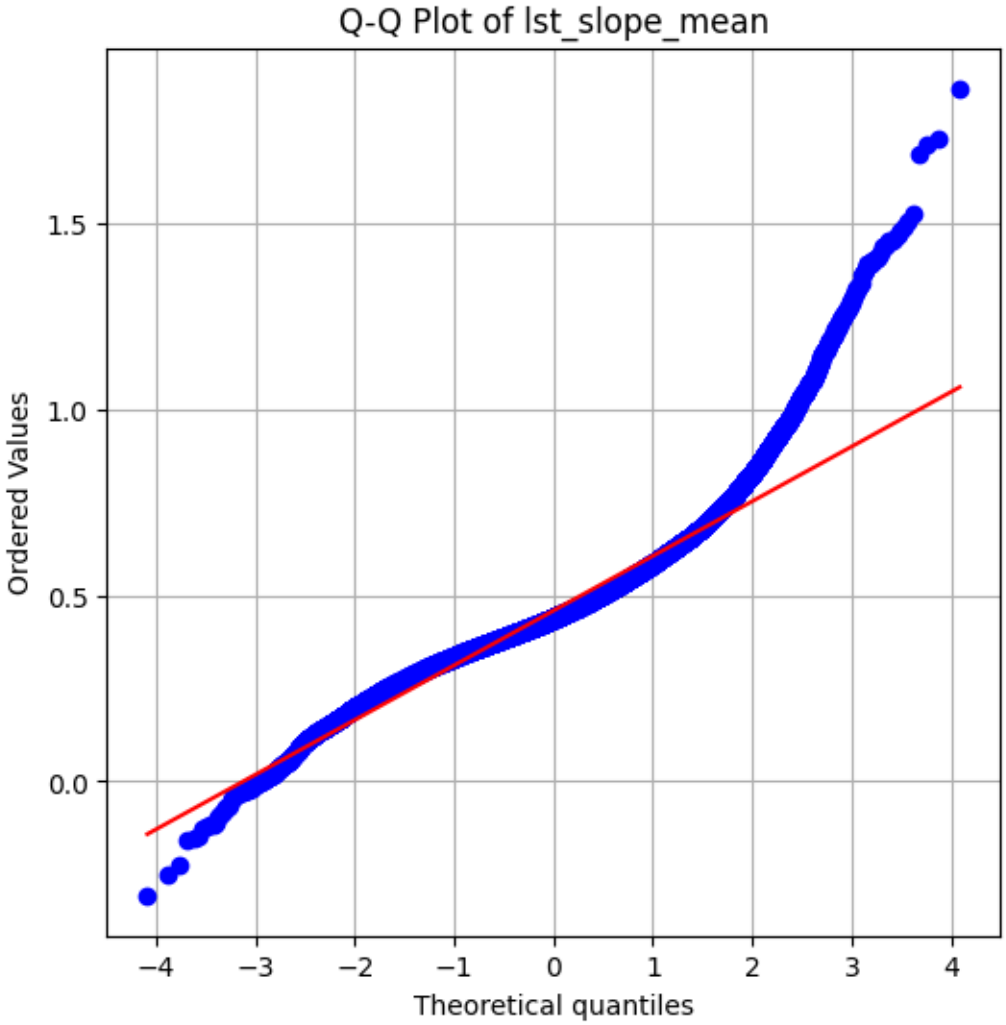

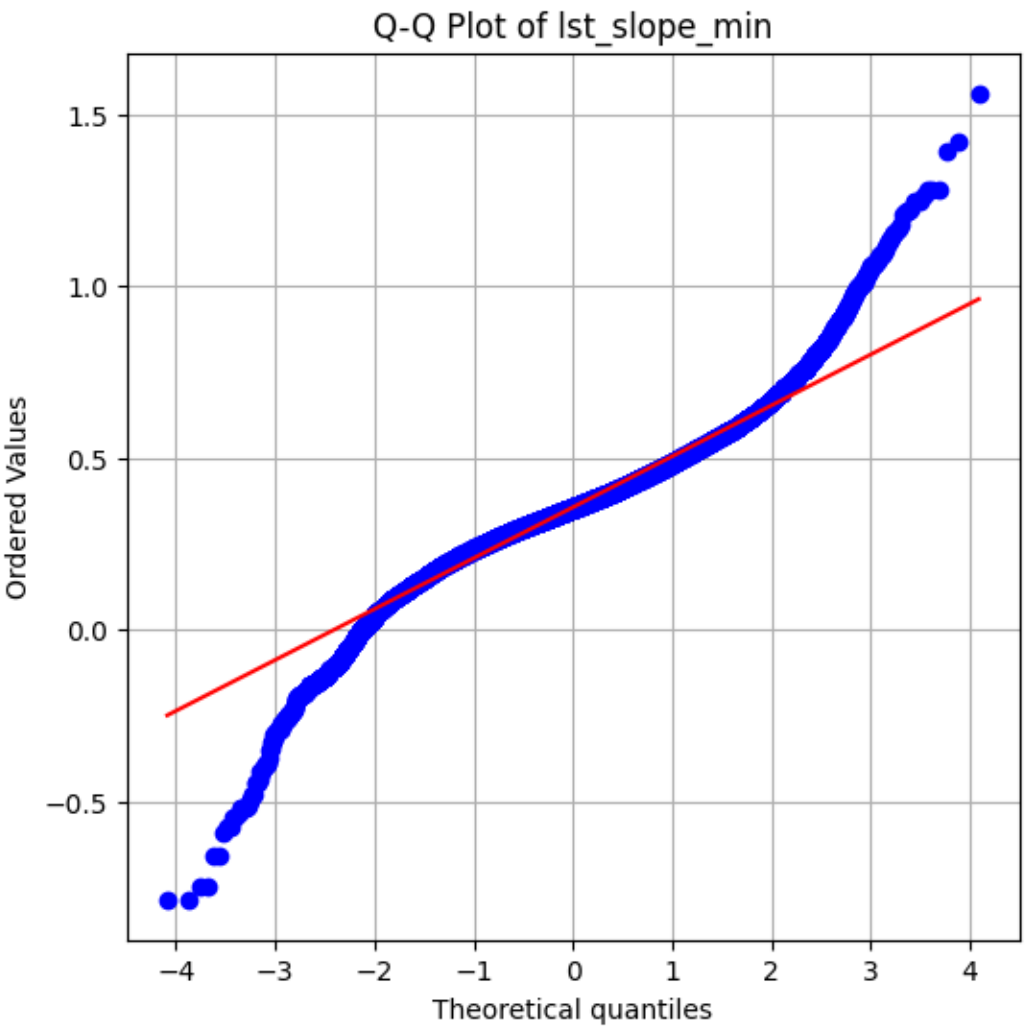
Q-Q Plot of lst_slope_min
Ordered Values
Theoretical quantiles
1.5
1.0
0.5
0.0
−0.5
−4
−3
−2
−1
0
1
2
3
4

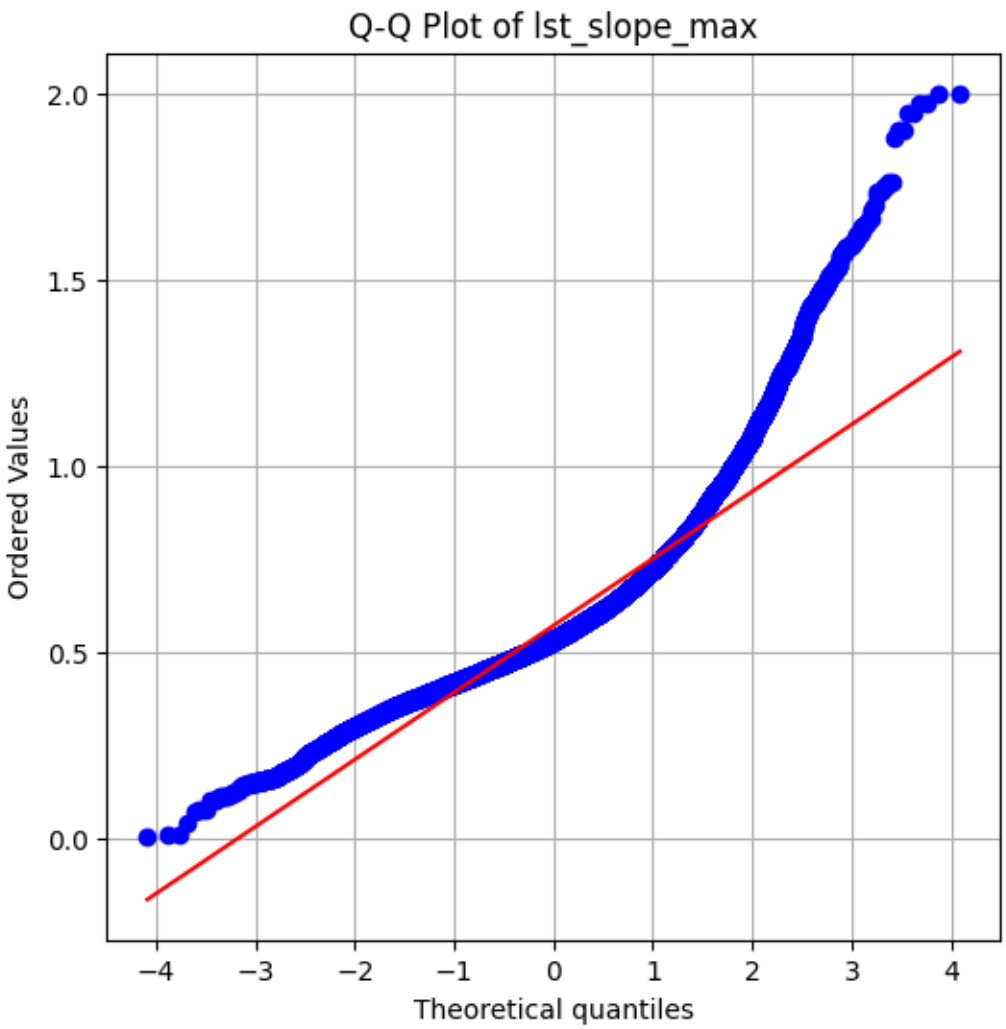
Q-Q Plot of lst_slope_max
Ordered Values
Theoretical quantiles
2.0
1.5
1.0
0.5
0.0
−4
−3
−2
−1
0
1
2
3
4

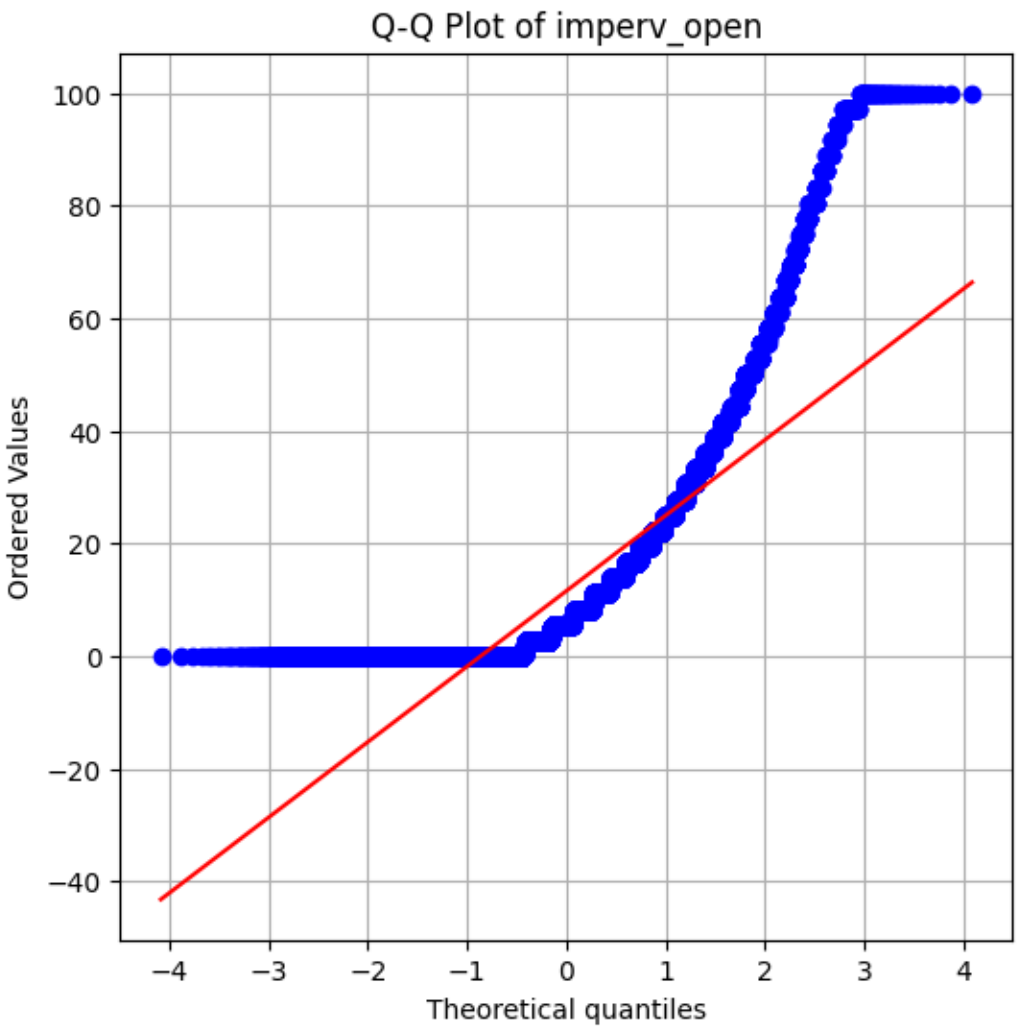
Q-Q Plot of imperv_open
Ordered Values
Theoretical quantiles
100
80
60
40
20
0
−20
−40
−4
−3
−2
−1
0
1
2
3
4

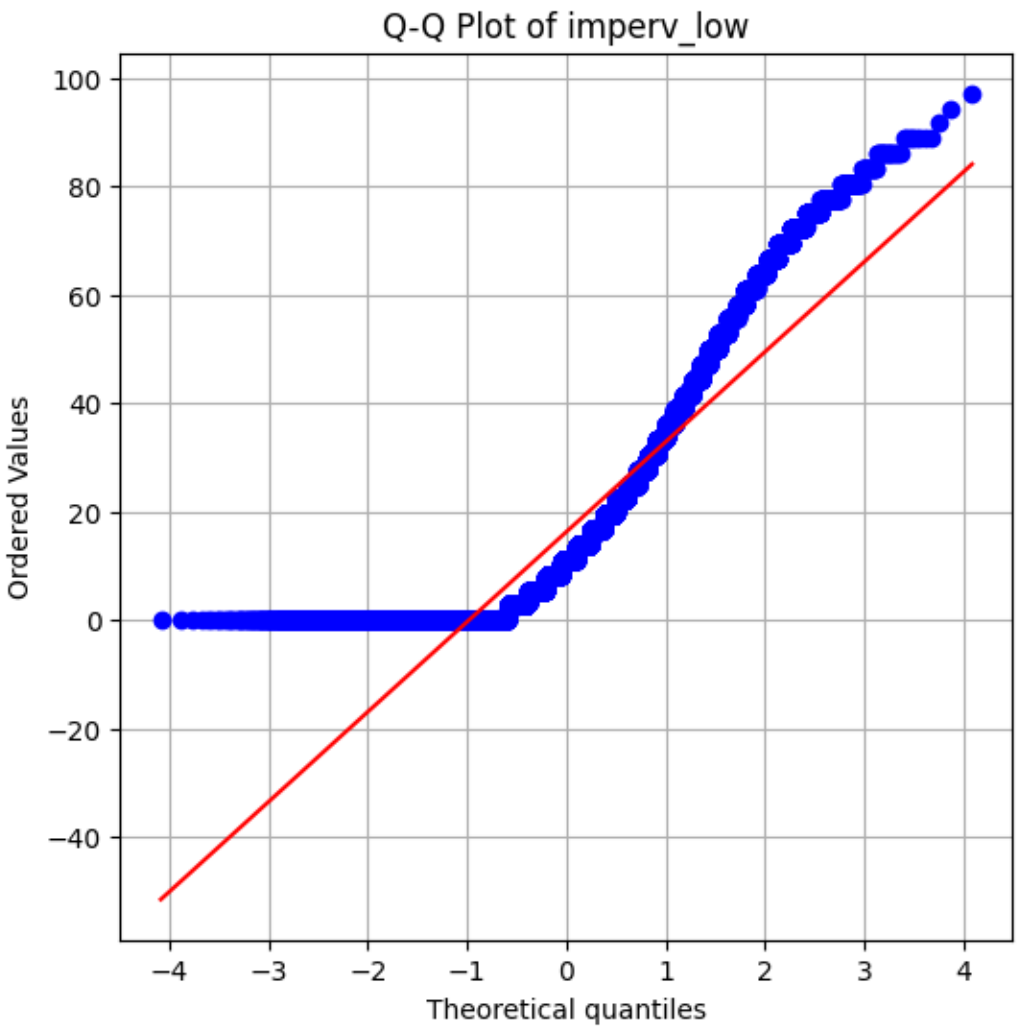
Q-Q Plot of imperv_low
Ordered Values
Theoretical quantiles
100
80
60
40
20
0
−20
−40
−4
−3
−2
−1
0
1
2
3
4

.

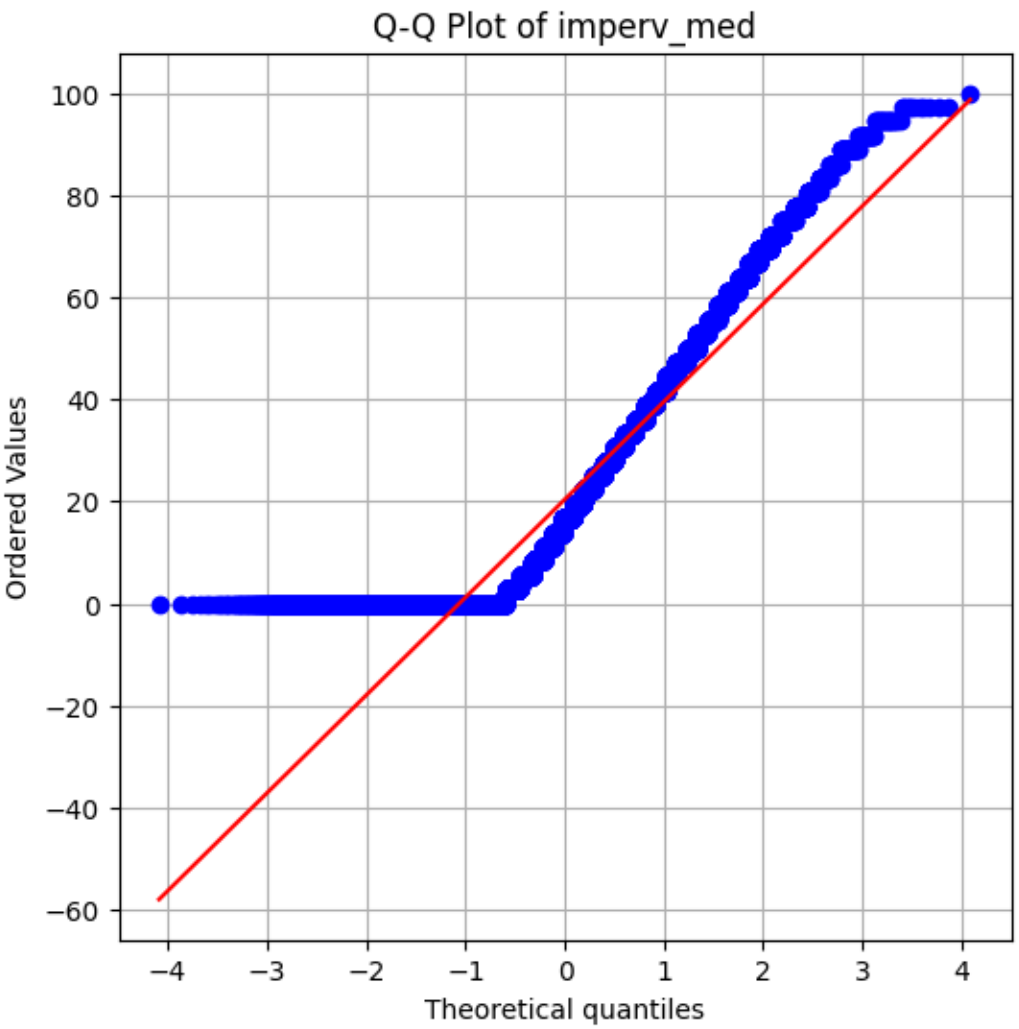
Q-Q Plot of imperv_med
Ordered Values
Theoretical quantiles
100
80
60
40
20
0
−20
−40
−60
−4
−3
−2
−1
0
1
2
3
4

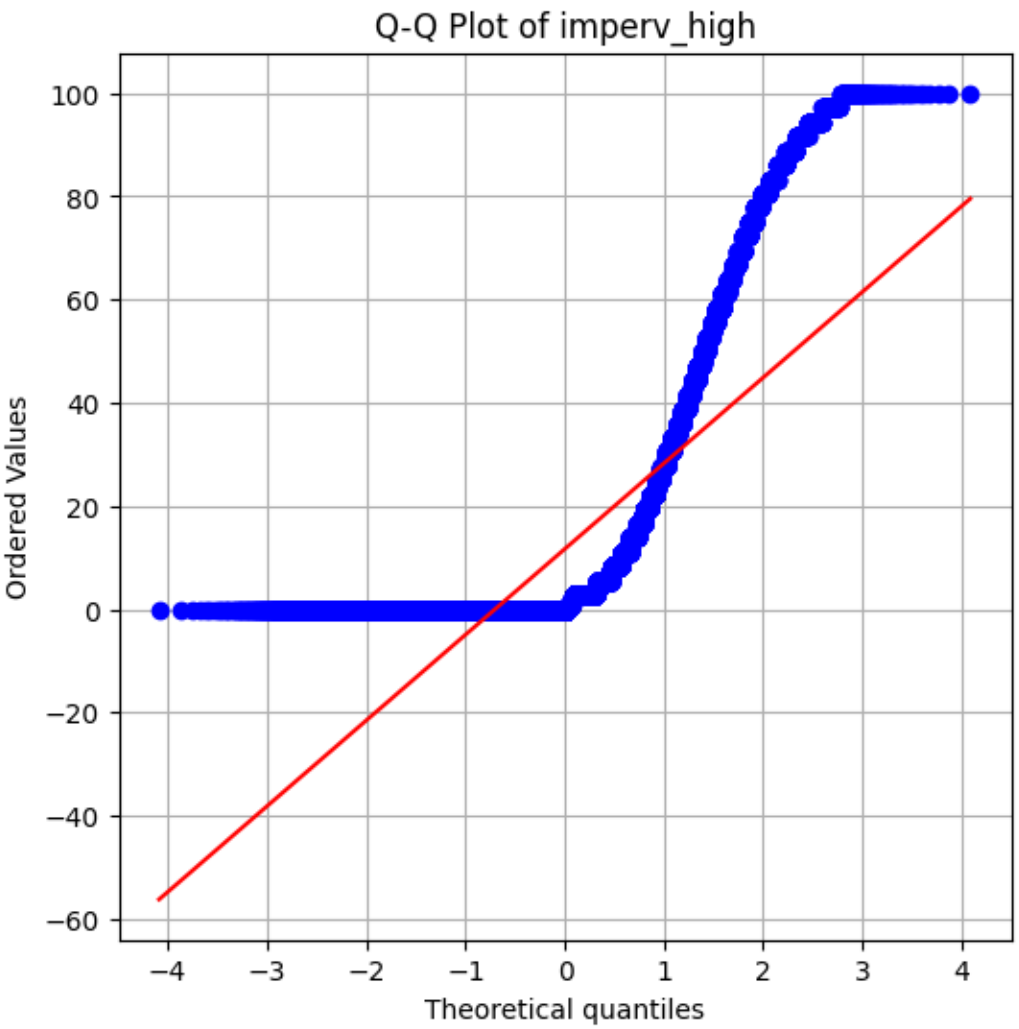
Q-Q Plot of imperv_high
Ordered Values
Theoretical quantiles
100
80
60
40
20
0
−20
−40
−60
−4
−3
−2
−1
0
1
2
3
4

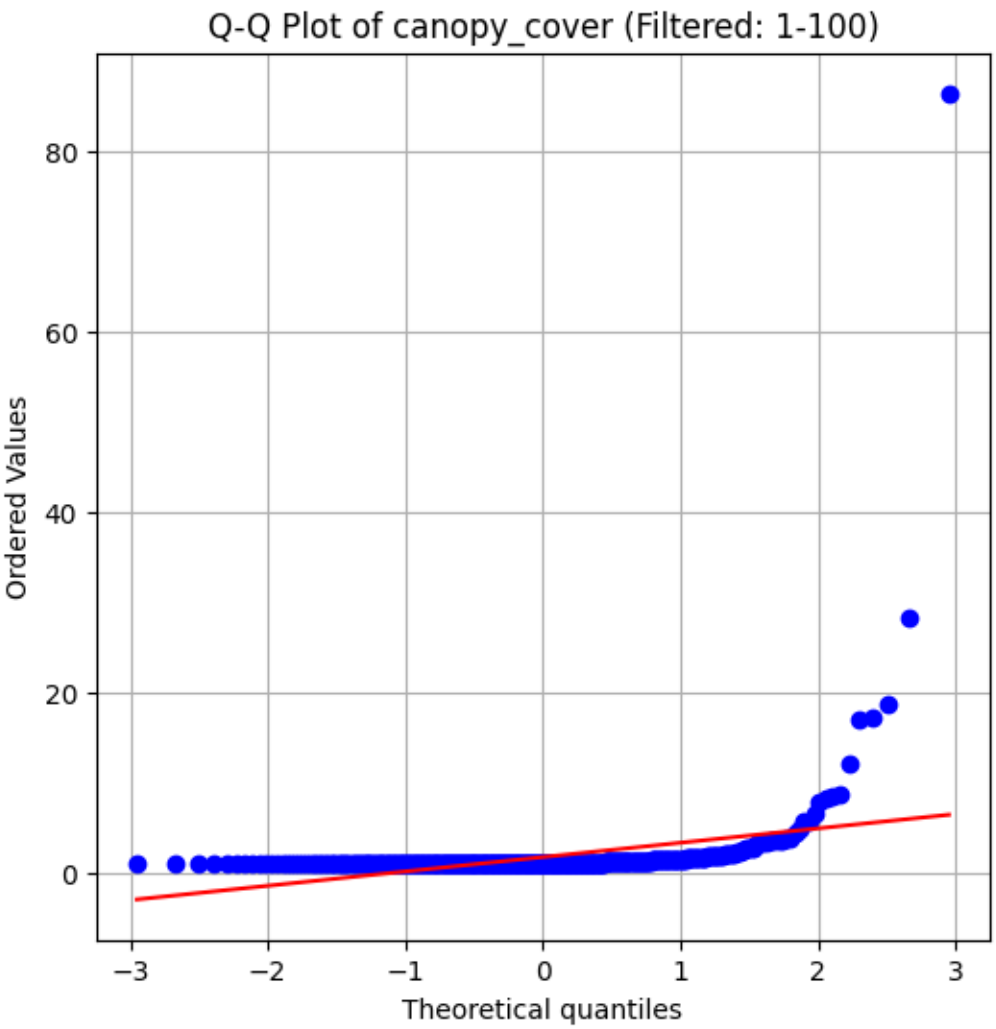
Q-Q Plot of canopy_cover (Filtered: 1-100)
Ordered Values
Theoretical quantiles
0
20
40
60
80
−3
−2
−1
0
1
2
3

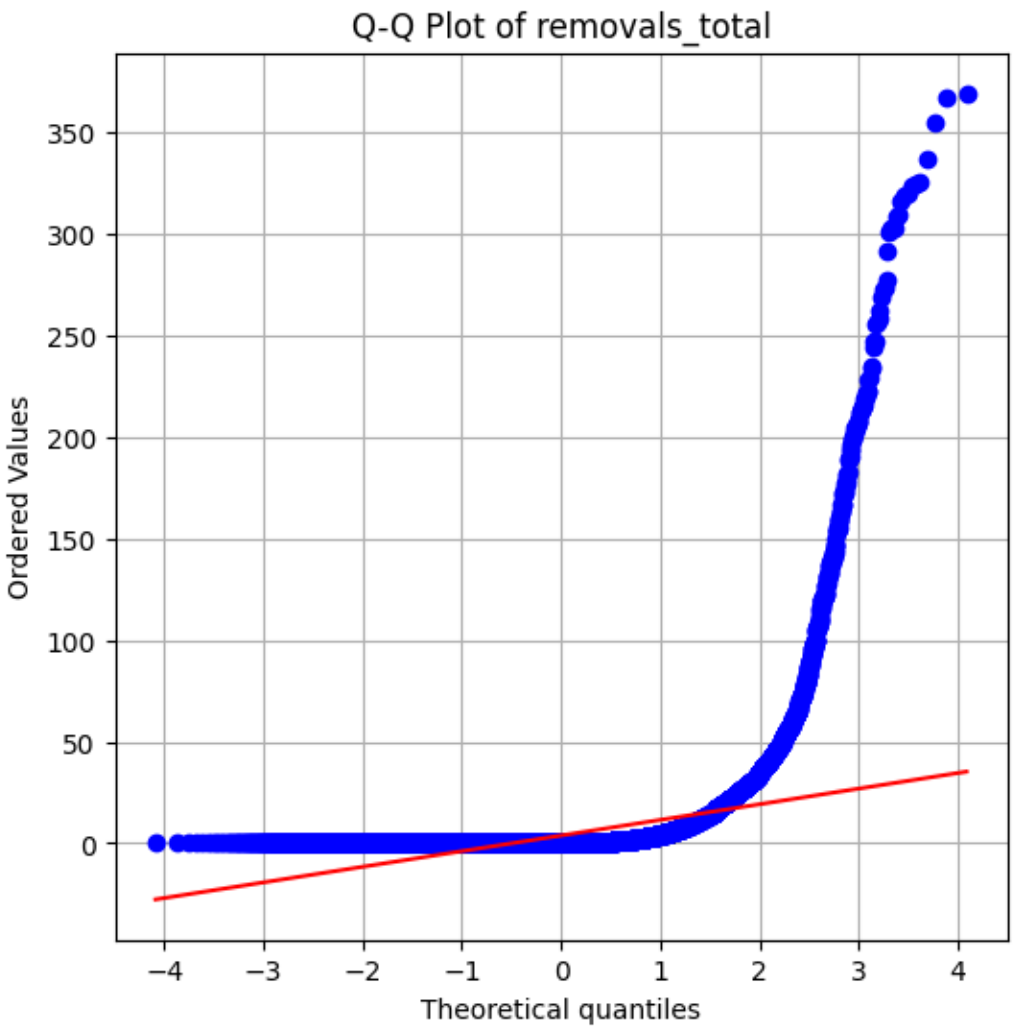
Q-Q Plot of removals_total
Ordered Values
Theoretical quantiles
350
300
250
200
150
100
50
0
−4
−3
−2
−1
0
1
2
3
4

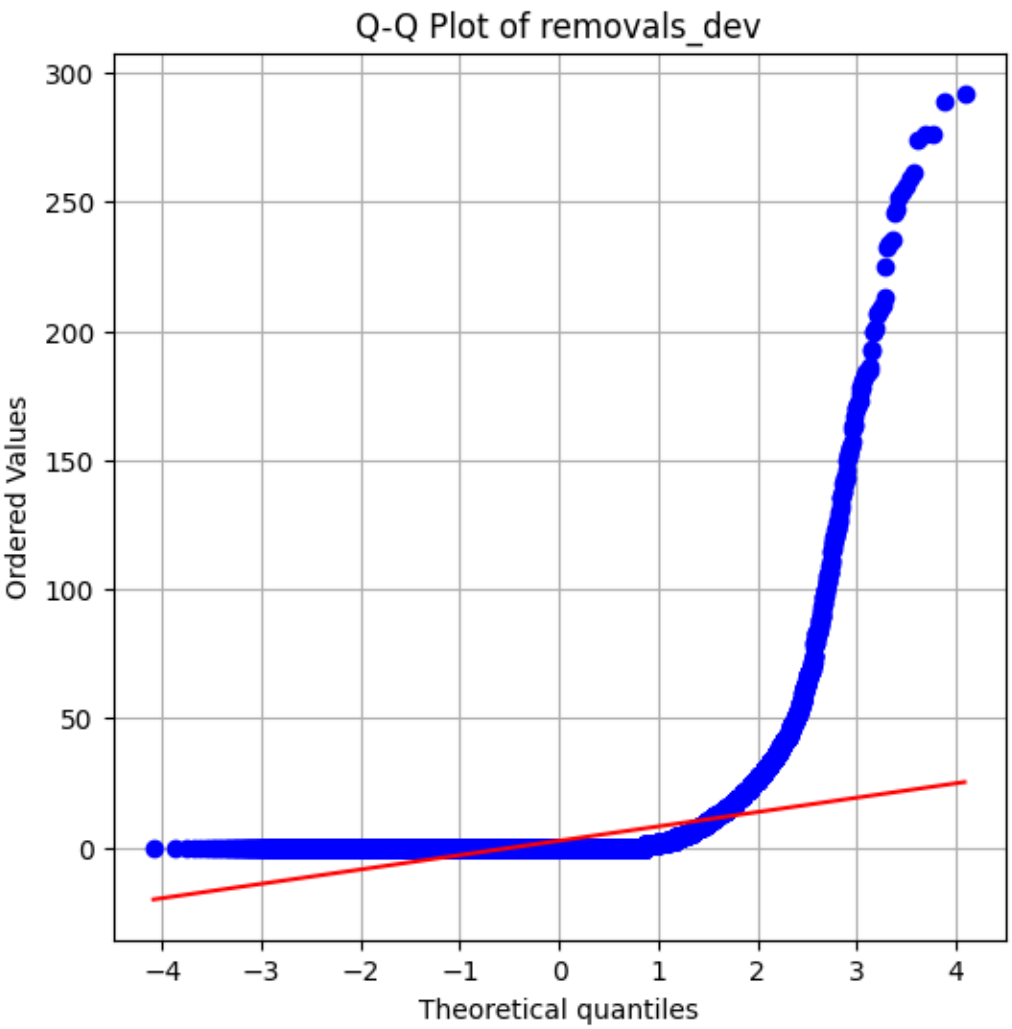
Q-Q Plot of removals_dev
Ordered Values
Theoretical quantiles
300
250
200
150
100
50
0
−4
−3
−2
−1
0
1
2
3
4

.

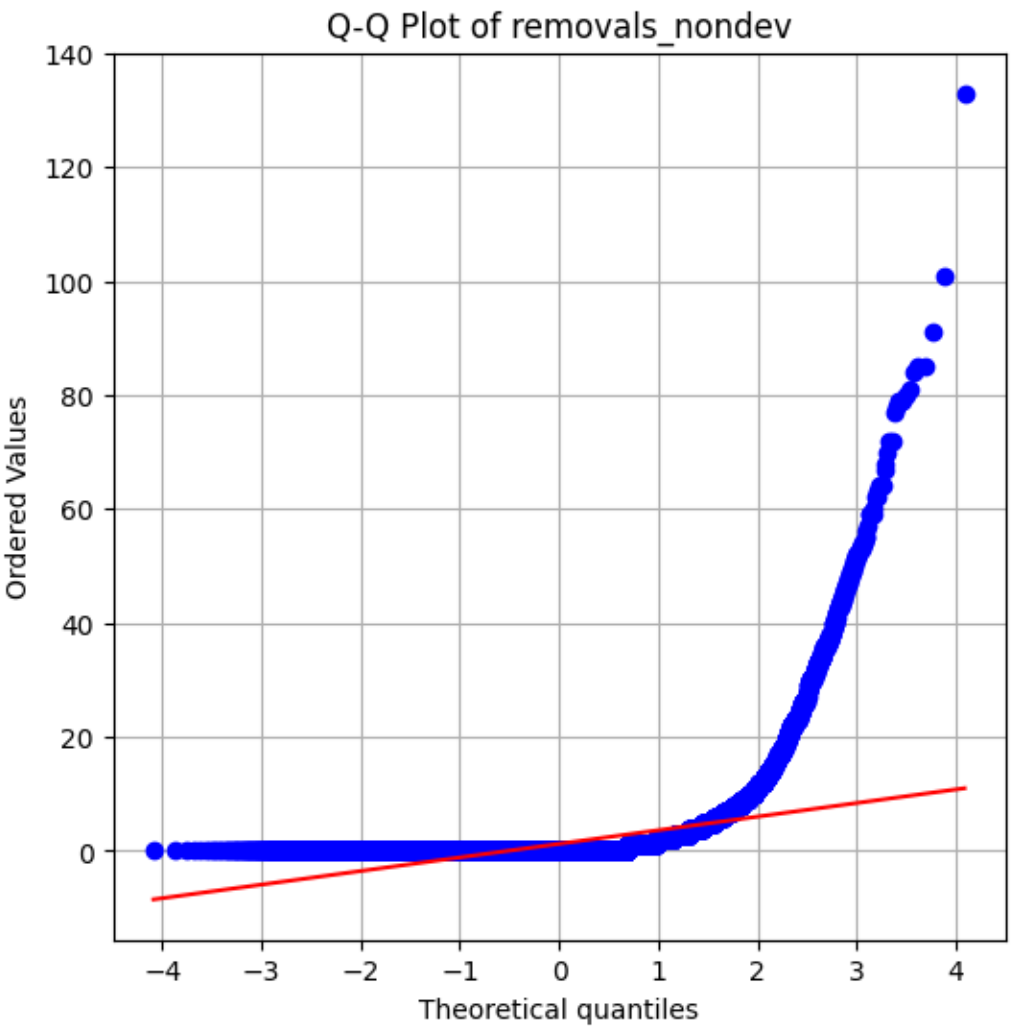
Q-Q Plot of removals_nondev
Ordered Values
Theoretical quantiles
140
120
100
80
60
40
20
0
−4
−3
−2
−1
0
1
2
3
4

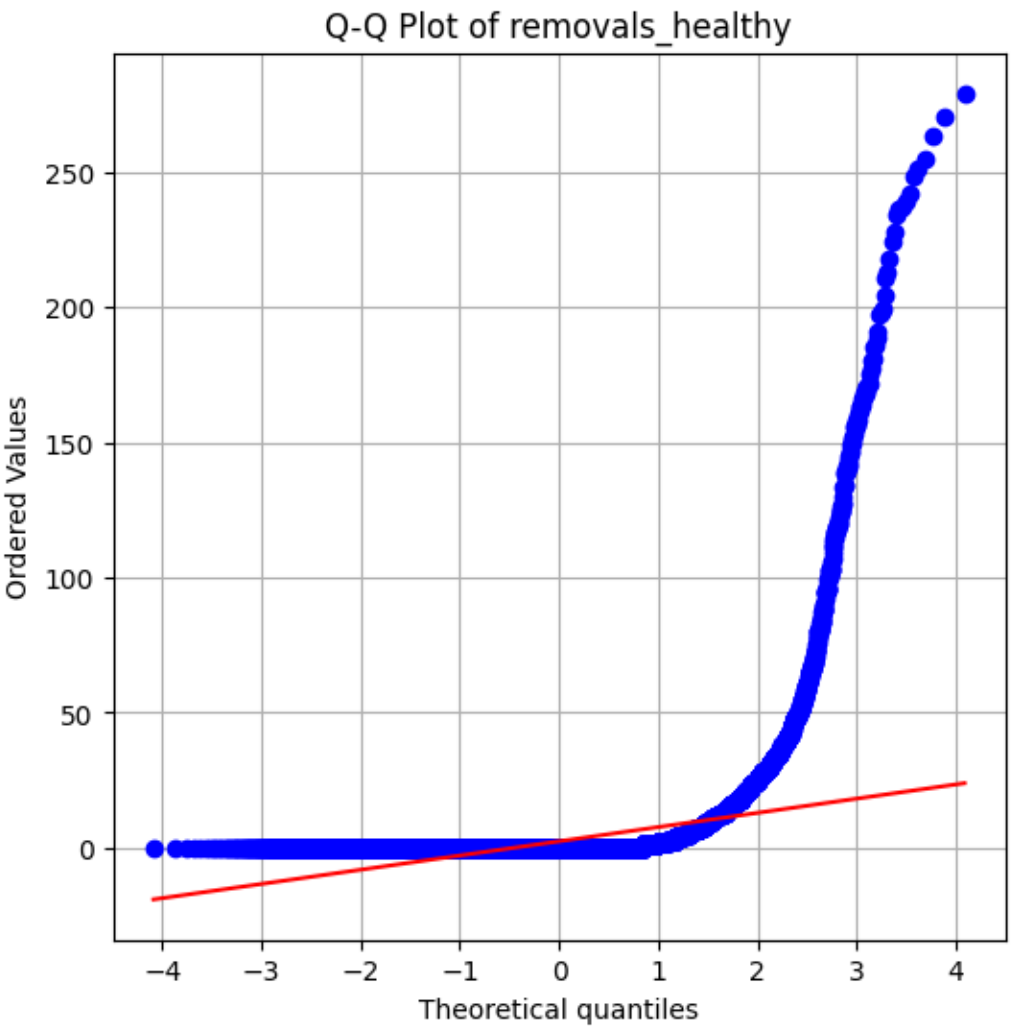
Q-Q Plot of removals_healthy
Ordered Values
Theoretical quantiles
250
200
150
100
50
0
−4
−3
−2
−1
0
1
2
3
4

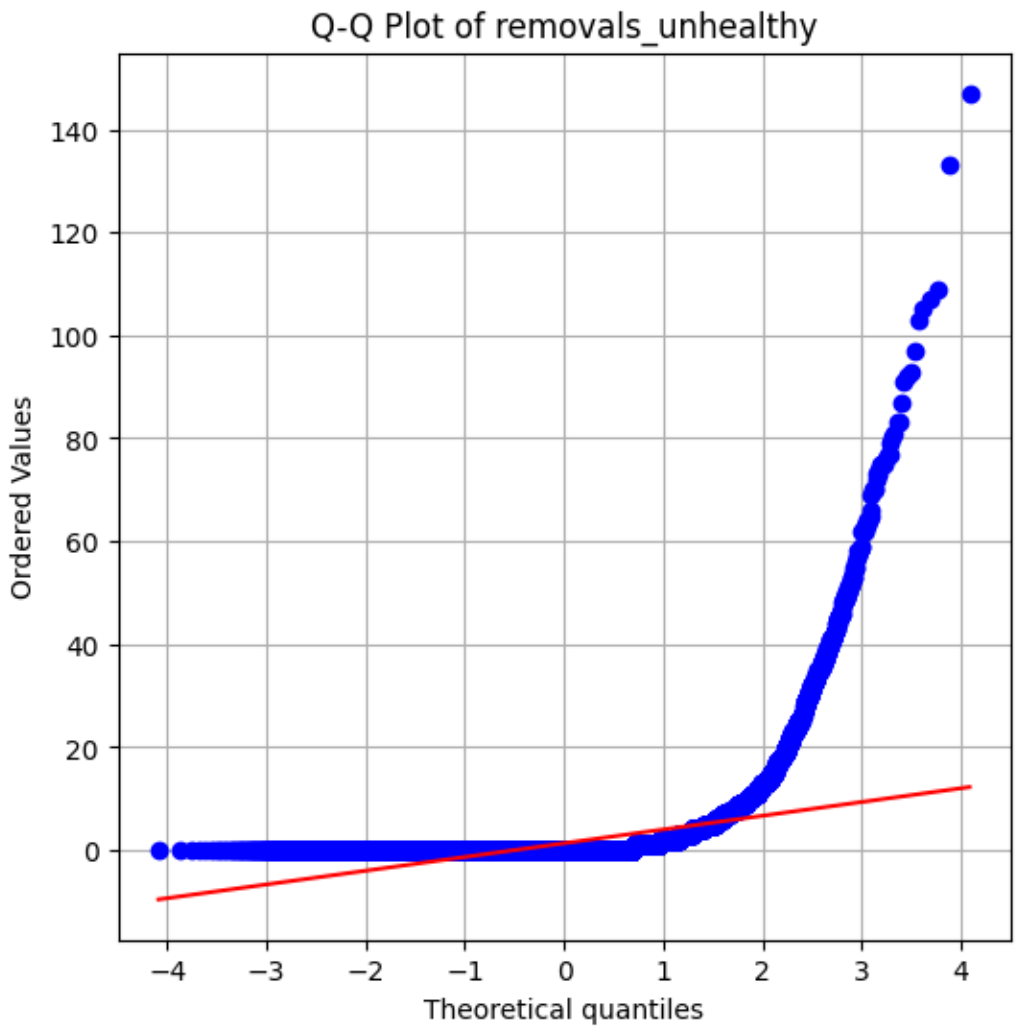
Q-Q Plot of removals_unhealthy
Ordered Values
Theoretical quantiles
140
120
100
80
60
40
20
0
−4
−3
−2
−1
0
1
2
3
4

Vita

Personal Background

Hannah Elese Buckhalter

Tacoma, Washington

Daughter of John Buckhalter and Deborah Buckhalter

Education

2018	Diploma, Stadium High School, Tacoma, WA
2022	Bachelor of Science, University of Montana, Missoula, MT

Experience

2023-2025	Graduate Teaching Assistant, Texas Christian University
2022-2023	Plant Healthcare Specialist, Bartlett Tree Experts
2022 (May-Aug)	Front Country Ranger, USDA Forest Service

Presentations

Buckhalter, H. and Lavy B. 2025. Examining the relationship between permitted tree removals and land surface temperature change in Austin, Texas. American Association of Geographers 2025 Annual Meeting. Detroit, Michigan.

Buckhalter, H. and Lavy, B. 2024. Examining the relationship between permitted tree removals and land surface temperature change in Austin, Texas. TCU Research and Creative Activities Poster Session. Fort Worth, TX.

Buckhalter, H. and Lavy, B. 2024. Examining the relationship between permitted tree removals and land surface temperature change in Austin, Texas. Michael and Sally McCracken Student Research Symposium. Texas Christian University Fort Worth, TX.

Awards

2024 $2,000 – SERC Graduate Research Grant Award, College of Science and Engineering, Texas Christian University
2024 $3,000 – ENSC Graduate Research Grant Award, Department of Environmental and Sustainability Sciences, Texas Christian University
2025 $400 – Graduate Student Travel Grant Award, Texas Christian University

Abstract

THE IMPACT OF PERMITTED TREE REMOVAL ON LAND SURFACE TEMPERATURE CHANGE IN AUSTIN, TEXAS

By Hannah Elese Buckhalter, M.S., 2025

Department of Environmental and Sustainability Sciences

Texas Christian University

Thesis Advisor: Dr. Brendan Lavy, Assistant Professor of Environmental and Sustainability Sciences

Thesis Committee: Dr. Gehendra Kharel, Assistant Professor of Environmental and Sustainability Sciences

Dr. Esayas Gebremichael, Assistant Professor of Geological Sciences

In the United States, instances of heat-related illnesses are increasing in urban areas. Trees help mitigate urban heat and reduce heat-related illnesses by providing cooling effects through evapotranspiration and shade. Urban development is a primary driver of urban forest loss. The city of Austin, Texas, adopted a tree preservation ordinance in 1984 to protect trees on private and public property. The amount of approved tree removals, however, has increased as Austin remains one of the fastest growing cities in the United States. We created a geographic information system to analyze the impact of over 58,000 tree removals on land surface temperature (LST) across Austin's city limits. Our results indicate that both total and development-related removals significantly impact the cities changing LST. This research contributes to the growing body of literature on urban forests and microclimates, providing information to support the conservation of urban trees and healthy environments for urban residents.